DETERMINATION OF TRACE AMOUNT OF SILVER NANOPARTICLES IN AQUEOUS MEDIA USING DITHIZONE AS A SELECITIVE COLORIMETRIC AGENT

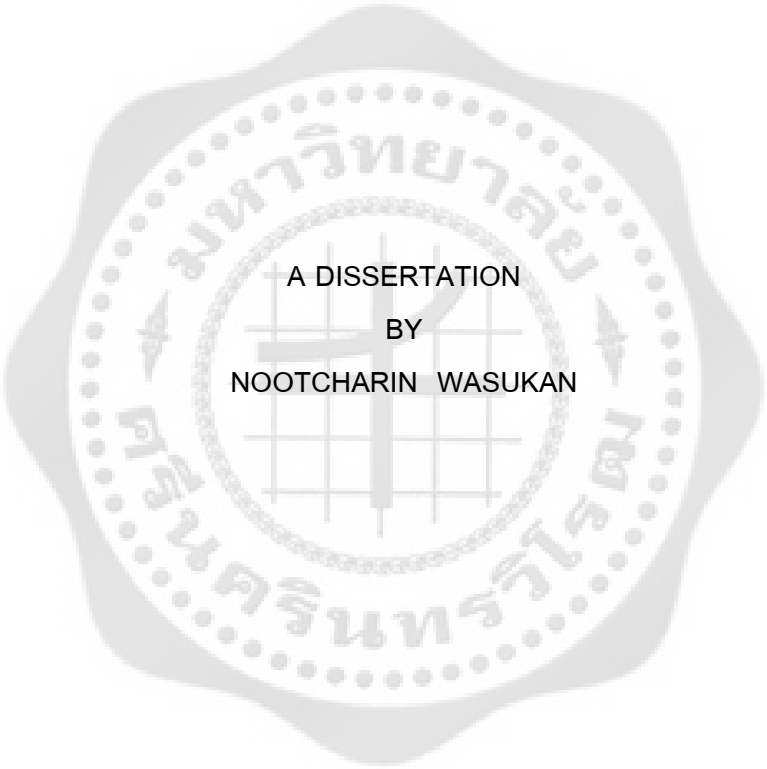

A DISSERTATION

BY

NOOTCHARIN WASUKAN

Presented in Partial Fulfillment of the Requirements for the

Doctor of Philosophy Degree in Applied Chemistry

at Srinakharinwirot University

August 2016

DETERMINATION OF TRACE AMOUNT OF SILVER NANOPARTICLES IN AQUEOUS MEDIA USING DITHIZONE AS A SELECITIVE COLORIMETRIC AGENT

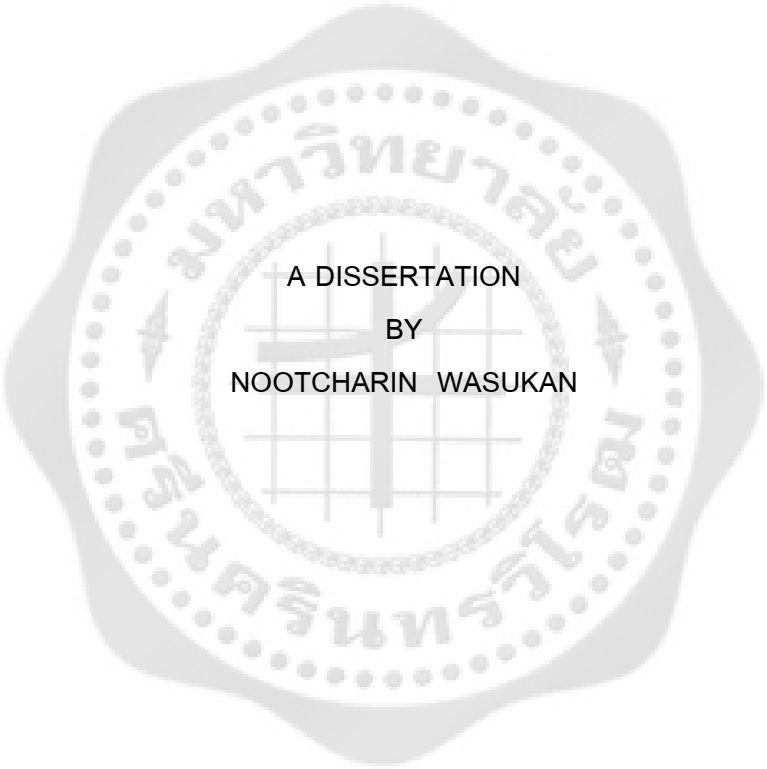

A DISSERTATION

BY

NOOTCHARIN WASUKAN

Presented in Partial Fulfillment of the Requirements for the

Doctor of Philosophy Degree in Applied Chemistry

at Srinakharinwirot University

August 2016

การวิเคราะห์อนุภาคนาโนของเงินปริมาณต่ำในตัวกลางที่เป็นของเหลว โดยใช้ไดไทโซนเป็นสารเทียบสีที่มีความจำเพาะ

บทคัดย่อ

ของ

นุจรินทร์ วะสุกัน

เสนอต่อบัณฑิตวิทยาลัย มหาวิทยาลัยศรีนครินทรวิโรฒ เพื่อเป็นส่วนหนึ่งของการศึกษา
ตามหลักสูตรปรัชญาดุษฎีบัณฑิต สาขาวิชาเคมีประยุกต์
สิงหาคม 2559

นุจรินทร์ วะสุกัน. (2559). *การวิเคราะห์อนุภาคนาโนของเงินปริมาณต่ำในตัวกลางที่เป็นของเหลวโดยใช้ไดไทโซนเป็นสารเทียบสีที่มีความจำเพาะ*. ปริญญานิพนธ์ ปร.ด. (เคมีประยุกต์) กรุงเทพฯ: บัณฑิตวิทยาลัย มหาวิทยาลัยศรีนครินทรวิโรฒ. อาจารย์ที่ปรึกษาปริญญานิพนธ์: อาจารย์ ดร.สุจิตรา ศรีสังข์, ภญ. ดร. รวิวรรณ มณีรัตนโชติ, ผู้ช่วยศาสตราจารย์ ดร. มะยูโซ๊ะ กูโน.

การนำอนุภาคนาโนของเงิน (AgNPs) มาใช้ประโยชน์ในผลิตภัณฑ์สำหรับผู้บริโภคมีหลากหลาย เนื่องจากมีคุณสมบัติต้านชื้อแบคทีเรียได้ ดังนั้นการปลดปล่อย AgNPs จากภาคอุตสาหกรรมหรือของเหลือทิ้งจากการใช้งานของผลิตภัณฑ์จึงอาจส่งผลกระทบต่อระบบนิเวศได้ ด้วยเหตุนี้การตรวจวัดที่ง่ายและมีความจำเพาะซึ่งวัด AgNPs ปริมาณต่ำได้จึงเป็นประโยชน์ในการเฝ้าระวังปริมาณ AgNPs ในสิ่งแวดล้อม ไดไทโซน (dithizone) สารเทียบสีเป็นหนึ่งในลิแกนด์ที่มีประสิทธิภาพและสามารถทำปฏิกิริยากับโลหะหนักเกิดเป็นสารประกอบเชิงซ้อนที่มีความเสถียรภาพ งานวิจัยนี้เป็นการศึกษาความจำเพาะของสารเทียบสีไดไทโซนเพื่อนำมาใช้สำหรับการตรวจวัด AgNPs ในตัวกลางที่เป็นของเหลว ประกอบด้วยการศึกษาเปรียบเทียบการใช้แบบจำลองทางคอมพิวเตอร์กับข้อมูลที่ได้จากการทดลองสำหรับการเกิดปฏิกิริยาระหว่างสารประกอบเชิงซ้อนของเงินและไดไทโซน โดยใช้ยูวีวิสสเปคโทรสโคปี (UV-Vis spectroscopy) และ FT-IR spectroscopy ด้วยระเบียบวิธี B3LYP/6-31G (d,p) รวมทั้งการใช้ ^{1}H NMR spectroscopy ด้วยระเบียบวิธี B3LYP/6-311+G (2d, p) ในการคำนวณ ผลการทดลองพบว่าสารประกอบเชิงซ้อนของเงินและไดไทโซนมีพลังงานต่ำและมีความเสถียรโดยเกิดกระบวนการแลกเปลี่ยนไฮโดรเจนไอออนของไดไทโซนกับอะตอมของเงิน ขณะที่โมเลกุลของไดไทโซนดูดกลืนแสงที่ความยาวคลื่น 447 นาโนเมตรและ 604 นาโนเมตร ให้สารละลายสีเขียว เมื่อเปรียบเทียบความจำเพาะของไดไทโซนกับอนุภาคนาโนของเงินและโลหะไอออนอื่นๆ เช่น Na^{+}, K^{+}, Cu^{2+}, Mg^{2+}, Ba^{2+}, Mn^{2+}, Fe^{3+}, Co^{2+}, Ni^{2+}, Cu^{2+}, Ag^{+}, Zn^{2+}, Cd^{2+}, Hg^{2+} และ Pb^{2+} ที่มีความเข้มข้นของโลหะไอออนเท่ากับ 0.1 มิลลิโมลาร์ พบว่าเมื่อสารละลายไดไทโซนทำปฏิกิริยากับอนุภาคนาโนของเงินและไอออนของโลหะจะเกิดการการเปลี่ยนแปลงสีจากสีเขียวเป็นสีส้มอย่างชัดเจนเมื่อเป็นสารประกอบเชิงซ้อนอนุภาคนาโนของเงินกับไดไทโซน (AgNPs-dithizone complex) เท่านั้น โดยมีการดูดกลืนแสงที่ความยาวคลื่น 477 นาโนเมตร และความเข้มข้นต่ำสุดของอนุภาคนาโนของเงินที่สามารถตรวจวัดได้เท่ากับ 0.071 มิลลิกรัมต่อลิตร ดังนั้นคุณสมบัติที่โดดเด่นของวิธีนี้สามารถนำไปใช้ในการตรวจวัดอนุภาคนาโนของเงินในตัวกลางที่เป็นของเหลวได้

DETERMINATION OF TRACE AMOUNT OF SILVER NANOPARTICLES IN AQUEOUS MEDIA USING DITHIZONE AS A SELECITIVE COLORIMETRIC AGENT

AN ABSTRACT
BY
NOOTCHARIN WASUKAN

Presented in Partial Fulfillment of the Requirements for the
Doctor of Philosophy Degree in Applied Chemistry
at Srinakharinwirot University
August 2016

Nootcharin Wasukan. (2016). *Determination of trace amount of silver nanoparticles in aqueous media using dithizone as a selective colorimetric agent*. Dissertation, Ph.D. (Applied Chemistry). Bangkok: Graduate School, Srinakharinwirot University. Advisor Committee: Dr. Sujittra Srisung, Dr. Rawiwan Maniratanachote, Asst. Prof. Dr. Mayuso Kuno.

Silver nanoparticles (AgNPs) are increasingly used in consumer products due to their antibacterial properties. The release of AgNPs from the industry or consumer product waste might have contributed affected on the ecosystem. Therefore, the measurement of AgNPs in trace amounts, using an easy and selective method, will help to monitor of AgNPs in the environment. Dithizone is one of the most effective chelating reagents for metal ions, which form stable complexes and generate intense colors. In this study, dithizone was selected for AgNPs detection in aqueous media. The complex formation between silver with dithizone was investigated by using UV-Vis spectroscopy and FT-IR spectroscopy. The results of computer simulation using B3LYP/6-31G(d,p) and ^{1}H NMR spectra calculation using B3LYP/6-311+G(2d,p) methods were compared with the experimental data. It was found that Ag-dithizone complex occurred via ion exchange interaction between hydrogen at thiol group of dithizone and a silver atom with low binding energies. In UV-Vis spectroscopy, dithizone was characterized by two peaks at about 447 nm and 604 nm, which were responsible for the green color of the solution. The selectivity of dithizone to AgNPs was also compared with the other metal ions such as Na^{+}, K^{+}, Cu^{2+}, Mg^{2+}, Ba^{2+}, Mn^{2+}, Fe^{3+}, Co^{2+}, Ni^{2+}, Cu^{2+}, Ag^{+}, Zn^{2+}, Cd^{2+}, Hg^{2+} and Pb^{2+} at the concentration of 0.1 mM. The results showed that a distinct color change from green to orange was noticed only in the case of AgNPs-dithizone complexes formation, with a maximum wavelength at 477 nm. The detection limit of the present method for AgNPs is 0.071 mg/L. Therefore, a remarkable feature of this method can be applied for determination of AgNPs in aqueous media.

The dessertation titled

“Determination of trace amount of silver nanoparticles in aqueous media using dithizone as a selective colorimetric agent”

by

Nootcharin Wasukan

Has been approved by the Graduate School as partial fulfillment of the requirements for the Doctor of Philosophy Degree in Applied Chemistry of Srinakharinwirot University.

.....Dean of Graduate School

(Assist. Prof. Dr. Chatchai Ekpanyaskul)

.....

Dissertation Committee

.....Major-advisor

(Dr. Sujittra Srisung)

.....Co-advisor

(Dr. Rawiwan Maniratanachote)

.....Co-advisor

(Asst. Prof. Dr. Mayuso Kuno)

Oral Defense Committee

.....Chair

(Maj. Gen. Assoc. Prof. Dr. Chainarong Cherdchu)

.....Committee

(Dr. Sujittra Srisung)

.....Committee

(Dr. Rawiwan Maniratanachote)

.....Committee

(Asst. Prof. Dr. Mayuso Kuno)

.....Committee

(Assoc. Prof. Dr. Siritron Samosorn)

Acknowledgements

I would like to express my sincere gratitude and appreciation to my supervisor, Dr. Sujittra Srisung, for her kindness, excellent advice, caring, helpful supervision, giving me a lot of suggestions, support and encouragement throughout the period of this dissertation.

I am also very grateful to my co-advisors, Dr. Rawiwan Maniratanachote and Asst. Prof. Dr. Mayuso Kuno for their endless kindness, helpful suggestion, valuable time, expert guidance and encouragement for the completeness of this dissertation.

I would like to thank the oral defense committee, Maj. Gen. Assoc. Prof. Dr. Chainarong Cherdchu and Assoc. Prof. Dr. Siritron Samosorn, for their great advice, valuable comments and feedback to improve my dissertation.

I am grateful to Professor Wesley R. Harris at Department of Chemistry and Biochemistry, University of Missouri-St. Louis, Missouri, USA for guiding my research, valuable time, helpful suggestion and support on documents during the process on my research.

I am thankful National Science and Technology Development Agency (NSTDA) Thailand Graduate Institute of Science and Technology Scholarship (TGIST), (Grant No. TG-55-17-55-055D) for supporting me and Nano Safety and Risk Assessment Laboratory, National Nanotechnology Center (NANOTEC) for providing chemicals and equipment including group meeting activities, good advice on my research.

I would like to thank The Graduate School, Faculty of Science, Srinakharinwirot University for research grant support from conducting this dissertation.

I would like to thank Department of Chemistry, Faculty of Science, Srinakharinwirot University for providing all chemicals, equipment and instruments on my research.

Special thanks are given to my teachers, friends, all member of inorganic laboratory (19-1008), colleagues and staff of the Department of Chemistry, Faculty of Science, Srinakharinwirot University for their friendship, kind support and encouragement.

Finally, I wish to appreciate my family for their love, care, unconditional, encouragement and understanding in every aspect throughout my whole life.

Nootcharin Wasukan

TABLE OF CONTENTS

TABLE OF CONTENTS (continued)

LIST OF TABLES

LIST OF TABLES (continued)

LIST OF FIGURES

LIST OF FIGURES (continued)

LIST OF FIGURES (continued)

LIST OF FIGURES (continued)

LIST OF FIGURES (continued)

LIST OF FIGURES (continued)

LIST OF FIGURES (continued)

CHAPTER 1
INTRODUCTION

1. Background

Nowadays, nanotechnology is rapidly growing together with production and utilization of nanoparticles in a wide range of commercial products throughout the world. Silver nanoparticles (AgNPs) are used in a variety of consumer products such as electronics, cosmetics, textiles, paints and medical devices due to their antimicrobial properties (Dastjerdi; & Montazer. 2010: 5-18; Gao; & Cranston. 2008: 60-72). However, safety of AgNPs on human health and the environment are of major concerns. Exposure of AgNPs for short- and long-term might affect to both human and ecosystem. In human, long term exposure to silver can cause a blue-gray pigmentation of the skin, which is an irreversible discoloration called “Argyria” (Greene; & Su. 1987: 151-154). Furthermore, silver accumulation in soil and water might lead to circulation into the food chain and aquatic life (De Schamphelaere; & Janssen. 2004: 6201-6209; Lee; et al. 2007: 133-143; Morgan; & Wood. 2004: 1261-1267). Thus, it has been of awareness and concern when silver, in any forms, are utilized. According to the World Health Organization (WHO. 2008: 434), the level of silver in drinking water up to 0.1 mg/L causes no risk to human health and occupational safety. The National Institute for Occupational Safety and Health (NIOSH) and the Occupational Safety and Health Administration (OSHA) suggest a limitation of silver exposure at 0.01 mg/m^3 with the limitation for immediately dangerous to life or health (IDLH) at 10 mg/m^3 (NIOSH. 2007: 280).

AgNPs are used increasingly in commercial products, which may cause a release of the nanoparticles into the environment (Benn; & Westerhoff. 2008: 4133-4139, Blaser; et al. 2008: 396-409 and Lorenz; et al. 2012: 817-824). Amount of silver in the form of ion can be determined by using analytical instruments such as atomic absorption spectroscopy (AAS), inductively coupled plasma mass spectroscopy (ICP-MS) and inductively coupled plasma atomic emission spectrometry (ICP-AES) (Cheng; et al. 2012: 507-515; Chwastowska; et al. 2004: 224-229; & Yua; Song; & Chen. 2011: 625-630). However, the disadvantages and limitations of these instruments are time-consuming, difficulty and high cost of operation, unable to detect silver in complex matrices, and non-portable for field monitoring. Therefore, development of a simple analytical technique with high sensitivity

and selectivity to AgNPs has been of interest. A wide variety of colorimetric sensors for detection of heavy metal ions has been reported (Das; et al. 2012: 3714-3721; Jiang; et al. 2012: 12-15; & Mei; et al. 2012: 1879-1883). The functions of these sensors are based on chemical reactions which immediately generate optical signal and can be visualized by naked-eyes. This method is simple and low-cost of operation comparing to the AAS and ICP. Dithizone ligand is considered one of the most effective chelating reagents for many metal ions. It can interact and form stable complex with metal ions and generate specific colors. Dithizone was also applied for removing of heavy metal ions (Safavi; & Bagheri. 2005: 53-58; & Takahashi; Danwittayakul; & Suzuki. 2009: 1380-1385). Also, the study on the dithizone is available dye for detecting of cyanide anions (CN^-) through the use of a cationic chemosensor and this method could have applied to analysis of Co^{2+} and CN^- for water samples (Tavallali; et al. 2013: 121-130; Tavallali; et al. 2014: 139-146).

There are several ligands used for detection of silver ion (Ag^+) in the samples such as Cu_2O nano-colloid (Andal; & Buvaneswari. 2011: 653-658) and *o*-phenylenediamine (OPDA) (Yang; & Wang. 2011: 5005-5011). Therefore, the developing colorimetric sensors for AgNPs with dithizone and dithizone derivatives using computer simulation for the prediction of the molecular structure and compared the stability of dithizone and dithizone derivatives were studied. The computational methods using the density functional theory (DFT) was applied for calculated model in term of silver-dithizone complex. This method has been very popular and selected for this study due to their designing an item as a model on a computer before building the real item in the reason of time saving and risk decreasing. Moreover, theoretical calculations based on quantum mechanics were investigated to compose reliable predictions. This calculation could be used to explain possible foundation of molecular structures, energy and other parameter properties.

So far, there is no information about the detection of AgNPs using chemical ligands as colorimetric agents. This study aimed to determine stability, selectivity and sensitivity of dithizone and dithizone derivatives for detection of AgNPs in aqueous media by visualizing the color changes and using a UV-Vis spectroscopy, as well as computer simulation.

1.1 Objectives of the study

1. To compare stability of dithizone, dithizone derivatives, silver-dithizone complex, AgNPs-dithizone complex and silver-dithizone derivative complex by computer simulation.

2. To study on the selectivity and sensitivity of dithizone with other metal ions.

3. To develop method for trace amount measurement of AgNPs in aqueous media.

1.2 Significance of the study

Currently, the consumer products containing AgNPs are widely used. The nanoparticles can be exposed and affected on human health and the environment. According to the point of safety concern on their release in to aquatic environment, it is important and challenging to monitor amount of AgNPs in those media. However, there is no portable instrument available to detect AgNPs for the field study. Therefore, development of colorimetric sensor, by using chemical ligands, with high selectivity and sensitivity to the nanoparticles is promising. This would be of advantage as a simple and low-cost technique for determining even trace amount of AgNPs in aqueous media.

1.3 Scope of the study

In the first part, the computer simulation was used to predict and design the structure of dithizone derivative with electron-withdrawing groups; $-NO_2$, $-SO_3H$, -CN, $-CF_3$, -F, -Cl, and -Br. Then the method will be optimized to determine the possible structures of dithizone and dithizone derivatives by calculating the minimum energy of structure using B3LYP/6-31G(d,p) level of calculations. Interactions between Ag ion and AgNPs with dithizone derivatives were also investigated. The lowest binding energy indicates the most stable complexes.

In the second part, the stability constant of silver-dithizone complexes were estimated. Effects of other parameters including pH on selectivity and sensitivity of the complexes were also investigated. This method will be developed and applied to determine AgNPs in product samples.

CHAPTER 2
REVIEW OF LITERATURES

This chapter proposes the reviews of literature for both theoretical and related topics of AgNPs information, colorimetric sensor, computer simulation, stability of complexes and dithizone ligand which are illustrated as follows:

1. Theory and related topics

1.1 AgNPs

AgNPs are colloidal silver defined as particle size at least one dimension between of approximately 1 and 100 nm (ISO/TS 27687; 2008). AgNPs have attracted interest in widespread applications including, electronics, biosensing, textiles, cosmetics, paints, and medical tools because of their antibacterial effect. AgNPs is black powder and the color of AgNPs suspension is light yellow. The change in color of AgNPs depends on the size of particle resulting AgNPs that have distinct, unique physical, chemical and optical properties. The wavelength of the plasmon absorption change depends on the electron oscillation surface of the AgNPs absorption. Meanwhile, the different sizes of AgNPs depend on localized surface plasmon resonance (SPR). There are the increasing interests in various products and sensors due to optical properties of AgNPs as evaluated with SPR (Mulfinger. 2007: 322-325). However, the characteristics and properties of AgNPs are attractive for various commercial products leads to concerns of potential risk for humans and the environment.

1.2 Colorimetric chemosensor

Colorimetric sensors are based on an optical signal due to the bindings between ligand and metal ion that lead to the color change of complexation that depend on the specificity and selectivity of ligand. Colorimetric sensors are widely used in analyte-sensing systems and are interesting in the environmental and biomolecular applications. This method is increasing in the attraction because of their simplicity, convenience, ease of measurement, high sensitivity and low cost for analysis (Kaur; & Kumar. 2011: 9233-9264). In addition, hard and soft acids and bases (HASB) theory was considered of the specificity

of ligand and metal ion in the colorimetric sensor which hard acid prefers to interact with hard bases, soft acids prefer to interact with soft bases, while a borderline acid tends to bond to borderline bases (Pearson. 1963: 3533-9). Therefore, its application to colorimetric sensing of silver was tested. According to HASB theory, the interaction between silver as soft acids and sulfur as a soft bases ligand was considered. Sulfur atom established the high affinity for silver as coordination sites were designed and synthesized. Meanwhile, the development of a new molecule for sensing is important. Furthermore, the molecules are difficult in synthesis and time consuming. The synthetic reaction may be high risk and danger. However, the specificity and selectivity of the molecule, including the binding of ligand-metal complexes was used to predict the detection of targets. Finally, the computer simulation method was carried out to design as a molecule on a computer for sensing.

1.3 Computational chemistry

Computational chemistry is a part of chemistry that uses computer simulation to the solution of interesting chemical problems. The method was used with theoretical chemistry, combined into able computer programs to calculate the structures and properties of molecules and solids or simulated experimental results. Generally, computational results consist of the information obtained by the chemical experiments. Until now, it can in some cases predict unmonitored chemical phenomena. This method was designed and investigated the possibility of molecules, including prediction of changes in structure before the synthesis of the actual molecule. Therefore, the methods are widely used because of their time saving, without risk and good prediction of changes in trends or patterns. Therefore, it is the most widely applied in the invention of new drugs and materials (Summers. 1998: 119-131).

1.4 Stability of complexes

The stability of metal – ligand complexes are indicated by stability constants or equilibrium constants. Generally, potentiometry and spectrophotometry are used to determine constants. Stability constant is a measure of the stability of a complex (ML) formed by a metal ion (M) with a ligand (L) in aqueous solution, and refers to the equilibrium:

$$M + L \underset{k_{-1}}{\overset{k_1}{\rightleftharpoons}} ML$$

The corresponding stability constant can be defined by Equation 1.;

$$K = \frac{[ML]}{[M][L]}$$

Equation 1.

In this research, there was carried out with spectrophotometry to estimate for stability constant. The additions of different concentration of Ag ion and AgNPs to dithizone ligand were investigated, which a new absorption band was appeared related to the complex formation of dithizone with Ag ion and AgNPs, respectively. The formation constants of the complexes were considered from Benesi and Hildebrand equation (Benesi; & Hildebrand. 1949: 2703-2707; Tayade; et al. 2014: 19-26).

$$\frac{1}{A - A_0} = \frac{1}{(\varepsilon_{ML} - \varepsilon_L)} + \frac{1}{(\varepsilon_{ML} - \varepsilon_L)\, K[M_0]}$$

Equation 2.

Where, $[M_o]$ is the silver concentration; A_o and A are absorbance of the free dithizone ligand solutions and the corresponding silver-dithizone complexes, at a given wavelength; ε_L and ε_{ML} are the molar extinction coefficients of the dithizone ligands and silver-dithizone complexes, respectively and K is the stability constant for silver-dithizone complexes From Equation. (2), plot of $x = 1/[M_0]$ versus $y = 1/A\text{-}A_0$ gives a *y*-intercept = $1/ (\varepsilon_{ML}\text{-} \varepsilon_L)$ and slope = $1/(K(\varepsilon_{ML}\text{-} \varepsilon_L))$ which gives the value of K. The results of stability constant were calculated from the plots of $1/[M_0]$ versus $1/A\text{-}A_0$ by using the SigmaPlot software (Systat Software, San Jose, CA)

1.5 Dithizone

Dithizone is a chelating agent containing sulfur (S) and nitrogen (N) donor atoms as shown in (Figure 1). It is a black color powder and not soluble in a water. However, dithizone are soluble in ethanol, acetone, chloroform, toluene and dimethyl sulfoxide. Dithizone was used for extraction, removal and preconcentration of many metal ions. Moreover, the dithizone has been used for the selectivity and specificity of various heavy metal ions such as Pb, Cd, Cu and Hg (Antônio; et al. 2002: 674-678; Danwittayakul; et al. 2008: 37-40; Yin; et al. 2012: 207-212). Because dithizone consists of thiol group as soft base, the interaction between dithizone and metal ions such as Pb, Zn and Hg can cause a high intense color of complexes (Kiwan; 1997: 947-950; Salih; et al. 1998: 1205-1213).

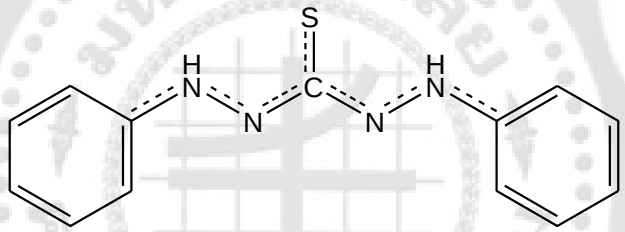

FIGURE 1 Structure of dithizone.

AgNPs have been widely used in commercial products due to their antibacterial effect. For a variety of consumer products,the toxic effect of AgNPs is a major concern. Due to an increasing use and disposal of the product can cause release of AgNPs into the aquatic environment. Therefore, the previous studies related to release of AgNPs into the aquatic environment from the commercial available product are as shown below.

In 2008, Benn and Wenterhoff proposed a method to determine nanosilver release from commercial socks into the water. The six brands of commercially available socks were prepared by the digestion method and analyzed initial concentration of silver using inductively coupled plasma optical emission spectroscopy (ICP-OES). Then, the sock samples were washed in ultrapure water. Consequently, the release of silver was detected in the washwater. In the presence of silver release from sock sample into the washwater at

different rates and silver amount in the 500 mL washwater ranged from 3 to 1300 ppb (Benn; & Westerhoff. 2008: 4133-4139).

In 2010, Kaegi; et al. proposed a method to investigate the release of AgNPs contained in paints from outdoor facades. After the facade runoff, samples were collected for a one year into natural water. Then, the sample was prepared by the acid digestion method and the quantity of AgNPs was analyzed by using inductively coupled plasma mass spectrometry (ICP-MS). They found that the initial concentration of AgNPs being 145 μAg/L andnd 30% of the AgNPs were released into the environment. The limit of detection method was 0.08 μg/L (Kaegi; et al. 2010: 2900-2905).

In 2012, Lorenz; et al. proposed a method to characterize the release of silver from commercially available silver-textiles during a washing and rinsing cycle. The eight different textiles were prepared and digested by the wet acid digestion method before analysis of silver amount by using ICP-OES. In the presence of initial silver amount of the textiles were between 1.5 and 2925 mg/kg. The amount of silver release in the washing of textiles was between 0.32 and 38.5 mg/L and in the rinsing solution between 0.36 and 22.7 mg/L. The limit of detection method was 0.005 mg/L (Lorenz; et al. 2012: 817-824).

In 2012, Pasricha; et al. proposed a method to investigate the silver released from the fabric into water during washing. Three different types of fabric were prepared by contained the synthesized AgNPs. After that fabrics were washed three times in ultrapure water and the quantities of AgNPs loading and releasing from the fabrics were measured by using atomic absorption spectrophotometry (AAS). With the appearance of the fabrics, release into the wash water at different rates, the percentage loading of AgNPs is in the ranged from 10-30% and the percentage releasing is between 12% and 25% of silver content (Pasricha; et al. 2012: 852-859).

From the research mentioned above, the methods were used for analysis of AgNPs by using AAS and ICP-MS. The two techniques are time consuming, complicated and expensive instruments. Therefore, it is not appropriate for field monitoring in routine analysis so that the colorimetric sensor method is an interesting alternative in AgNPs analysis due to their advantage such as simplicity, rapid, low cost and high selectivity that suitable for detection AgNPs in the aquatic environment. There are previous studies on the determination of Ag ion by using various types of ligand as shown below.

In 2006, Bhardwaj; et al. presented as a simple method for silver (I) determination in aqueous medium by using mesitylene based azo-coupled chromogenic tripodal receptors. The complex formation between ligand and silver (I) were observed the

color changes of the solution from yellow to red upon addition of silver (I) with the naked eyes. Therefore, the silver (I) is selectivity and specificity for the binding ligand in the aqueous medium. The detection of silver (I) in water samples at a very low concentration was 50 μM (Bhardwaj; et al. 2006: 7878-7886).

In 2011, Andal and Buvaneswari proposed a simple method for silver (I) determination in aqueous medium by using a simple method of preparation of Cu_2O nano-colloid as colorimetric sensor. The Cu_2O nano-colloid was prepared by using sodium alginate as a capping agent after that addition of silver (I) solution the color change of Cu_2O nano-colloid was observed from yellow to brown. Therefore, Cu_2O nano-colloid is high selectivity for silver (I) through an ion exchange process and non-toxic and environment friendly (Andal; & Buvaneswari. 2011: 653-658).

In 2011, Yang and Wang developed a method for silver (I) and copper (II) determination in sewage by using *o*-phenylenediamine (OPDA) as autocatalytic sensor. The reaction between OPDA and silver (I) and copper (II) changing the color of the samples were observed to light yellow. Moreover, this method was applied to test paper for silver (I) and copper (II) with the naked eyes. The limit of detection method was 60 nM for silver (I) and for copper (II) was 2.5 nM (Yang; & Wang. 2011: 5005-5011).

As indicated above mentioned researches, we are interested and have developed methods for detection of AgNPs with ligand in this study. Therefore, the plans for the design of these sensors are important for detection of silver depend on specific ligand analyze complex formation lead to the change of colors that can be easily observed by the naked eyes. Dithizone ligand is interested because of their selective and sensitive for metal ions. Moreover, dithizone consist of a thione group (C=S) on its molecule was introduced to the binding site that interaction with heavy metal ion possess a highly specific and the change of the optical sensing properties by the naked eyes. There are many researches that proposed the use of dithizone ligand for detection of heavy metal ion in the actual water sample as shown below.

In 2013, Tavallali; et al. developed a method for cyanide and cobalt (II) determination in dimethyl sulfoxide/water media by using dithizone (DTZ) as dual-analyte colorimetric chemosensor. The interaction between DTZ and cobalt (II) through the nitrogen and sulfur atoms of DTZ was coordinated with cobalt (II) into the complex formation changes green to red upon the addition of cobalt (II). Then, $[Co(DTZ)_2]^{2+}$ complex was changed to orange upon addition of cyanide that was attracted on azo a double bond of complexes. The limit of detection method was 0.04 μmol L^{-1} for cobalt (II) and the detection

limit for cyanide of the interaction complex $[Co(DTZ)_2]^{2+}$ is 0.43 μmol L^{-1} in dimethyl sulfoxide/water media. This method can be applied to the detection of cyanide in water samples (Tavallali; et al. 2013: 121-130).

In 2014, Tavallali; et al. presented a simple method and developed a method for cyanide determination in aqueous media by using dithizone as colorimetric sensor. The proposed interaction between dithizone and cyanide by color changes from green to yellow observed with the naked eyes. Due to the nucleophilic attack of cyanide was performed between azo double bond and thione group of molecules. The detection limit of the new chromogenic probe was measured to be 0.48 μmol L^{-1}. This method can be applied to the detection of cyanide in a variety of real samples (Tavallali; et al. 2014: 139-146).

From the research mentioned above, there is no information on colorimetric sensors for AgNPs. Therefore, the developing colorimetric sensors for AgNPs using dithizone and dithizone derivative with electron-withdrawing group; $-NO_2$, $-SO_3H$, -CN, $-CF_3$, -F, -Cl, -Br. In this work, there was carried out with dithizone and dithizone derivatives due to the structure of the molecule as chromophores, having the resonance stabilization of the molecule leading to absorption band and colorimetric changes for applying to determine of AgNPs in aqueous media. There are previous studies on the effect of electron-withdrawing for the sensitivity and binding properties as shown below.

In 2011, Lv Y; et al. presented a designed and synthesized three simple indole based colorimetric anion sensors 1-3 containing anthrone, 1,3'-indanedione and malononitrile as electron-withdrawing and chromogenic groups for detection of various anions. The investigated on the anion binding properties of three indole-based colorimetric sensors with the introduction of electron-withdrawing groups have a positive effect. The result showed that sensor 1 sensitivity for fluoride anion with a color change from pale yellow to light blue indicate that the deprotonation of chromophore-modified indole NH. The ability of anion sensors was found to be related to the electron-withdrawing of chromophores occurs by hydrogen bonds or deprotonation (Lv Y; et al. 2011: 973-977).

In 2011, Wang L; et al. presented the anion binding properties of the nitro-substituted 3,3'-bis(indolyl)methane receptors. The electron-withdrawing nitro group into the indole units and meso-phenyl ring of 3,3'-bis(indolyl)methane may be induced deprotonation of the indole NH and/or meso-position CH can lead to selectivity in colorimetric sensing of fluoride anion in comparison with other anions tested. The result shows that nitro derivative were found to display selective colorimetric sensing of fluoride anion. The binding site of

chemosensor occurred by the single CH proton based on a proton transfer process which the solution change from orange-yellow to purple-red (Wang L; et al. 2011: 726-731).

In 2015, Ghosh S; et al. presented a designed molecule selectively detect fluoride anion shown that the color change from colorless to red by naked-eyes. The investigated effects of the position of $–NO_2$ group (ortho, meta and para) in the benzohydrazide base Schiff bases (1-3) on the sensitivity and color of species. The result of Schiff bases (1–3) which reasons intramolecular charge transfer (ICT) between the electron deficient $–NO_2$ group and electron rich –N which impacts the ICT process resulting a color change from colorless to red. Moreover, test paper coated with the benzohydrazide base can be selective with fluoride anion by naked-eyes (Ghosh S; et al. 2015: 869-874).

From the research mentioned above, the effect of electron-withdrawing lead to the binding site of chemosensor, sensitivity and color of the species. Therefore, computer simulations were used for prediction of the molecular structure and compared the stability of dithizone and dithizone derivatives.

CHAPTER 3

EXPERIMENTAL

1. Apparatus

1.1 UV-Visible spectrophotometer (UV-Vis)

The absorbance spectra of metal ions, dithizone and dithizone derivatives were recorded by a UV-Visible spectrophotometer (Shimadzu UV-2401PC) at the wavelength range of 200-800 nm.

1.2 pH meter

The pH of AgNPs and dithizone solution were determined by Mettler S20 pH meter.

1.3 Homogenizer

Cream base and silver nanoparticle powder mixtures were prepared on Homogenizer model Pro 200.

1.4 Fourier Transform Infrared spectroscopy (FTIR) Absorption Spectra

The spectra of dithizone, dithizone derivatives and silver-dithizone complexes were measured on Perkin Elmer FT-IR spectrum BX spectrometer by using potassium bromide (KBr) disc as a calibrator.

1.5 Transmission Electron Microscopy (TEM)

The morphology of the AgNPs-dithizone complex was characterized by TEM, on JEM-2100 at an accelerating voltage of 120 kV.

2. Physical Property

2.1 Solubility

The solubility of dithizone was monitored by dissolving with ethanol, methanol, hexane, acetone, acetonitrile, dimethyl sulfoxide and DI water.

3. Chemicals and reagents

A chemicals and reagents used in this study were of analytical reagent grade and were shown in Table 1.

TABLE 1 Chemicals and reagent list

Chemicals and reagents	**Suppliers**
Dithizone ($\geq$99.0%)	Sigma-Aldrich (St. Louis, MO, USA)
Sodium iodide (NaI)	Carlo Erba (Milano, Italy)
Potassium iodide (KI)	Fisher Scientific (Pittsburgh, PA, USA)
Barium chloride dihydrate ($BaCl_2.2H_2O$)	Carlo Erba (Milano, Italy)
Calcium chloride ($CaCl_2$)	Laboratory Unilab Reagent (Sydney, Australia)
Aluminum nitrate nonahydrate ($Al(NO_3)_3.9H_2O$)	Fluka (Buchs, Switzerland)
Nickel chloride hexahydrate ($NiCl_2.6H_2O$)	Carlo Erba (Milano, Italy)
Copper nitrate Trihydrate ($Cu(NO_3)_2.3H_2O$)	Fisher Scientific (Pittsburgh, PA, USA)
Cadmium acetate dihydrate ($Cd(CH_3COO)_2.2H_2O$)	Fluka (Buchs, Switzerland)
Manganese sulfate monohydrate ($MnSO_4.H_2O$)	Fluka (Buchs, Switzerland)
Zinc sulfate heptahydrate ($ZnSO_4.7H_2O$)	Fluka (Buchs, Switzerland)
Iron sulfate heptahydrate ($FeSO_4.7H_2O$)	Fluka (Buchs, Switzerland)
Cobalt chloride hexahydrate ($CoCl_2.6H_2O$)	Merck (Darmstadt, Gemany)
Lead nitrate ($Pb(NO_3)_2$)	Laboratory Unilab Reagent (Sydney, Australia)
Magnesium sulfate heptahydrate ($MgSO_4.7H_2O$)	Laboratory Unilab Reagent (Sydney, Australia)
Mercury chloride ($HgCl_2$)	Sigma-Aldrich (St. Louis, MO, USA)
Silver nitrate ($AgNO_3$)	Fisher Scientific (Pittsburgh, PA, USA)

TABLE 1 (continued)

Chemicals and reagents	**Suppliers**
Silver nanoparticles (AgNPs), 20 nm particle size	Sigma-Aldrich (St. Louis, MO, USA)
Silver nanoparticles (AgNPs), 100 nm particle size	Sigma-Aldrich (St. Louis, MO, USA)
Silver nanoparticles powder	Sigma-Aldrich (St. Louis, MO, USA)
Potassium chloride (KCl)	Carlo Erba (Milano, Italy)
Potassium nitrate (KNO_3)	Carlo Erba (Milano, Italy)
p-nitroaniline ($C_6H_6N_2O_2$)	Himedia (Mumbai, India)
Sodium sulfide Nonahydrate ($Na_2S.9H_2O$)	Fisher Scientific (Pittsburgh, PA, USA)
Sodium acetate Trihydrate ($CH_3COONa.3H_2O$)	Laboratory Unilab Reagent (Sydney, Australia)
Sodium nitrite ($NaNO_2$)	Carlo Erba (Milano, Italy)
Nitro methane (CH_3NO_2)	Fisher Scientific (Pittsburgh, PA, USA)
Sodium hydroxide (NaOH)	Carlo Erba (Milano, Italy)
Potassium hydroxide (KOH)	Fisher Scientific (Pittsburgh, PA, USA)
Nitric acid (HNO_3)	Carlo Erba (Milano, Italy)
Hydrochloric acid (HCL)	Fisher Scientific (Pittsburgh, PA, USA)
Sulfuric acid (H_2SO_4)	Fisher Scientific (Pittsburgh, PA, USA)
Glacial acetic acid (CH_3COOH)	Fisher Scientific (Pittsburgh, PA, USA)
Ammonium hydroxide solution 28% NH_3 in H_2O, $\geq$99.99%	Fisher Scientific (Pittsburgh, PA, USA)
Acetone (C_3H_6O)	Carlo Erba (Milano, Italy)
Ethanol (C_2H_5OH)	Carlo Erba (Milano, Italy)
Methanol (CH_3OH)	Carlo Erba (Milano, Italy)
Ethyl acetate (C_4H_8O)	Carlo Erba (Milano, Italy)
Hexane (C_6H_{14})	Carlo Erba (Milano, Italy)
Dichloromethane (CH_2Cl_2)	Carlo Erba (Milano, Italy)
Dimethyl sulfoxide (C_2H_6OS)	Fisher Scientific (Pittsburgh, PA, USA)
Dimethysulfoxide-d_6 (DMSO-d_6)	Sigma-Aldrich (St. Louis, MO, USA)
Acetonitrile (CH_3CN)	Carlo Erba (Milano, Italy)

4. Preparation of chemicals and reagents

4.1 Preparation of dithizone and dithizone derivative solution

A 0.5 mmol dithizone solution was prepared by dissolving 128 mg with 100 mL of ethanol, methanol, acetone, acetonitrile, dimethyl sulfoxide and DI water.

4.2 Preparation of metal ions solution

The solution of metal ions was dissolved with DI water to the concentration of 1×10^{-5} M.

4.3 Preparation of AgNPs suspension

AgNPs of approximately 20 and 100 nm with the concentration of 20 mg/L were diluted with DI water to the concentration of 0.2 mg/L.

5. Molecular simulation

5.1 Computational details

The geometry optimization, vibrational frequency and binding energies were determined using the density functional approaches B3LYP (B3 Becke 3-parameter exchange and Lee_Yang_Parr correlation) functionals with the 6-31G(d,p), 6-31G(d), 6-31+G(d), 6-31+G(d,p), 6-31++G(d,p), 6-311G(d,p), 6-311+G(d,p) and 6-311++G(d,p) basis set. All calculations were carried out using the Gaussian 2003 package (Frisch; et al. 2003) running on a Linux PC.

5.2 Optimized structure of dithizone and dithizone derivatives

For comparison, the structure of dithizone and dithizone derivatives were using the B3LYP/6-31G(d,p) level of calculations. Meanwhile, the B3LYP/3-21G basis set was used for silver in the case of the silver-dithizone complex, silver-dithizone derivative complexes and AgNPs-dithizone complex. The structures of dithizone (Figure 2) and dithizone derivative with the nitro group (Figure 3) were optimized which the structures were investigated proton transfer on the sulfur and nitrogen atoms in the molecule. Moreover, The structures of dithizone derivative with electron-withdrawing group; $-SO_3H$, -CN, $-CF_3$, -F, -Cl and -Br were optimized as shown in (Figure 4). The possible structures of dithizone and dithizone derivatives were confirmed by the minimum energy conformations. Therefore, the lowest energy was demonstrated the stability of the structure.

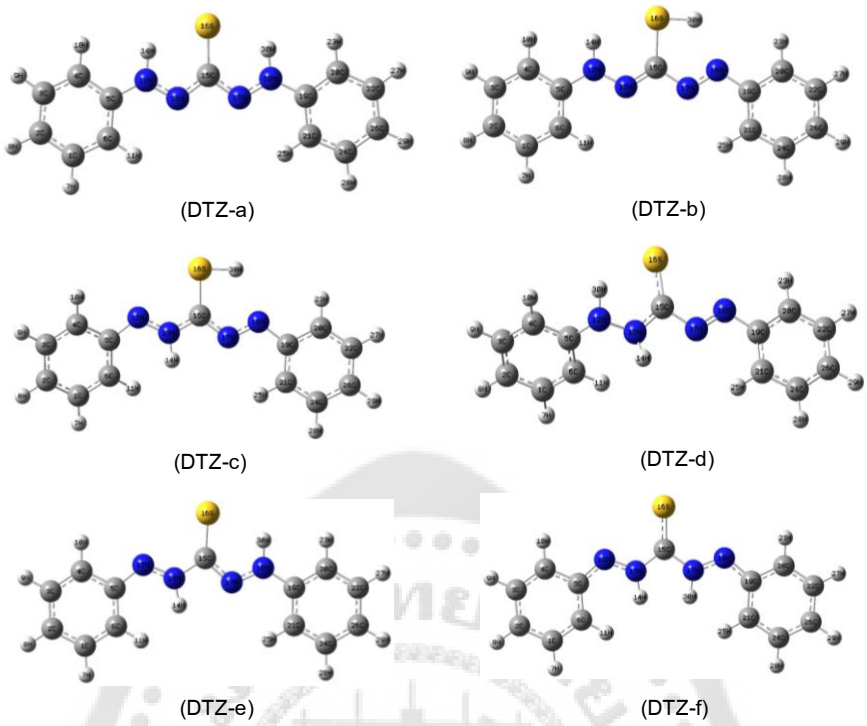

FIGURE 2 Optimized molecular structures of dithizone.

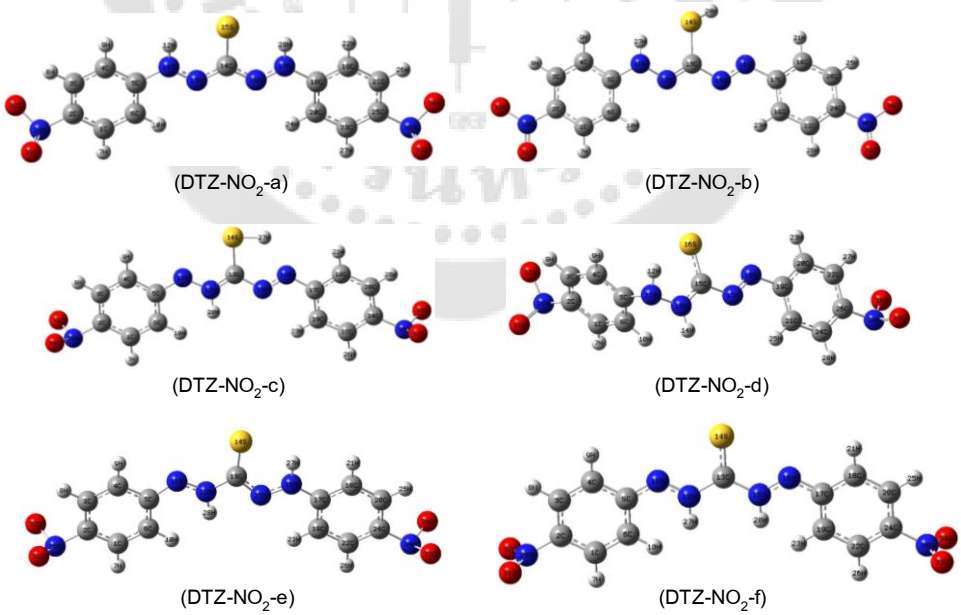

FIGURE 3 Optimized molecular structures of dithizone derivative with nitro group.

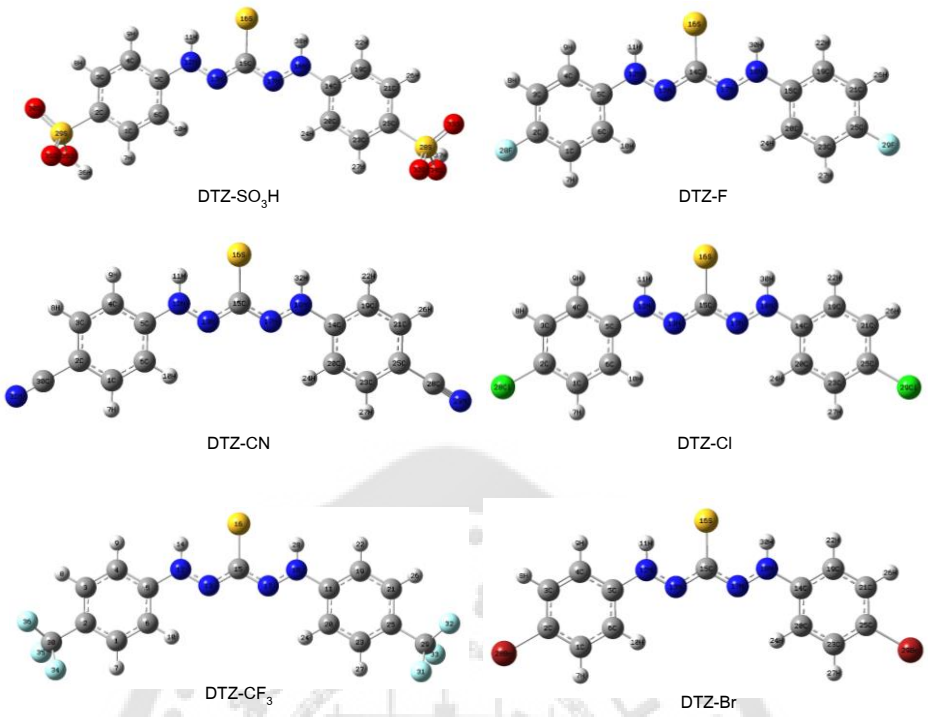

FIGURE 4 Optimized molecular structures of dithizone derivative with electron-withdrawing group; -SO_3H, -CN, -CF_3, -F, -Cl, and -Br.

5.3 The interaction of complexes

The interactions between the Ag ion and AgNPs react with dithizone and dithizone derivative with electron-withdrawing group; -NO_2, -SO_3H, -CN, -CF_3, -F, -Cl, and -Br complexes were studied using the B3LYP/6-31G(d,p) level of calculation on the three different initial location of silver such as between N12 and S16 atom (location 1) or between N18 and S16 atom on the side of dithizone molecule (location 2) or between N13 and N17 atom below of dithizone molecule (location 3) as shown in (Figure 5). Then, a comparison between locations I, II and III of silver with possible structures of dithizone and dithizone derivatives are studied. The interactions between silver and dithizone derivatives were calculated of binding energies by the minimum energy of complex depend on the location of silver. Finally, the binding energy between silver and dithizone derivatives were evaluated the stability of the complex.

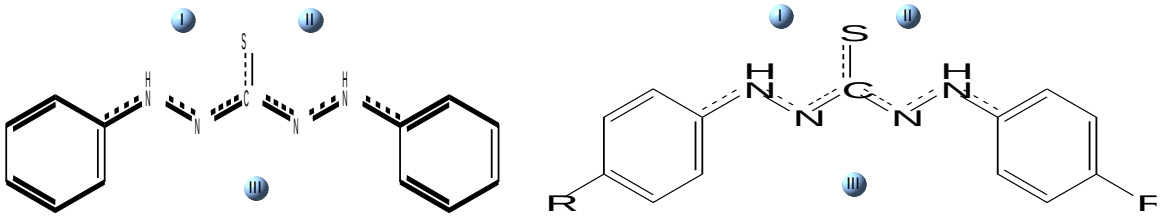

FIGURE 5 The interaction of Ag ion and AgNPs with dithizone and dithizone derivative with electron-withdrawing group; -NO_2, -SO_3H, -CN, -CF_3, -F, -Cl and -Br complexes.

5.4 Spectroscopy studies of experimental section and theoretical calculations

For the experimental details, The UV-Vis spectra of dithizone and silver-dithizone complex were recorded by a Shimadzu UV-2401PC UV-Vis spectrophotometer in the wavelength range of 400-800 nm. In the case of FT-IR spectrum, the silver-dithizone complex was prepared by 10 mg of dithizone was dissolved in DMSO solvent and 6.63 mg of $AgNO_3$ was dissolved in DI water. Then, both solutions were mixed and stirred at room temperature for 72 h. A black precipitate of the product was filtered and washed with DI water follow by washing with a little of cool methanol and ethanol solvent. Finally, the product was dried at room temperature and the silver-dithizone complex was recorded on Perkin Elmer FT-IR spectrum BX spectrometer by using potassium bromide (KBr) disc. The experiment of ^{1}H NMR was prepared by the 10 mg of dithizone was dissolved in DMSO-d_6 solvent, and silver-dithizone complex was obtained by adding silver nitrate ($AgNO_3$) (6.63 mg) to dithizone (10 mg) and dissolved in DMSO-d_6 solvent. Then, the dithizone ligand and silver-dithizone complexes were recorded on a Bruker AVANCE 300 NMR spectrometer. Theoretical calculations, the UV–Vis spectra of dithizone and silver-dithizone complex was investigated by using TD-DFT calculations with B3LYP/6-31G(d,p) method. Moreover, The calculated FT-IR vibration frequencies of dithizone and silver-dithizone complex were obtained with B3LYP/6-31G(d,p) basis sets. Moreover, the spectrum of ^{1}H NMR theoretical determination with the use of computer simulations were investigated by the B3LYP/6-311+G(2d,p) method.

The conceptual framework of this research is shown in the figure below.

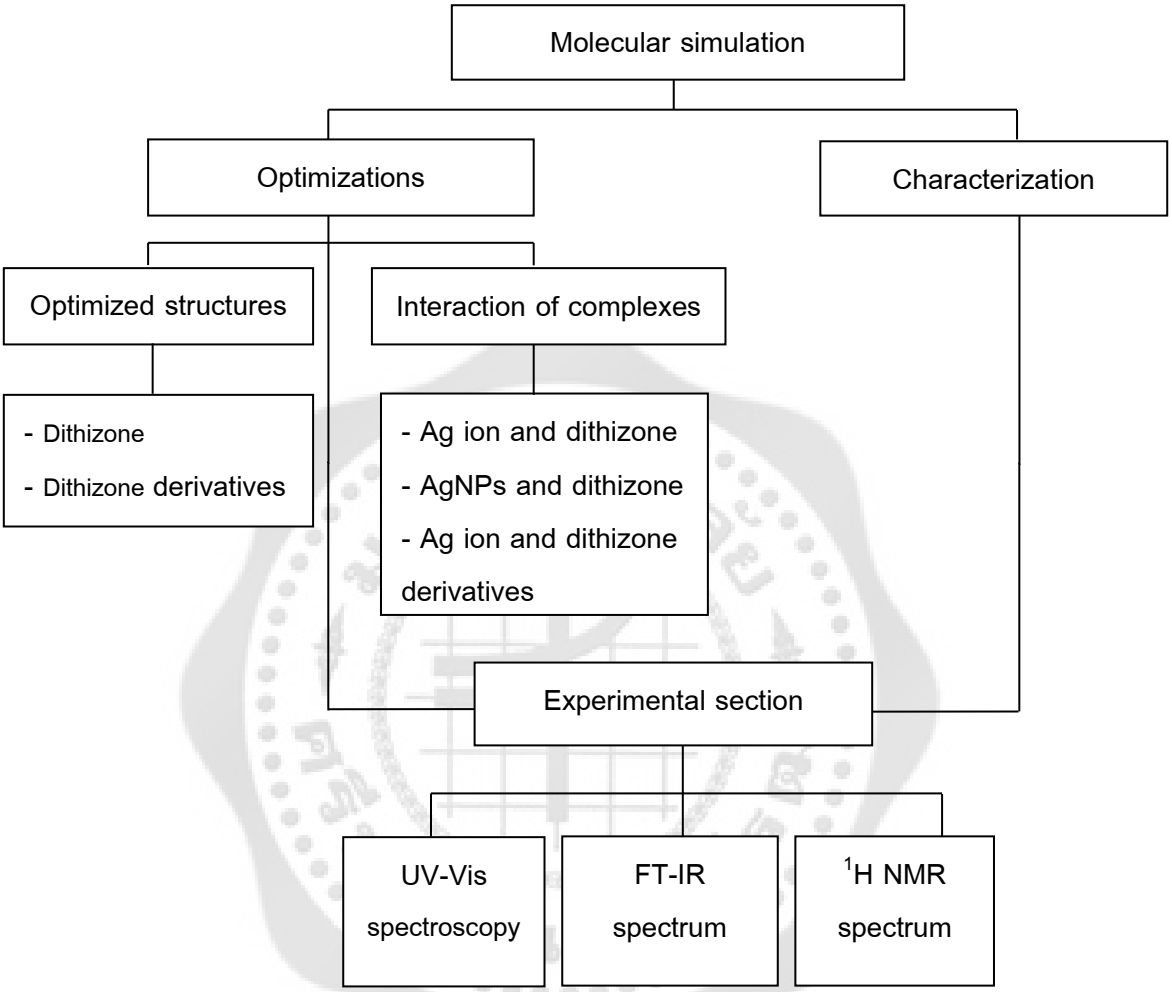

FIGURE 6 The proposed procedure of interaction between Ag ion and AgNPs with dithizone and dithizone derivatives and spectroscopy studies.

6. Optimization of assay conditions

6.1 Solubility of dithizone

A 50 mg of dithizone was prepared by dissolving with 100 mL of various organic solvents ethanol, methanol, hexane, acetone, acetonitrile and dimethyl sulfoxide. The dithizone solution was investigated by using UV-Vis spectrophotometry.

6.2 Characterization of dithizone, Ag ion and AgNPs

The characterization of Ag ion was dissolved in DI water and AgNPs with particle diameters of 20 and 100 nm were diluted with DI water. While, the dithizone was dissolved in ethanol, acetonitrile and dimethyl sulfoxide. All of the solutions were measured by UV-Vis spectroscopic studies. The spectra were recorded on a UV visible spectrophotometer from 200 to 800 nm. The resulting in the wavelength of maximum absorption of 20 and 100 nm AgNPs is shown at 406 and 492.5 nm, respectively.

6.3 Effect of pH

The pH condition for colorimetric detection of AgNPs was optimized. Then, the investigation consisted of 20 and 100 nm AgNPs stock solution at the concentration of 0.2 mg/L with a series of spectrophometric that covered at pH 2, 4, 6, 8 and 10. The pH of the sample was adjusted by using 0.1 M HNO_3 or 0.1 M NaOH and the solution was allowed to equilibrate by adding the final volume with DI water. All measurements were made in the absorbance mode.

6.4 Selectivity

The selectivity of dithizone and dithizone derivative for AgNPs was evaluated by testing other metal ions, Na^+, K^+, Ba^{2+}, Ca^{2+}, Al^{3+}, Cu^{2+}, Mg^{2+}, Mn^{2+}, Fe^{2+}, Co^{2+}, Ni^{2+}, Cr^{2+}, Ag^+, Zn^{2+}, Cd^{2+}, Hg^{2+}, Pb^{2+} and AgNPs with the particle size of 20 and 100 nm were tested by colorimetric analysis. Initially, the selectivity of the ligand in the sensing of the metal ions was tested by adding 2 mL of ligand to a mixture solution containing 2 mL of each metal ion. All of the experiments were prepared at room temperature. After the additions of ligand, other metal ions were monitored color change of the solution to the naked eyes. Meanwhile, the different color changes of solution were compared to the other metal ions.

6.5 Detection limit of dithizone, Ag ion and AgNPs

The limit of detection for dithizone, Ag ion and AgNPs were estimated in different concentrations. The interactions between of Ag ion and AgNPs with dithizone were observed the color change. This method was investigated the selectivity of dithizone for minimum amount measurement of Ag ion and AgNPs in aqueous solution.

7. Applications

7.1 Paper based sample

7.1.1 Preparation of the paper based devices

Cast coat paper (2.5 x 10 cm^2) will be cut into a sphere with a diameter of 12 mm. Then, peel sticker paper on top and the Whatman filter paper, putting in the middle, which covered by a sticker paper on the top. Finally, the Whatman filter paper (No. 42) was created into the channel or holes with a diameter of 12 mm pattern of paper based devices as shown in (Figure 7).

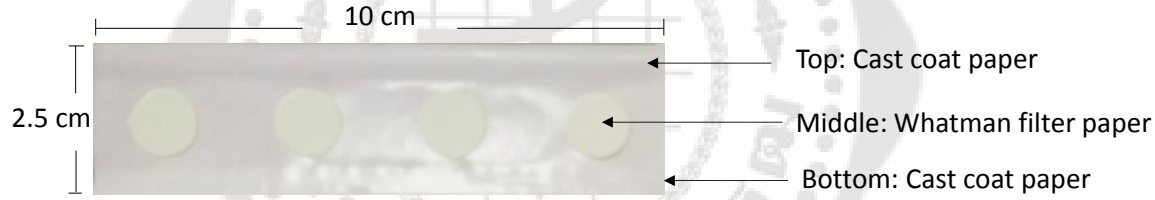

FIGURE 7 Design of the paper based device.

7.1.2 Colorimetric measurements

To indicate a convenient and easy-to-use paper based for the detection of AgNPs in aqueous media, the interactions between AgNPs and the paper based will be investigated. Meanwhile, the optimal parameter for the operation of the paper based were determined, including the effect of concentration, effect of reaction time and the detection limit of dithizone and AgNPs on the paper based.

7.1.3 Effect of concentration in paper based

The dithizone solution was diluted from stock dithizone solution with different concentration (40 mg/L, 60 mg/L, 80 mg/L and 100 mg/L). The dithizone solution was maintained at room temperature. The dithizone solution was dropped into the loading

zone of the paper based in various concentrations. After a 5 µL of Ag ion and AgNPs in each concentration was added onto the paper based, resulting in the color change visual by naked eyes.

7.1.4 Effect on reaction time in paper based

In order to consider the effect of time on the colorimetric response of the paper based. The paper based was investigated that a 80 mg/L dithizone solution was prepared and 5 µL of this solution was dropped into the loading zone of paper based. After a 5 µL of Ag ion in each concentration was added onto the paper based, resulting in the color change visual by naked eyes. The response time of the system was monitored.

7.1.5 Detection limit of Ag ion and AgNPs in paper based

The sensitivity of the paper based was investigated for different dithizone, Ag ion and AgNPs concentrations in aqueous solutions. The color intensity of the paper based with a visual detection limit of them.

7.1.6 Analysis of AgNPs in aqueous samples of the paper based

Aqueous samples of commercial, personal care nanoproducts containing silver nano were obtained by purchasing at department stores. Before analysis, samples were prepared by filtrated through a whatman filter paper. Then, at 5 µL of the solution was dropped on the paper based and dried at room temperature, resulting in the color change visual by naked eyes.

7.2 Cream based sample

7.2.1 Analysis of spiked AgNPs powder in cream based

About 20 g of the cream based was accurately weighed into a beaker and homogeneously mixed with silver nanoparticles (2 mg) for 20 minutes. The mixture sample was diluted to four concentrations (12.5 mg/L, 25 mg/L, 50 mg/L and 100 mg/L). The 0.4 g of each sample was added with 50 µL of dithizone solution (80 mg/L). The color of sample change was observed by naked-eyes. The response time of the system and the detection limit of AgNPs was investigated.

7.2.2 Analysis of the spiked AgNPs solution in cream based

Cream base 0.4 g was added 50 µL of dithizone solution in a concentration of 80 mg/L. While, the AgNPs solutions in various concentrations of 0.4 mg/L, 0.6 mg/L, 0.8 mg/L, 1.25 mg/L, 2.5 mg/L, 5 mg/L and 10 mg/L were prepared. Then, cream based was added in different concentration of AgNPs solution. After the addition a 50 µL of dithizone solution (80 mg/L), the color change was observed visual by naked eyes was shown the response time of the system and the detection limit of AgNPs was investigated.

7.2.3 Analysis of AgNPs in cream sample

The cream sample of commercial, personal care nanoproducts was purchased from department stores. Cream sample was carried out for detection of AgNPs by using dithizone.

7.3 Aqueous samples

7.3.1 Analytical performance of dithizone-based sensing for AgNPs in aqueous sample

7.3.1.1 Calibration curve

Standard AgNPs solutions were prepared by dissolving the known amount of silver in water. The dithizone solution was used to detect the AgNPs in standard AgNPs solution and the calibration curve was plotted between absorbance ratios ($A_{477\ nm}/A_{604\ nm}$) against the AgNPs concentration.

7.3.1.2 Analysis of AgNPs in aqueous sample

Aqueous samples of commercial, personal care nanoproducts containing silver nano were obtained from department stores. In this work, aqueous sample was carried out to detect the amount of silver which aqueous sample that claimed on their labels to contain ‘‘Nano-silver”. Aqueous sample was prepared by filtrating through a whatman filter paper before subjected to further analysis.

The conceptual framework of this research is shown in the figure below.

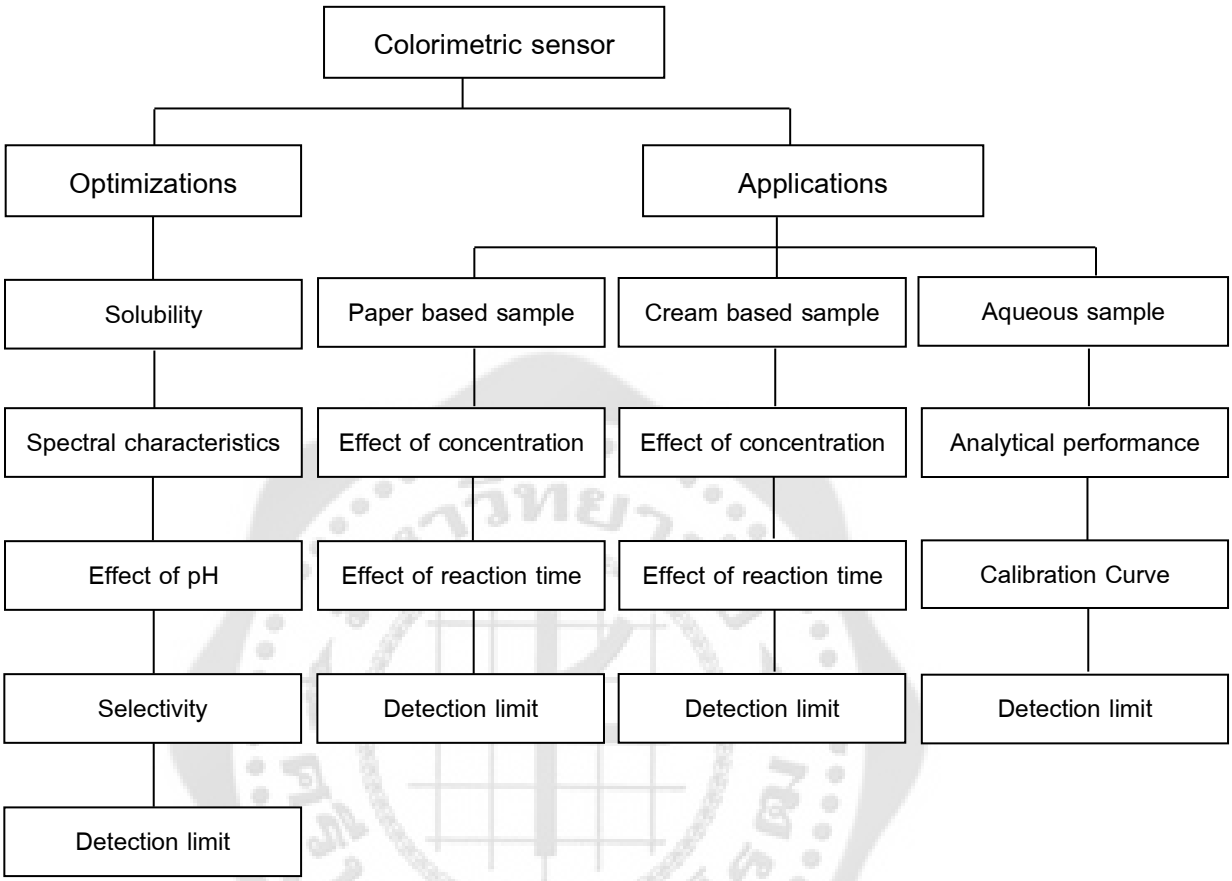

FIGURE 8 The proposed method of determination of Ag ion and AgNPs by dithizone.

8. Stability constant (K) and Characterization

8.1 UV-Vis titration of dithizone with Ag ion and AgNPs

All titration experiments were carried out at room temperature and monitored by UV-Vis spectroscopy. Meanwhile, the mentioned 3 mL solution of solvent was transferred into both sample and reference quartz cuvette after a spectrophotometric baseline was recorded in the ranging from 200-800 nm. Then, a solution of dithizone was added to the sample cuvette while an equal volume of solvent was added to the reference cuvette before recording the absorption spectra obtained in the titrations. Next, AgNPs solution was transferred to the dithizone solution and the dithizone derivative solution to prepare AgNPs complex. After mixing them for a few minutes, UV-Vis spectra was recorded. Finally, the absorbance spectra changes of AgNPs complex upon addition of AgNPs were shown. The additions of different concentration of Ag ion and AgNPs to dithizone ligand were investigated, which a new absorption band was appeared related to the complex formation of dithizone with Ag ion and AgNPs, respectively. The formation constant of the complexes was considered from Benesi and Hildebrand equation (Benesi; & Hildebrand. 1949; 2703-2707 and Tayade; et al. 2014: 19-26). The corresponding stability constant can be defined by equation 2.

$$\frac{1}{A - A_0} = \frac{1}{(\varepsilon_{ML} - \varepsilon_L)} + \frac{1}{(\varepsilon_{ML} - \varepsilon_L)\ K[M_0]}$$

Equation 2.

Where, $[M_o]$ is the silver concentration; A_o and A are absorbance of the free dithizone ligand solutions and the corresponding silver-dithizone complexes, at a given wavelength; ε_L and ε_{ML} are the molar extinction coefficients of the dithizone ligands and silver-dithizone complexes, respectively and K is the stability constant of silver-dithizone complexes From Equation. (2), plot of $x = 1/[M_0]$ versus $y = 1/A\text{-}A_0$ gives a *y*-intercept = $1/ (\varepsilon_{ML}\text{-} \varepsilon_L)$ and slope = $1/(K(\varepsilon_{ML}\text{-} \varepsilon_L))$ which gives the value of K. The results of stability constant were calculated from the plots of $1/[M_0]$ versus $1/A\text{-}A_0$ by using SigmaPlot software program (Systat Software, San Jose, CA).

8.2 Characterization of AgNPs-dithizone complex

A 30 µL of this suspension was dropped on lacey carbon-coated copper grids and dried overnight in a desiccator. The morphology of the AgNPs-dithizone complex was investigated by transmission electron microscopy.

The conceptual framework of this research is shown in the figure below.

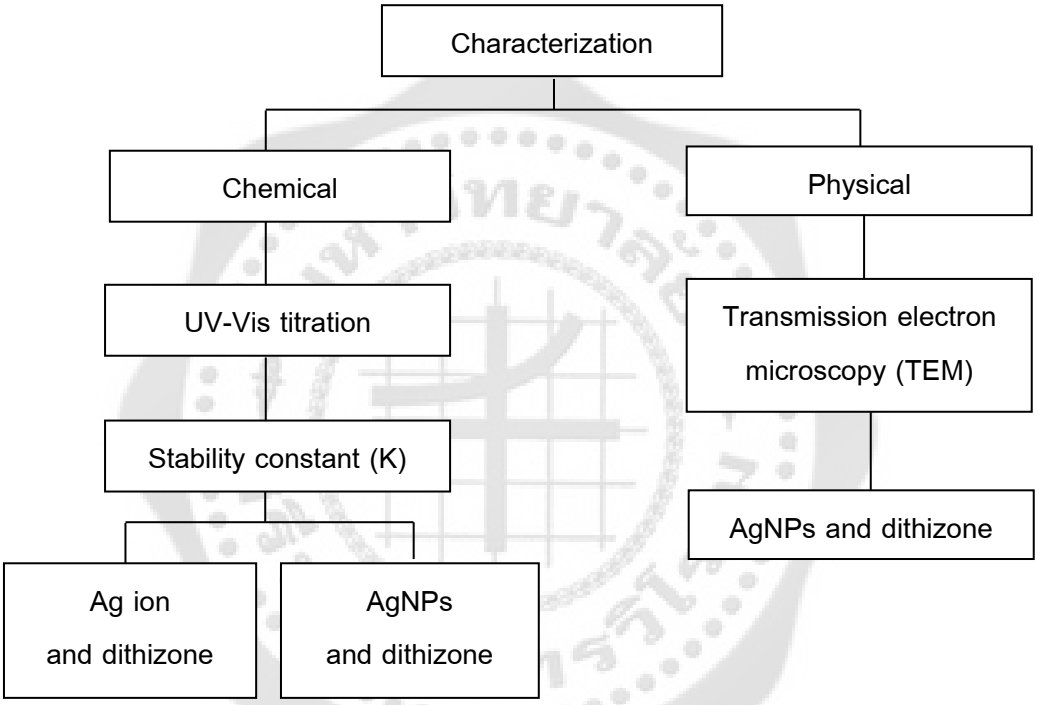

FIGURE 9 The proposed method of determination of stability constant of Ag ion and AgNPs with dithizone and characterization of AgNPs-dithizone complex.

CHAPTER 4

RESULTS AND DISCUSSION

1. Optimized structure of dithizone and dithizone derivatives

1.1 Optimized structure of dithizone

The optimized six possible structures of dithizone are shown in (Figure 10) obtained at B3LYP/6-31G(d), B3LYP/6-31G(d,p), B3LYP/6-31+G(d), B3LYP/6-31+G(d,p), B3LYP/6-31++G(d,p), B3LYP/6-311G(d,p), B3LYP/6-311+G(d,p) and B3LYP/ 6-311++G(d,p) level of calculations. The lowest energy was demonstrated in the case of isomer DTZ-a showing that the symmetrical DTZ-a isomer is more stable than isomers DTZ-b, DTZ-d, DTZ-e, DTZ-c and DTZ-f, respectively. The proton transfer on the sulfur and nitrogen atoms in the molecule can be the reason of the structural differences. In addition, the interaction between Ag ion and dithizone which can cause the loss of one proton of the symmetrical structure of dithizone as a dithizone anion. All three optimized possible structures of dithizone anion were confirmed by the minimum energy conformations as shown in (Figure 11). The results of geometry optimization indicate that the DTZ-g-anion is more stable than DTZ-i-anion and DTZ-h-anion, respectively. The comparison between the structures of the DTZ-a and DTZ-anion showed that DTZ-a is more stable than DTZ-anion isomer because of the symmetrical structure of the DTZ-a with twelve protons while the unsymmetrical structure of the DTZ-anion resulting from the loss of one proton which can cause interaction with Ag ion.

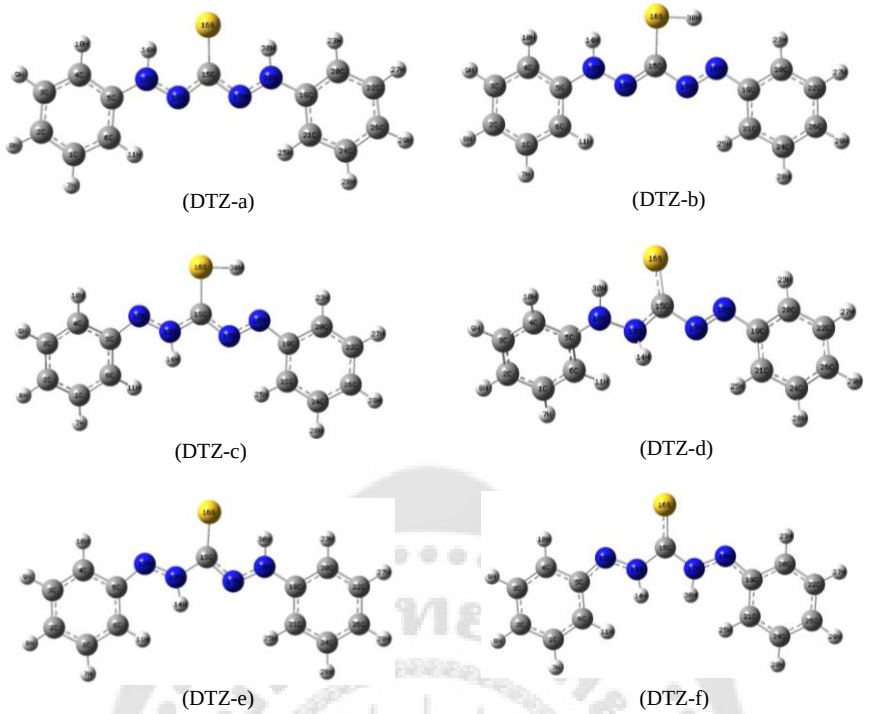

FIGURE 10 Optimized molecular structures of dithizone.

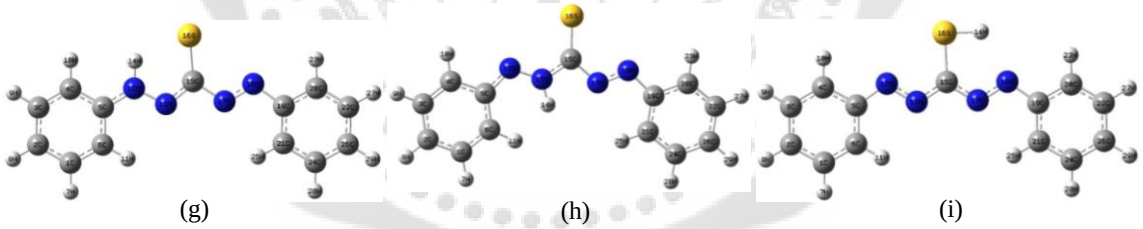

FIGURE 11 Structures of dithizone anion.

Compared the relative energy of isomers DTZ-a, DTZ-b, DTZ-d, DTZ-e, DTZ-c and DTZ-f with in the gas phase and DMSO solvent for eight basis sets are shown in (Table 2.) The result showed that the lowest energy of the DTZ-a isomer is more stable than DTZ-b, DTZ-d, DTZ-e, DTZ-c and DTZ-f in both gas and DMSO solvent phases. Meanwhile, the relative energy results of eight basis sets are not differences in gas phase even in a higher basis set. In case of DMSO results, they are similar to in gas phase as shown in (Figure 12). Therefore, in this work, the B3LYP/6-31G(d,p) basis set was considered in the studies for the next step.

TABLE 2 The calculated DFT relative energies of six isomers (a-f) obtained by B3LYP/6-31G(d), B3LYP/6-31G(d,p), B3LYP/6-31+G(d), B3LYP/6-31+G(d,p), B3LYP/6-31++G(d,p), B3LYP/6-311G(d,p), B3LYP/6-311+G(d,p) and B3LYP/6-311++G(d,p) calculations in gas phase and DMSO solvent.

Isomer	6-31G(d)		6-31G(d,p)		6-31+G(d)		6-31+G(d,p)		6-31++G(d,p)		6-311G(d,p)		6-311+G(d,p)		6-311++G(d,p)	
	Non solvent	DMSO	Non solvent	DMSO	Non solvent	DMSO	Non solvent	DMSO	Non solvent	DMSO	Non solvent	DMSO	Non solvent	DMSO	Non solvent	DMSO
a	0.00	0.00	0.00	0.00	0.00	0.00	0.00	0.00	0.00	0.00	0.00	0.00	0.00	0.00	0.00	0.00
b	7.02	10.43	7.20	10.53	6.31	9.30	6.34	9.30	6.34	9.30	6.60	9.74	6.01	8.86	6.00	8.85
c	19.21	22.06	19.54	22.31	18.00	20.64	18.23	20.80	18.20	20.77	18.51	21.11	18.03	20.51	18.02	20.50
d	10.89	10.99	11.55	11.12	9.70	9.86	9.89	9.95	9.87	9.93	10.28	10.32	9.47	9.59	9.45	9.57
e	13.50	9.99	13.75	10.21	13.05	9.71	13.25	9.89	13.25	9.89	13.31	9.73	13.12	9.77	13.10	9.80
f	40.86	30.46	41.41	30.88	40.11	29.54	40.41	29.83	40.35	29.79	40.69	30.15	40.08	29.73	40.05	29.72

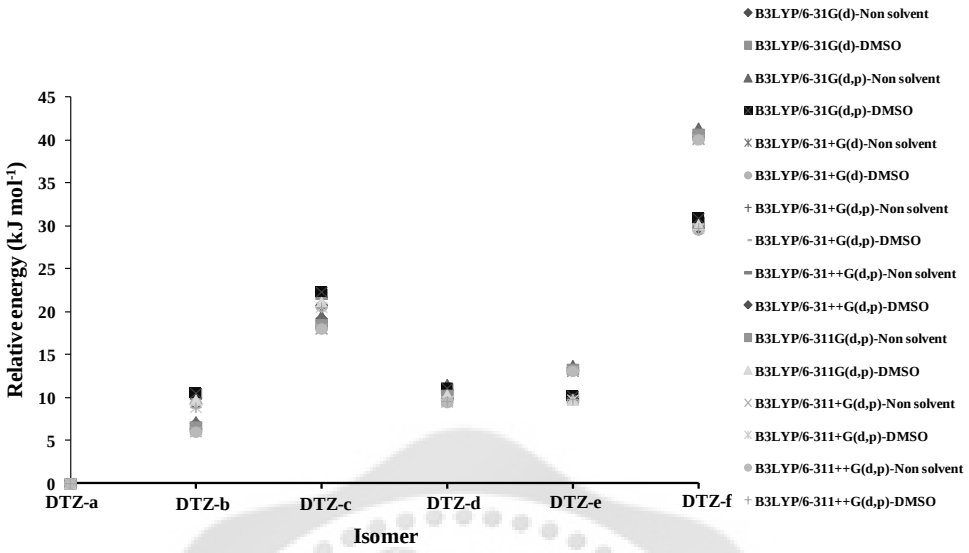

FIGURE 12 DFT calculated relative energies of six isomers (a-f) obtained by B3LYP/6-31G(d), B3LYP/6-31G(d,p), B3LYP/6-31+G(d), B3LYP/6-31+G(d,p), B3LYP/6-31++G(d,p), B3LYP/6-311G(d,p), B3LYP/6-311+G(d,p) and B3LYP/6-311++G(d,p) calculations in gas phase and DMSO solvent.

Result of the study on optimized structures of dithizone, using B3LYP/6-311G(d,p) level of calculation, showed that DTZ-reference is more stable than the other conformations of dithizone (Eschwege; et al. 2011: 14637-14646). In this study, the comparison between structures of DTZ-a and DTZ-reference were determined using different methods in which the structure of DTZ-a was optimized at B3LYP/6-31G(d,p) level of calculation while structure of DTZ-reference was obtained at B3LYP/6-311G(d,p) level of calculation. The results showed that the structure of DTZ-a and DTZ-reference are similar which both structures are symmetrical and having conjugated systems. The results of calculated bond length for optimized structures at B3LYP method using 6-311G(d,p) and 6-31G(d,p) basis sets are presented in (Table 3). It was found that the bond lengths obtained from B3LYP/6-31G(d,p) level of calculations are similar to B3LYP/6-311G (d,p) level of calculation. Although B3LYP/6-311G(d,p) level of calculation has improved accuracy but the equal of standard deviation (SD) in both calculations were found in good agreement. Therefore, in this study, the B3LYP/6-31G(d,p) level of calculation was selected for further calculation.

TABLE 3 Comparison of B3LYP/6-311G(d,p) and B3LYP/6-31G(d,p) level of calculation bond length, including standard deviation (SD) of differences between these values.

Bond lengths (Å)	Expt.	B3LYP	
		6-311G(d,p)	6-31G(d,p)
		Calc.	Calc.
C15-S16	1.712	1.728	1.728
N13-C15	1.344	1.356	1.359
N12-N13	1.299	1.290	1.295
C5-N12	1.380	1.400	1.399
SD[a]		0.017	0.017

[a] Standard deviation (SD) = $[\Sigma(X_{Cal.} \_ X_{Expt.})^2/n -1]^{1/2}$.

The optimized bond lengths and bond angles for the six possible structures of dithizone are shown in (Table 4). The C15–S16, N13–C15, N12–N13 and C5–N12 bond length of the dithizone in the range of 1.652–1.797 Å, 1.300–1.394 Å, 1.282–1.382 Å and 1.378–1.400 Å , respectively. The bond angle of N13–C15–S16, N12–N13–C15 and C5–N12–N13 were observed in the range of 119.31°–126.34°, 114.00°–124.54° and 115.99°–123.09°, respectively. The bond length and bond angle variations depend on the transfer of proton in the molecules. In addition, the bond lengths and bond angles of three dithizone anion were also listed in (Table 4). The bond lengths of the C15–S16, N13–C15, N12–N13 and C5–N12 were found to be 1.686–1.813 Å , 1.333–1.368 Å , 1.298–1.322 Å and 1.370–1.398 Å , respectively. The bond angles of N13–C15–S16, N12–N13–C15 and C5–N12–N13 were in the range of 120.63°–125.92°, 113.55°–126.49° and 113.61°–122.33°, respectively. The bond distances and bond angles of three dithizone anion were different due to the position of proton in the molecules. Therefore, this bond distance can be used as a principle of the strength of interaction between dithizone anion and Ag ion. The structures of DTZ-b, DTZ-c and DTZ-i-anion representing to the hydrogen bond to sulfur in molecule lead to the similar bond angle C15–S16–H30 of three structures. While, the C15–S16–H30bond angle of three structures of DTZ-b, DTZ-c and DTZ-i-anion were investigated that found to be 89.26°, 89.44° and 89.46° as shown in (Table 4). Meanwhile, the structure of DTZ-i-anion can interact in three locations of Ag ion showing complex (1i),

complex (2i) and complex (3i) that cause the bond angle of C15–S16–H14 in the ranges of 93.03°, 92.63°, 91.53°as shown in (Table 5). The result shows that the bond angle of complex (1i) is larger than that of complex (2i) and complex (3i) due to the Ag ion (location 1) interacts with sulfur atom of molecule. In the case of complex (2i) having the Ag ion in location 2, the complex was interacted with hydrogen atom pushing of atom in molecule. The complex (3i) has the smallest bond angle because the Ag ion in location 3 bonded to N13 and N17 atoms in below of molecule causing the bond angle are narrow.

TABLE 4 The optimized structure of dithizone (DTZ-a-DTZ-f) and dithizone anion (DTZ-g-DTZ-i) for bond lengths (Å) and bond angles (deg) obtained by B3LYP/6-31G(d,p) calculations.

Parameters	Structure								
	DTZ-a	DTZ-b	DTZ-c	DTZ-d	DTZ-e	DTZ-f	DTZ-g	DTZ-h	DTZ-i
Bond Lengths (Å)									
C15-S16	1.728	1.797	1.756	1.664	1.687	1.652	1.735	1.686	1.813
N13-C15	1.359	1.300	1.342	1.353	1.394	1.392	1.333	1.368	1.342
N12-N13	1.295	1.324	1.305	1.382	1.282	1.302	1.343	1.322	1.298
C5-N12	1.399	1.400	1.389	1.418	1.388	1.378	1.372	1.370	1.398
Bond Angels (deg)									
N13-C15-S16	125.78	124.34	119.31	124.29	125.89	126.34	125.70	125.92	120.63
N12-N13-C15	114.00	119.32	124.54	122.48	124.54	122.82	113.55	126.49	115.66
C5-N12-N13	123.09	121.70	115.99	117.72	118.04	117.62	122.33	115.75	113.61
C15-S16-H13	-	89.26	89.44	-	-	-	-	-	89.46

TABLE 5 Selected bond distances (Å) angle (deg) and binding energy (Kcal mol^{-1}) of the silver-dithizone complex calculated at the B3LYP/6-31G(d,p) level of calculation.

Parameters	Complexes								
	1g	2g	3g	1h	2h	3h	1i	2i	3i
Bond lenght (Å)									
S16-Ag30	2.489	2.504	4.561	2.515	2.511	4.980	2.608	2.691	4.577
C15-S16	1.771	1.775	1.690	1.723	1.735	1.662	1.833	1.855	1.766
Bond angle (deg)									
N13-C15-S16	126.66	122.34	126.75	127.14	119.95	125.46	124.10	118.13	122.83
S16-C15-N17	122.80	128.86	127.76	125.69	132.99	129.36	118.52	124.15	124.74
N13-C15-N17	110.54	108.80	105.49	107.16	107.05	105.08	117.36	117.69	112.42
C15-S16-H14	-	-	-	-	-	-	93.03	92.63	91.53
Binding energy (Kcal mol^{-1})	-149.12	-167.31	-148.80	-167.54	-168.71	-134.18	-149.10	-144.37	-150.06

4.6.2.2 Optimized structures of dithizone derivatives

The optimized structure of dithizone derivative with electron-withdrawing group; $-NO_2$, $-SO_3H$, -CN, $-CF_3$, -F, -Cl, and -Br were compared with the dithizone structure. The method was carried out to investigate the dithizone derivatives being similar to study on the dithizone. The result shows that the structure of dithizone derivative with the nitro group (DTZ-NO_2-a) according to (Figure 13), is the most stable and similar to dithizone (DTZ-a) due to the symmetrical structure of molecules. Whereas, there are three possible structures of dithizone derivative anion (DTZ-NO_2-M, DTZ-NO_2-N and DTZ-NO_2-O) were optimized as shown in (Figure 14) which the dithizone derivative anion are lose of one proton in molecule due to their interaction with Ag ion. The results show that a geometry optimization structure of dithizone derivative anion (DTZ-NO_2-O) is more stable than DTZ-NO_2-N and DTZ-NO_2-M, respectively.

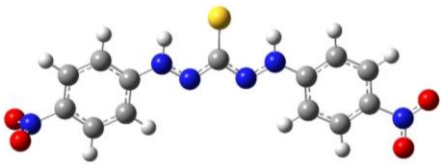

(DTZ-NO_2-a)

FIGURE 13 The structure of dithizone derivative with the nitro group (DTZ-NO_2-a).

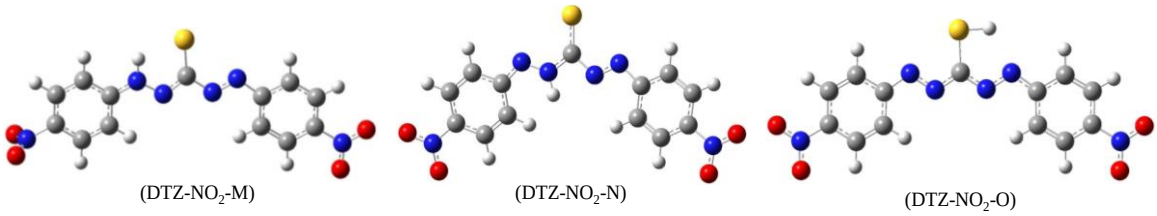

FIGURE 14 Structures of dithizone derivative anion with the nitro group.

Moreover, structures of dithizone derivative anion with electron-withdrawing group; $-SO_3H$, -CN, $-CF_3$, -F, -Cl and -Br were optimized as shown in (Figure 15) which each structure of the dithizone derivative anion corresponding to the interaction of Ag ion (location 2) between N18 and S16 atom on the side of the dithizone derivative molecule. The final geometries were confirmed as minima of the energy in conformation. The result show that geometry optimization structure of the dithizone derivative anion (DTZ-Br) is more stable than dithizone derivative anion (DTZ-SO_3H), (DTZ-Cl), (DTZ-CF_3), (DTZ-F) and (DTZ-CN), respectively.

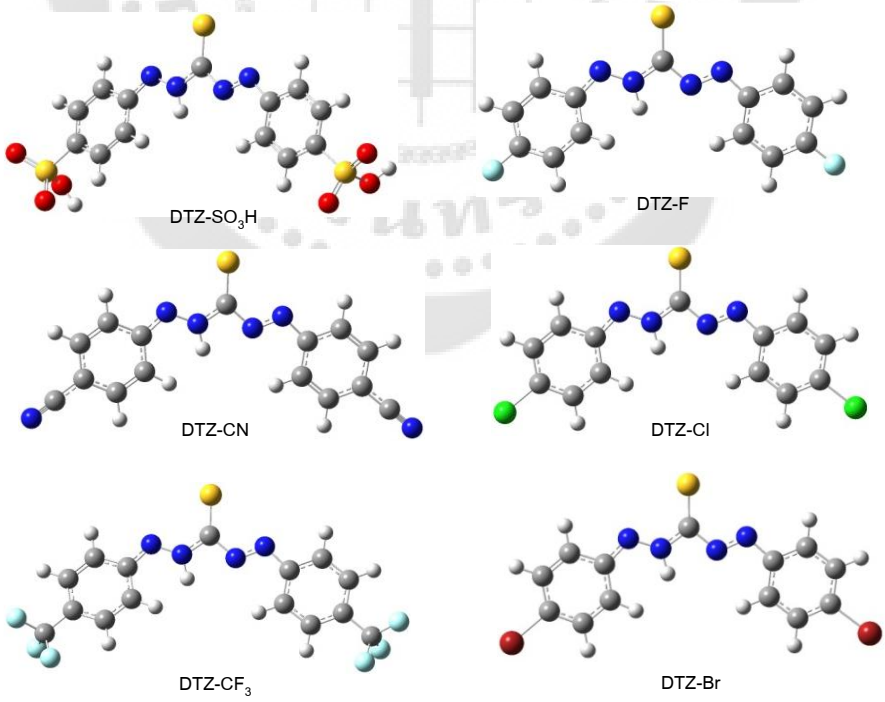

FIGURE 15 Optimized molecular structures of dithizone derivative anion with electron-withdrawing group; $-SO_3H$, -CN, $-CF_3$, -F, -Cl and -Br.

2. The interaction of complexes

2.1 The interaction between Ag ion and dithizone

Ag ion has drawn considerable interest in the interaction with various ligands and has been studied because of its antibacterial property. Previously, the interaction of Ag ion with Buckyball (C_{60}) was reported and the complexes are associated with medical and drug delivery systems. As the result, the Ag atom is able to be adsorbed on C_{60} to generate AgC_{60} which the disulfide bond were destroyed and resulted in the prevention of HIV-1 activity (Azizi; & Sohrabinia. 2012: 354-359). Moreover, interaction between N-acetyl-L-cysteine and Ag ion was reported to occur through sulfur atom. This silver complex showed the high cytotoxic activity at a concentration of 200 $\mu molL^{-1}$ (Abbehausen; et al. 2011: 579-583). In addition, because of its soft base property, silver can be coordinated with different ligands representing to the soft base ligands containing unsaturated nitrogen and sulfur atoms as shown in the interaction of 2-acetylthiazole and 2-acetylpyrazine. The ion is coordinated through imine-N and four *ortho*-ring-N atoms of the two ligands (Tan; et al. 2014: 119-132). In this study, the interactions of the silver and dithizone complexes were studied using the B3LYP/6-31G(d,p) level of calculation on the three different initial location of silver ion such as between N12 and S16 atom (location 1) or between N18 and S16 atom on the side of dithizone molecule (location 2) or between N13 and N17 atom below of dithizone molecule (location 3) as shown in (Figure 16). Therefore, a comparison between locations 1, 2 and 3 of Ag ion reacts with three possible structures of dithizone anion (DTZ-g, DTZ-h and DTZ-i) in (Figure 14) with nine possible structures of Ag ion and dithizone complexes were shown in (Figure 16). The calculated values of binding energies are given in (Table 5). For the calculation on the interactions of three initial locations of Ag ion and dithizone anion (DTZ-g), the results indicate the complex (2g) is more stable than complex (1g) and complex (3g), respectively in which the interaction energy of silver and dithizone (2g) is calculated to be -167.31 kcal mol^{-1}. The results of complexes (1h, 2h, 3h) of Ag ion and dithizone (DTZ-h) showed that the energy of 2h complex was about -168.71 kcal mol^{-1} more stable than the complex (1h) and complex (3h), respectively. Finally, it was found that the binding energy of complex (3i) was estimated to be -150.06 kcal mol^{-1} being more stable than complex (1i) and complex (2i), respectively.

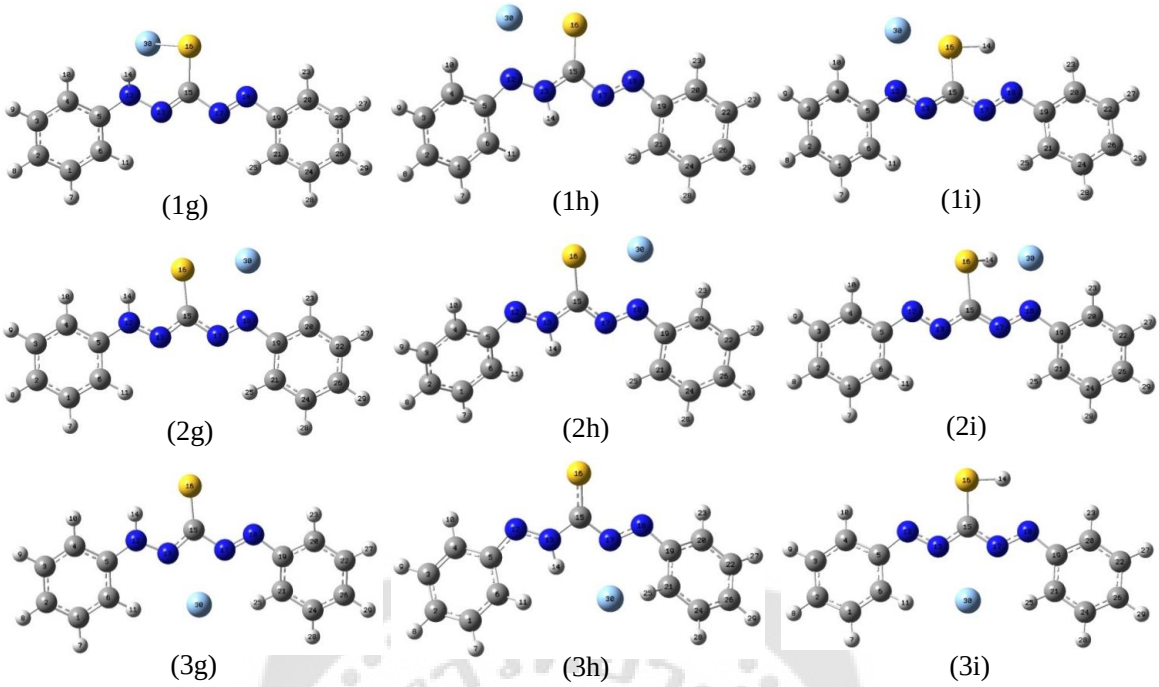

FIGURE 16 The interaction of silver-dithizone complexes.

In addition, the comparisons between the bond lengths of the C15–S16 bond for dithizone anion (DTZ-g, DTZ-h and DTZ-i) are presented in (Table 4) and silver-dithizone complex are listed in (Table 5). The results showed that the bond lengths of the C15– S16 bond in dithizone anion (DTZ-g) were increased from 1.735 Å to 1.771 Å and 1.775 Å in complex (1g) and complex (2g), respectively. However, the bond length for complex (3g) is decreasing to be 1.690 Å. Whereas, the calculated bond lengths for C15–S16 bond of the dithizone anion (DTZ-h) was 1.686 Å and for C15–S16 bond lengths were 1.723 Å, 1.735 Å and 1.662 Å in the complex (1h), complex (2h) and complex (3h), respectively.

Moreover, the C15–S16 bond length of the dithizone (i) was observed 1.813 Å and these bond lengths for three complexes of 1i, 2i and 3i were 1.833 Å, 1.855 Å and 1.766 Å, respectively. As the above mentioned, when the locations 1 and 2 of silver atom react with three possible dithizone anion structures (DTZ-g, DTZ-h, and DTZ-i) for the complexes of 1g, 2g, 1h, 2h, 1i and 2i, the results indicated that the C15–S16 bond lengths are longer as compared with each structures of dithizone anion (DTZ-g, DTZ-h,and DTZ-i) corresponding to the interaction of Ag ion with N atom to form N=N bond and with S atom to form C=S bond. Whereas, the shorter values of the C15–S16 bonds in complex 3g, 3h and 3i as compared with each structures of dithizone (DTZ-g, DTZ-h and DTZ-i) are caused by the

location 3 of silver atom between N13 and N17 to form N=N bond but they do not interact with S atom for C=S bond. Furthermore, the results showed the increasing of the N13–C15–S16 bond angle in complexes 1g, 1h and 1i, and the increasing of the S16–C15–N17 bond angles of complex 2g, 2h and 3i compared to structure of dithizone anion (DTZ-g, DTZ-h and DTZ-i). Therefore, the increasing of bond angles depends on the location of Ag ion effect and the repulsion of Ag ion with N and S atoms. However, the values of N13–C15–N17 bond angles are decreasing in the complexes 3g, 3h and 3i because the location 3 of silver atom interact with N13 and N17 to form N=N bond and may be due to the interaction with hydrogen atom. The results showed that complex 2h is more stable than complexes 1h, 2g, 3i, 1g, 1i, 3g, 2i and 3h, respectively, having the binding energy between silver and dithizone to be -168.71 kcal mol^{-1} (Table 5). From the results, we could conclude that the ion-exchange between the hydrogen and silver atom were observed in the complex of silver-dithizone.

2.2 The interaction between AgNPs and dithizone

Previously, the studies have shown that the interaction between Ag ion and dithizone complex was found that the complex 2h was the most stable. On the other hand, all three optimized possible structures of dithizone with AgNPs were investigated as shown in (Figure 17). The structure of complex (J) is similar to complex 2h of the dithizone reacts with AgNPs. In case of the complex (K) and complex (L) were evaluated for the anion dithizone binding to three Ag^0 atom clusters (AgNPs clusters) which ‘‘stand up’’ on the surface of dithizone as a slight gradient with geometry. Comparison of the observed two different locations of AgNPs cluster in complex (K) and complex (L) according to (Figure 17). The results of geometry optimization indicate that the distance between the AgNPs and sulfur atom of the complex (J), complex (K) and complex (L) are 2.491 Å, 2.598 Å and 2.574 Å, respectively. Moreover, the results show increasing of the S16–C15–N17 bond angles of complex (J) complex (K) and complex (L) as shown in (Table 6). Meanwhile, the complex (K) and complex (L) was compared two initial locations of AgNPs clusters, the resulting show that the complex (L) is more stable than complex (J) and complex (K), respectively. The lowest binding energy of complex (L) was estimated to be -53.543 kcal mol^{-1} in (Table 6). In this study, the molecule of dithizone having lone pair electrons of sulfur was found that AgNPs clusters bonding to on the surface of dithizone by occurs via a sulfur atom. Therefore, the behavior of AgNPs clusters adsorbs to the surface of the dithizone

molecule with a slight gradient (Bae; et al. 2002: 7076-7080; Chiniforoshan; et al. 2015: 56-61).

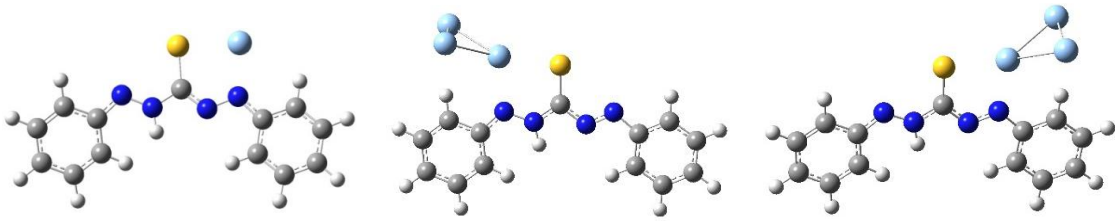

(J) (K) (L)

FIGURE 17 The interaction of AgNPs-dithizone complex.

TABLE 6 Selected bond distances (Å) angle (°) and binding energy (Kcal mol^{-1}) of the AgNPs-dithizone complex calculated at the B3LYP/6-31G(d,p) level of calculation.

Parameters	Complexes		
	J	K	L
Bond lenght (Å)			
S16-Ag30	2.491	2.598	2.574
C15-S16	1.771	1.717	1.727
Bond angle (deg)			
N13-C15-S16	117.27	125.02	121.32
S16-C15-N17	132.48	127.84	130.85
N13-C15-N17	110.24	107.14	107.84
C15-S16-H14	18.41	14.32	16.26
Binding energy(Kcal mol^{-1})	-45.67	-50.77	-53.54

Furthermore, the complex (K) and complex (L) were simulated at TD-DFT calculations with B3LYP/6-31G (d,p) level of theory in gas phase and in the DMSO solvent. For TD-DFT calculations, the complex (K) and complex (L) in the gas phase were investigated the absorption spectra which the result shows the maximum absorption spectra at 3389.77 nm and 8423.47 nm, respectively, compared with in DMSO solvent the maximum absorption band appeared at about 755.42 nm and 697.38 nm, respectively as summarized in (Table 7). In the case of study on the calculation of complex (K) and complex (L) in DMSO solvent which the result reveals the maximum absorption bands at 755.42 nm and 697.38 nm, respectively as shown in (Figure 18), (Specdis v1.64). From

the result found that in the gas phase have a higher error than in DMSO solvent depend on the polarity of solvent can cause the stability of the complex.

TABLE 7 The calculated absorption wavelength (λ, nm) of dithizone and AgNPs-dithizone complex in gas phase and DMSO solvent.

Complex	Non-solvent		Solvent	
	Excitation energy	Oscillator strength	Excitation energy	Oscillator strength
Complex (K)	3389.77	0.0564	755.42	0.3366
Complex (L)	8423.47	0.0111	697.38	0.2673

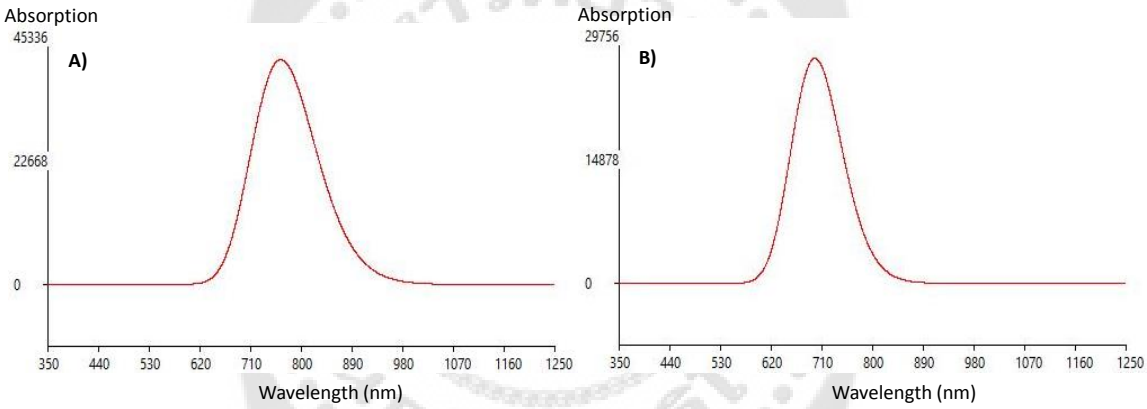

FIGURE 18 The calculated UV-Vis spectral of AgNPs-dithizone complex in DMSO solvent. A) complex (K) and B) complex (L).

4.6.3.3 The interaction between Ag ion and dithizone derivatives

Moreover, studies of the nine possible structures of interaction between Ag ion and dithizone derivative anion with the nitro group were investigated as shown in (Figure 19). The three possible locations of Ag ion react with dithizone derivative anion with the nitro group were compared. The binding energy of Ag ion with dithizone derivative with the nitro group are present in (Table 8). Therefore, the results show that the complexes (1M, 2M, 3M) of Ag ion and dithizone derivative (DTZ-NO_2-M) displayed that the energy of complex (2M) was about -160.86 kcal mol^{-1} more stable than the complex (1M) and complex (3M), respectively. The result of Ag ion and dithizone derivative (DTZ-NO_2-N)

showed that the complex (2N) to binding energy was estimated to be -147.75 kcal mol^{-1} being more stable than complex (1N) and complex (3N), respectively. Finally, the complexes (1O, 2O, 3O) of Ag ion and dithizone (DTZ-NO_2-O) were studied that the binding energy of complex (3O) was about -129.78 kcal mol^{-1} more stable than the complex (1O) and complex (3O), respectively. Although, the complex (2M) is the lowest of binding energy. However, the interaction of the complex (2h) and complex (2M), the resulting show the binding energy of complex (2h) is lower than complex (2M). Finally, the structure of complex (2h) is the most stable. After the simulation studies of silver interaction with dithizone and dithizone derivative with the nitro group were determined and all results were found.

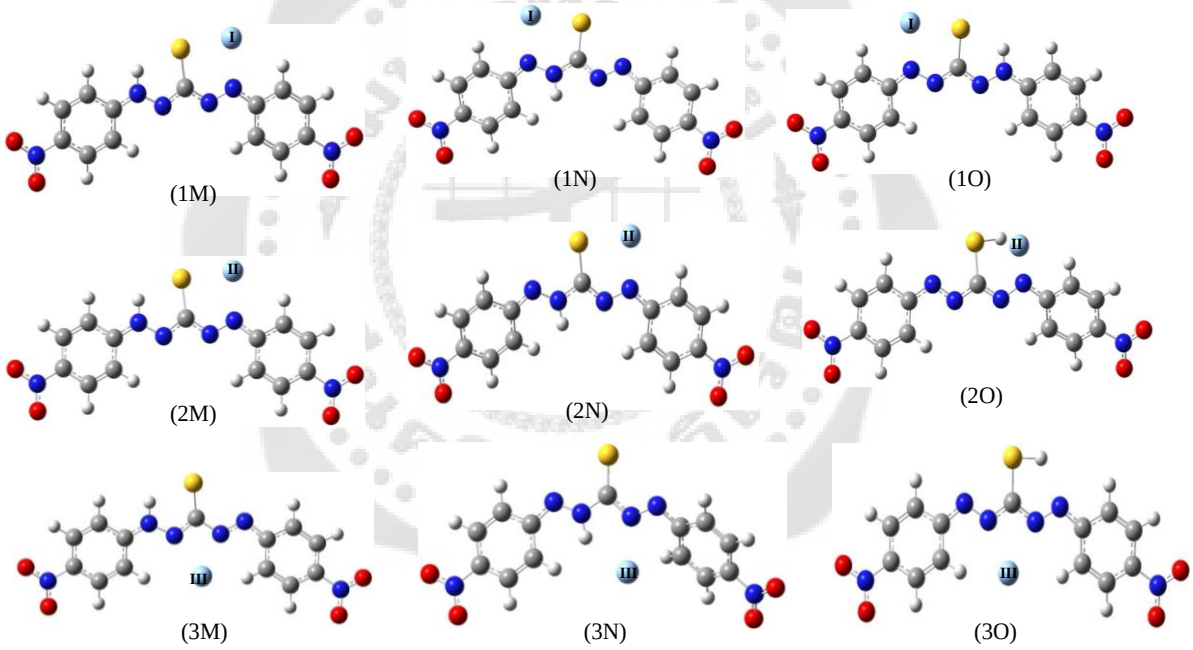

FIGURE 19 The interaction of silver-dithizone derivative with the nitro group complexes.

TABLE 8 Selected bond distances (Å) angle (deg) and binding energy (Kcal mol^{-1}) of the silver-dithizone derivative with the nitro group complexes calculated at the B3LYP/ 6-31G(d,p) level of calculation.

Parameters	Complexes								
	1M	2M	3M	1N	2N	3N	1O	2O	3O
Bond lenght (Å)									
S16-Ag30	2.475	2.507	4.568	2.526	2.521	4.976	2.613	2.687	4.582
C15-S16	1.769	1.766	1.684	1.714	1.726	1.656	1.830	1.852	1.761
Bond angle (deg)									
N13-C15-S16	126.444	122.718	127.115	127.467	120.385	125.642	123.907	118.382	122.457
S16-C15-N17	123.050	129.004	127.574	125.747	133.036	129.269	119.318	124.528	125.339
N13-C15-N17	110.506	108.278	105.311	106.786	106.579	105.024	116.773	117.067	112.203
C15-S16-H14	-	-	-	-	-	-	89.813	93.629	91.303
Binding energy (Kcal mol^{-1})	-142.48	-160.86	-142.27	-147.22	-147.75	-111.27	-129.28	-124.81	-129.78

Furthermore, the proposed structure of silver-dithizone derivative with electron-withdrawing group; -SO_3H, -CN, -CF_3, -F, -Cl and -Br complexes are reported. The DFT studies of a silver-dithizone derivative complexes, the six possible complexes were proposed the interaction of the dithizone derivatives structure with Ag ion through between N18 and S16 atom (location 2) on the side of the dithizone derivatives molecule as shown in (Figure 20). The binding energies show that the most stable form of the silver-dithizone derivative (DTZ-F) complex is -165.62 Kcal mol^{-1} as shown in (Table 9). Meanwhile, The silver-dithizone derivative (DTZ-F) complex is more stable than silver-dithizone derivative (DTZ-Cl), (DTZ-Br), (DTZ-CF_3), (DTZ-CN) and (DTZ- SO_3H) complex, respectively.

From the result of comparison the interaction between silver-dithizone complex and silver-dithizone derivative with electron-withdrawing group; -NO_2, -SO_3H, -CN, -CF_3, -F, -Cl and -Br complexes, the resulting show that the silver-dithizone complex (2h) is more stable than the other of silver-dithizone derivative complexes with the lowest of binding energy was -168.71 Kcal mol^{-1}.

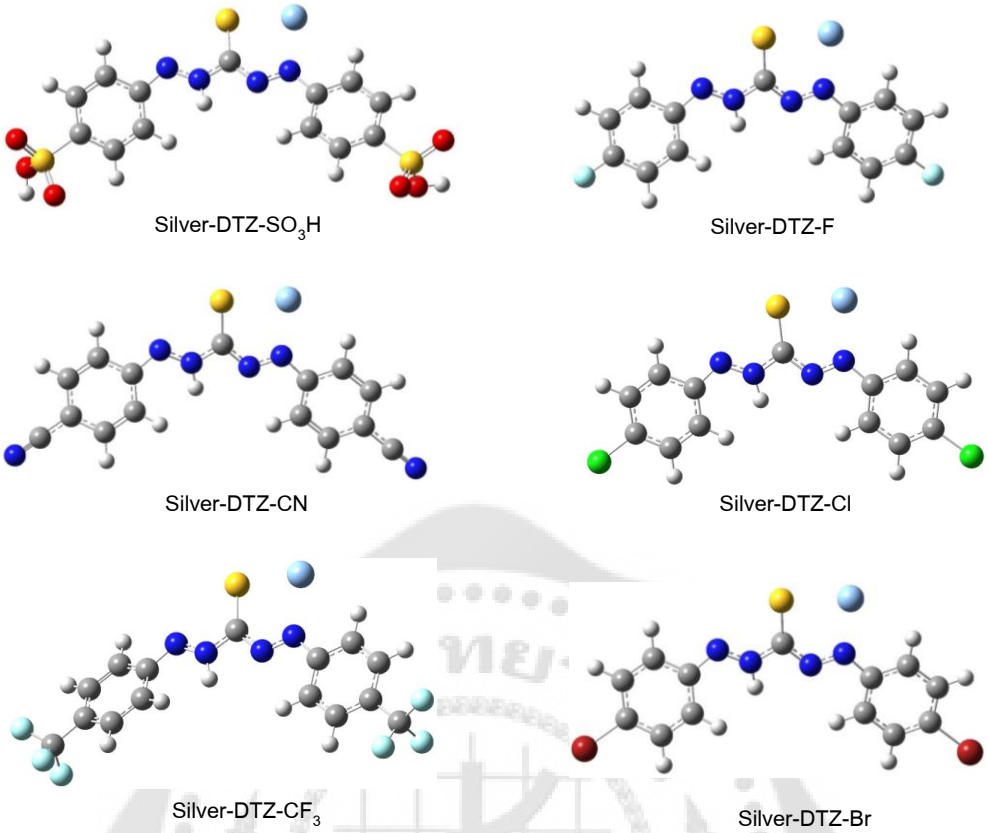

FIGURE 20 The interaction of silver-dithizone derivative with electron-withdrawing group; -SO_3H, -CN, -CF_3, -F, -Cl and -Br complexes.

TABLE 9 The binding energy (Kcal mol^{-1}) of the silver-dithizone derivative (DTZ-R = -SO_3H, -CN, -CF_3, -F, -Cl, -Br) complexes were calculated at the B3LYP/6-31G(d,p) level of calculation.

Complexes	Binding energy (BE) Kcal mol^{-1}
Silver-DTZ-SO_3H	-150.71
Silver-DTZ-CN	-152.01
Silver-DTZ-CF_3	-157.90
Silver-DTZ-F	-165.62
Silver-DTZ-Cl	-161.83
Silver-DTZ-Br	-161.70

3. Spectroscopy studies of experimental section and theoretical calculations

3.1 UV-Vis spectroscopy

3.1.1 Spectral characteristic

The characterization of dithizone in DMSO solvent was measured by UV-Vis spectroscopic studies. The spectra were recorded on a UV-Vis spectrophotometer from 400 to 800 nm. The absorbance spectrum of the dithizone is characterized by two peaks at about 455 and 620 nm, which are responsible for the green color of the solution and the absorbance spectrum at 505 nm are responsible for the silver-dithizone complex (Figure 21).

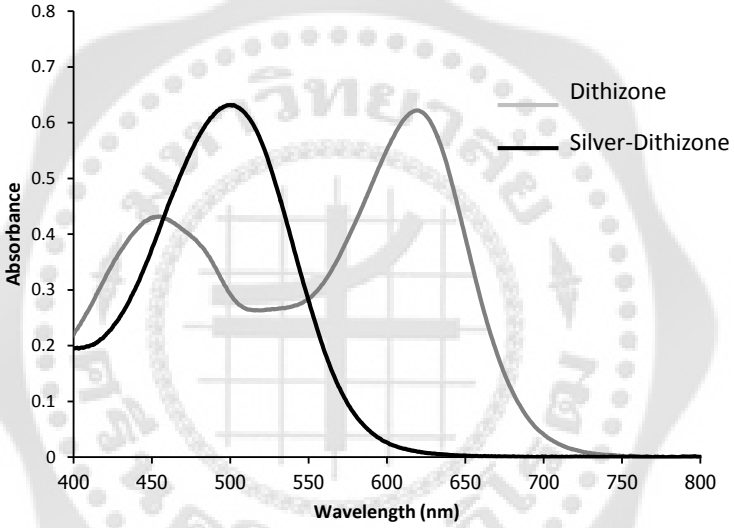

FIGURE 21 UV-Vis spectral of dithizone and silver-dithizone complex in DMSO solution.

3.1.2 UV-Vis spectroscopic study of silver-dithizone complex

The spectral characteristic of dithizone showed two peaks with the maximum absorbance at 455 and 620 nm. The red shift occurred in wavelength of maximum absorption from 455 nm to 505 nm after the addition of Ag ion. Meanwhile, the corresponding UV-Vis spectrum, the absorption at 620 nm disappeared (Figure 22) and the increase in the absorbance intensity of a new band appears at 480 nm with a significant blue-shift of the absorption maximum. Moreover, UV-Vis titration upon the addition of Ag ion was studied with the measured maximum absorbance at 620 nm corresponding to the formation of complex between Ag ion and dithizone as shown inset: (Figure 22). The sigmoidal curves were achieved by plotting the change in the absorbance intensity at 620

nm as a function of [Ag ion]. The binding of silver-dithizone complex was studied by UV-Vis titration experiments, which proposed the stoichiometric ratios in inset: (Figure 22). The results show that the sulfur atom of dithizone interacts with Ag ion in the ratio of 1:1.

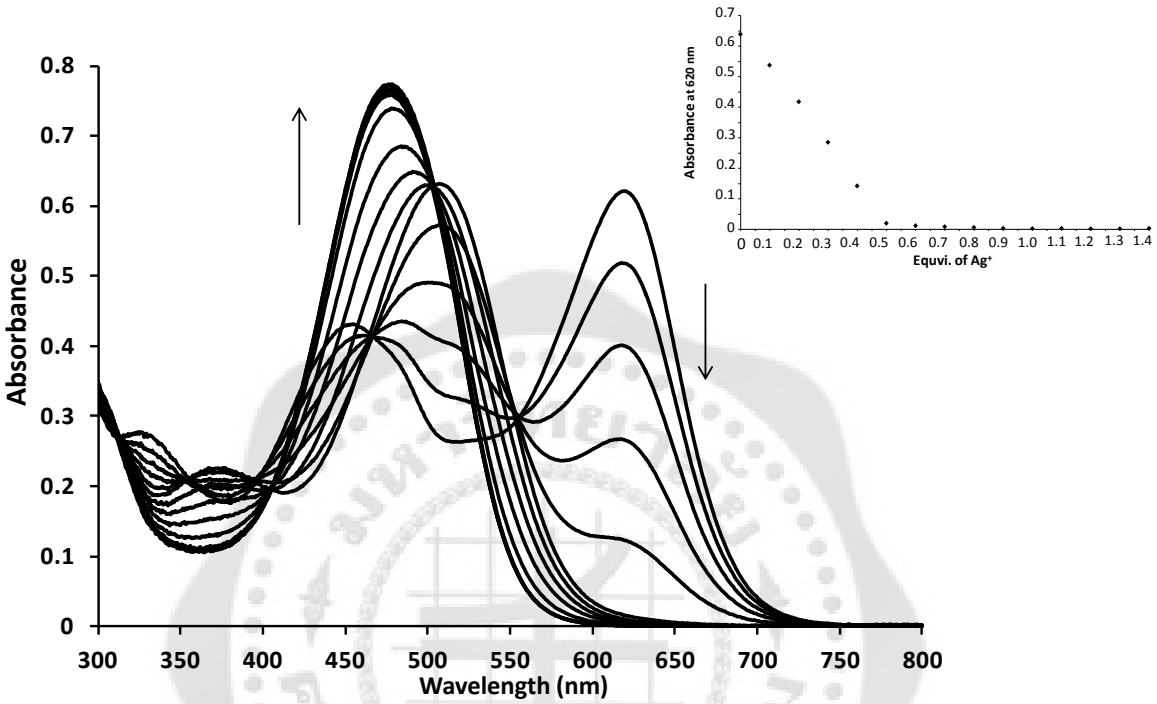

FIGURE 22 UV-Vis spectral titration of dithizone (3.9 x 10^{-4} M) in DMSO upon addition of (0 -0.28 x 10^{-3} M) Ag ion, Inset: the stoichiometry analysis between dithizone and Ag ion by molar ratio titration (λ_{max} = 620 nm).

The UV-Vis spectra are simulated at TD-DFT calculations with B3LYP/6-31G(d,p) basis set of theory in gas phase and in the DMSO solvent. The simulated UV-Vis spectra in the gas-phase and DMSO solvent were investigated with the maximum absorption bands at 412 and 712 nm in gas-phase and 432 and 601 nm in DMSO solvent as summarized in (Table 10). The comparison between the experimental and simulation of UV-Vis spectra show the result that maximum absorption values are blue shifted for the range of 43 nm and show a red shift of about 92 nm in gas-phase. The maximum absorption value of the DMSO solvent indicates the blue shifted with an error of about 19-23 nm. While, the maximum absorption are appeared at 432 and 601 nm as shown in (Table 10). This experiment results are similar to calculation spectra in DMSO solvent due to the polar

solvents giving the stable molecule. In addition, a comparison between the experimental and calculation spectra of silver-dithizone complex in gas phase and DMSO solvent as shown in (Table 10). The theoretical maximum absorption band is calculated at 560 nm for TD-DFT in gas phase and at 558 nm in DMSO solvent for silver-dithizone complex. While, the maximum absorption value of silver-dithizone complex is red shift by increasing for 55 nm in gas phase and 53 nm in DMSO solvent. The simulation result in DMSO solvent have a smaller error than that of gas phase which is depending on the solvent that the energy gap from ground to excited states moving to $\pi \rightarrow \pi^*$ transition.

TABLE 10 The experimental and calculated absorption wavelength (λ, nm) of dithizone and silver-dithizone complex in gas phase and DMSO solvent.

Sample	Condition	Experimental		TD-DFT/B3LYP/6-31G (d,p)			
		λ (nm)	λ(nm)	λ(nm)	0scillator strength	λ(nm)	0scillator strength
Dithizone	Gas phase	-	-	712	0.1159	412	1.0771
	DMSO solvent	455	620	601	0.3972	432	0.9305
Silver-dithizone complex	Gas phase	-	-	560	-	-	-
	DMSO solvent	505	-	558	-	-	-

3.1.3 FT-IR spectrum

The simulated frequencies are using density functional theory calculations with B3LYP/6-31G(d,p) basis sets. Comparisons of vibrational frequencies of the dithizone and silver-dithizone complex between experimental and calculated are as shown in (Table 11). The experimental FT-IR spectrum of dithizone, and silver-dithizone complex were presented in (Figure 23). In the FT-IR of dithizone, they are presented of C–H methylene vibrational absorption bands in the region 2960 $cm^{-1}$and the benzene ring stretching band appeared at 1492 and 1589 cm^{-1}. The absorption peaks at 1438 cm^{-1} was indicated to the C=S stretching mode. The deformation vibration of N–H bond was appeared at 1219 cm^{-1}. The C–H in plane bending vibration of benzene ring was attributed to the peak at 1141 cm^{-1}. Followed by, the N–N stretching mode was assigned in the peak at 890 cm^{-1}. Finally, the vibrational absorption bands in the region of 677 and 751 cm^{-1} are indicated to the benzene ring deformation vibration mode (Zhou; et al. 2011: 6731-6735).

Meanwhile, in the spectrum of silver-dithizone complex, the peak was shifts to 1433 cm^{-1} for the C=S stretching because the interaction between sulfur atom and Ag ion lead to silver-dithizone complex. Moreover, the deformation vibration of N–H bond and C–H in plane bending vibration of benzene ring were shift to 1217 $cm^{-1}$and 1142 cm^{-1} including the increasing a sharp of spectrum. The investigated and calculated frequencies of dithizone and silver-dithizone complex are shown in (Table 11). The optimized structure of dithizone is used in the vibrational frequency calculations DFT levels. The minimum energy of geometrical structure is obtained by using level 6-31G(d,p) basis sets (no imaginary frequency). In this study, the prediction FT-IR spectrum by using level B3LYP/6-31G(d,p) level was correlated between the optimal scaling factor of 0.9613 (Ullah; et al. 2014: 210-214). The comparison between the calculated vibrational frequencies and the experimental data are observed at 2960, 1492–1589, 1438, 1219, 1141, 890, 751 and 677 cm^{-1} of dithizone and the FT-IR vibrational frequencies are simulated at 3090, 1579–1589, 1397, 1228, 1142, 860, 701 and 607 cm^{-1}. The benzene ring stretching are observed at 1589 cm^{-1} and C–H bending at 1141 cm^{-1} showing correlation with the calculated vibrational frequencies of the dithizone. The FT-IR spectrum of silver-dithizone complex in experimental data are appeared at 2956, 1497, 1590, 1433, 1217, 1142, 890, 751 and 676 cm^{-1}. The result of calculated vibrational frequencies are investigated at 3084, 1585–1587, 1386, 1240, 1152, 897, 717 and 610 cm^{-1}. The peak in region of 1590 cm^{-1} for benzene ring stretching in the experimental was different to the simulated vibrational frequencies at 1587 cm^{-1} about 3 cm^{-1}. Therefore, the calculationof FT-IR spectrum are presented the strong correlation and good agreement with the experimental data.

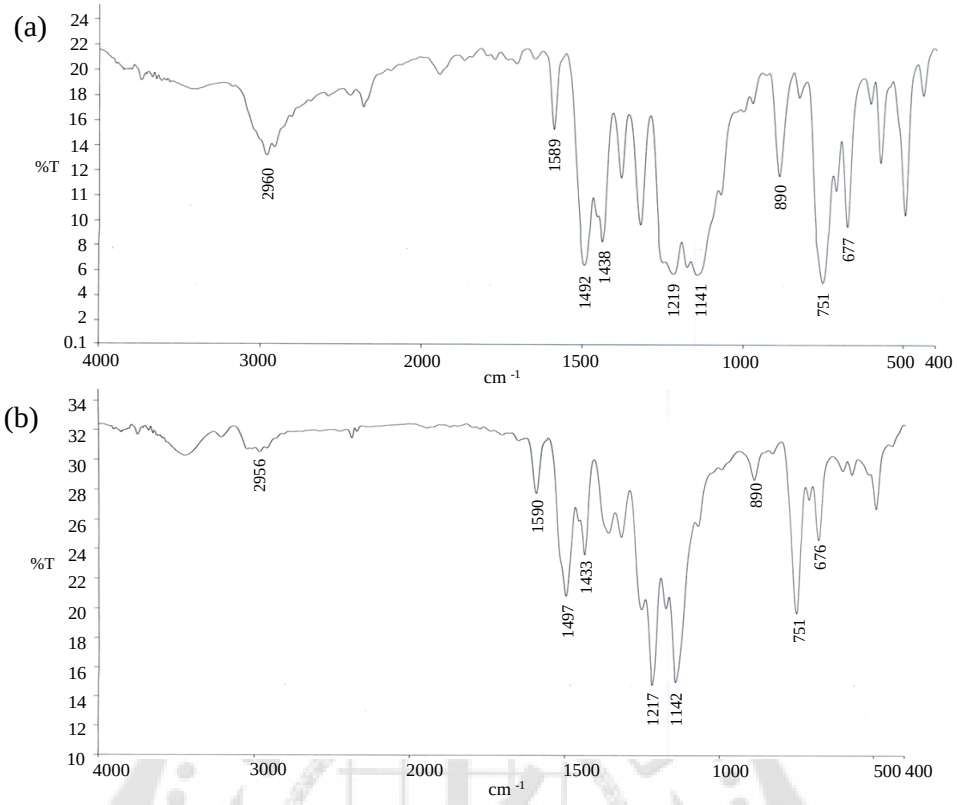

FIGURE 23 FT-IR spectra of dithizone (a) and silver-dithizone complex (b).

TABLE 11 Experimental FT-IR spectrum and calculated DFT:B3LYP/6-31G(d,p) vibrational wavenumbers for the dithizone and silver-dithizone complex.

S.NO	Expt.	Calculated frequency		Expt.	Calculated frequency		Approximate assignment
	Dithizone	Scaled	Un scaled	Silver-dithizone complex	Scaled	Un scaled	
1	2964	3090	3214	2956	3084	3208	C-H vibration
2	1589	1589	1653	1590	1587	1651	Benzene ring stretching
3	1492	1579	1643	1497	1585	1649	Benzene ring stretching
4	1438	1397	1453	1433	1386	1442	C=S stretching
5	1219	1228	1277	1217	1240	1290	N-H vibration
6	1141	1142	1188	1142	1152	1198	C-H bending
7	890	860	895	890	897	933	N-N stretching
8	751	701	729	751	717	746	Benzene deformation vibration
9	676	607	631	676	610	635	Benzene deformation vibration

3.1.4 NMR spectra

In addition, The ^{1}H NMR spectra of dithizone was compared between experimental data and computer simulation system by using the B3LYP/6-311+G(2d,p) method. For the experiment, the chemical shifts of ^{1}H NMR for all protons in structure of DTZ-a are shown in (Figure 24). This result indicates the hydrogen bonding interaction between water and dithizone can caused a small peak of N–H spectrum which are similar to the computer simulation's results. Therefore, the ^{1}H NMR data were applied to confirm the interaction between silver ion and dithizone ligand in the next step.

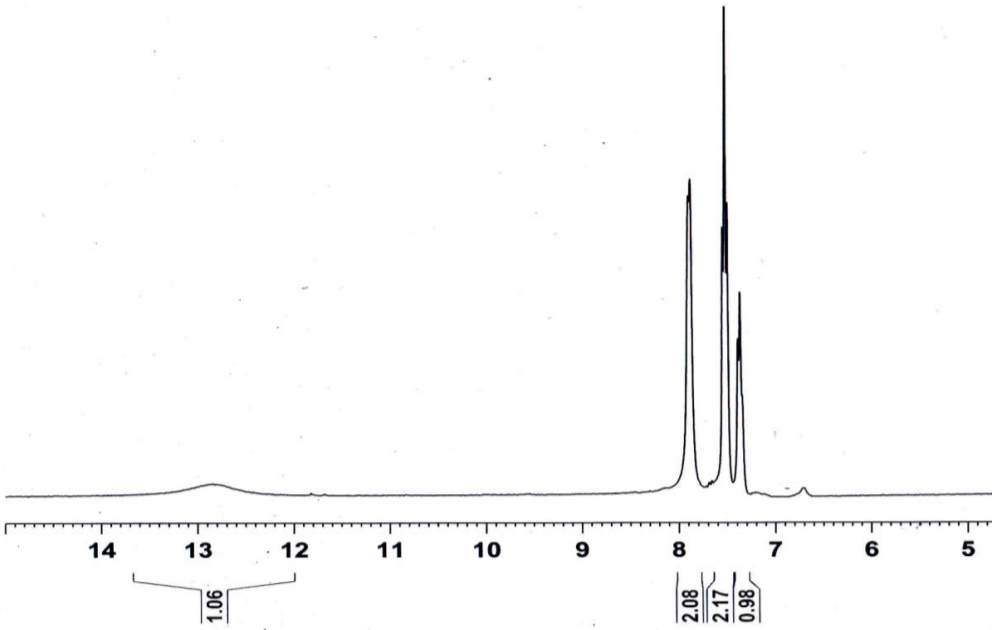

FIGURE 24 The experimental ^{1}H NMR spectrum of dithizone.

The theoretical chemical shift values were calculated by B3LYP method using 6-311+G(2d,p) basis set which the predicted chemical shifts values for the ^{1}H NMR studies of silver-dithizone complex were compared with the experiment as shown in (Figure 21). The chemical shifts of ^{1}H NMR for all protons in complex 2h are summarized in (Table 11). The calculations of ^{1}H NMR values in complex 2h were considered in case of DMSO solvent and non-solvent similar to NMR experiments. The predicted chemical shift of the proton (H14) at the nitrogen atom in complex 2h was compared with experimental data. The result showed the values of 11.67 and 11.35 ppm in DMSO and non-solvent, respectively, compared with the signal of 10.70 ppm in the experiment for H14 as shown in (Table 12). The data for non-solvent was plotted between the calculated ^{1}H NMR chemical shifts versus

experimentally measured chemical shifts in ppm. The result shows a correlation coefficient value of r^2 = 0.9773 as shown in (Figure 26). In the case of DMSO-d_6, the plot of calculated ^{1}H NMR chemical shifts versus experimentally measured chemical shifts in ppm, having a correlation coefficient value of r^2 = 0.9837 as shown in (Figure 27). The increasing of correlation coefficient value of complex 2h indicates the chemical shifts of protons depending on DMSO solvent.

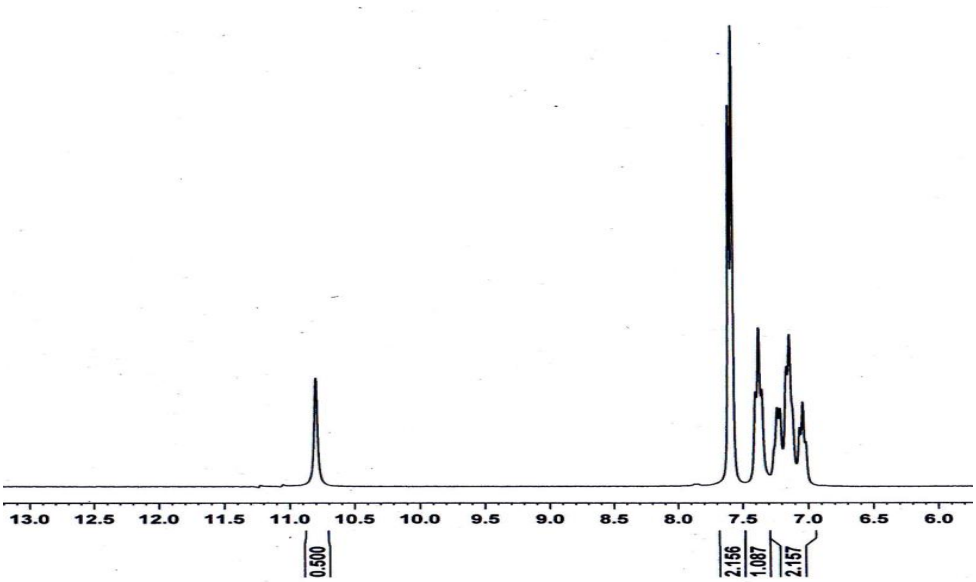

FIGURE 25 The experimental 1H NMR spectrum of interaction silver–dithizone complex in DMSO-d_6.

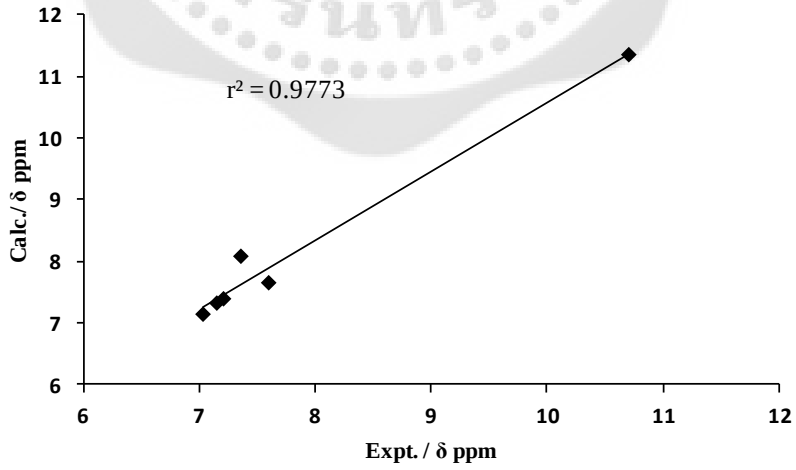

FIGURE 26 Plotted of complex 2h calculated ^{1}H NMR chemical shifts versus experimentally measured chemical shifts in ppm.

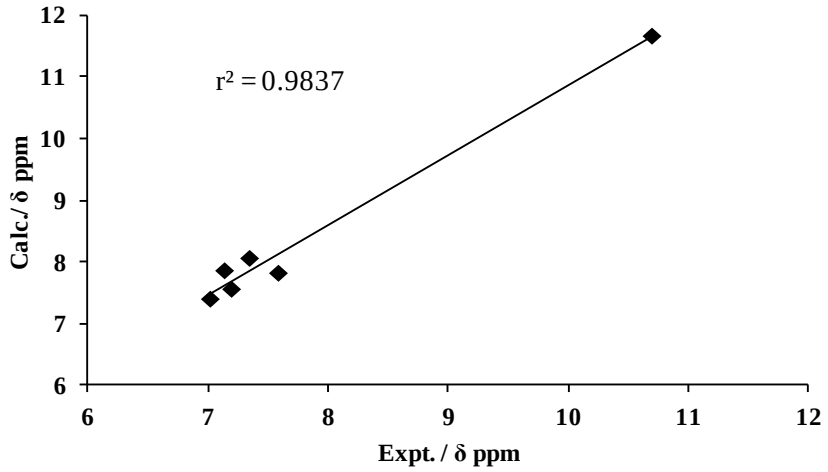

FIGURE 27 Plotted of complex 2h calculated ^{1}H NMR chemical shifts with DMSO-d_6 versus experimentally measured chemical shifts in ppm.

TABLE 12 Comparison of experimental and complex 2h calculated ^{1}H NMR chemical shifts (δ/ppm).

Proton	Expt.(δ/ppm)	Cal. (δ/ppm)	
		DMSO-d_6	Non-solvent
H_{14}	10.70	10.67	11.35
$H_{10,25}$	7.35	8.07	8.08
$H_{7,9,27,28}$	7.59	7.83	7.65
$H_{8,29}$	7.20	7.57	7.39
H_{23}	7.14	7.87	7.32
H_{11}	7.02	7.41	7.14

4. Optimization of assay conditions

4.1 Solubility of dithizone

The preparation of dithizone solution in various organic solvents such as methanol, ethanol, chloroform, acetone, hexane, dichloromethane, acetonitrile and dimethyl sulfoxide was studied. A 50 mg of dithizone was prepared by dissolving with 100 mL in various organic solvents as shown in (Figure 28A). The results show that the dithizone is soluble in all organic solvents. Then dithizone solution was added to 0.2 mg/L of AgNPs solution in the size of 20 nm or 100 nm is having the result show the separation layer with water in the case of dithizone in chloroform, hexane and dichloromethane because of its polarity solvent. However, dithizone in methanol, ethanol, acetone, acetonitrile and dimethyl sulfoxide are appeared the color change after the addition of 20 nm AgNPs solution, respectively, due to its high dielectric constant or polar solvents as shown in (Figure 28B). (Adam; et al. 2016: 192-208). While, the same results were found by using 100 nm AgNPs. The UV-Vis absorption spectra of dithizone in five organic solvents were tested as shown in (Figure 28C). The results show the maximum absorbance at about 600 nm which then gradually decreased and appeared by red shifts of this absorbance band in the solvent polarity. These observations were confirmed the optical spectra of dithizone in organic solvent depend on the lewis acidity of the solvent molecules (Das; et al. 2012: 3714-3721; Grimme; et al. 2010: 1402-1405). Therefore, the ethanol, acetonitrile and dimethyl sulfoxide solvent was selected for further experiments. Meanwhile, the results on during storage so that dithizone dissolved with dimethyl sulfoxide was unstable and decomposed compared to ethanol and acetonitrile, respectively. However, dithizone in acetonitrile found to be stable and the solution was maintained a green color for a month.

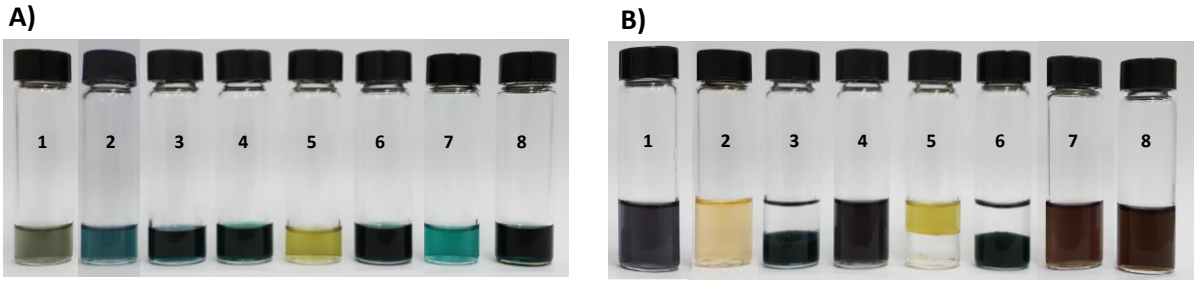

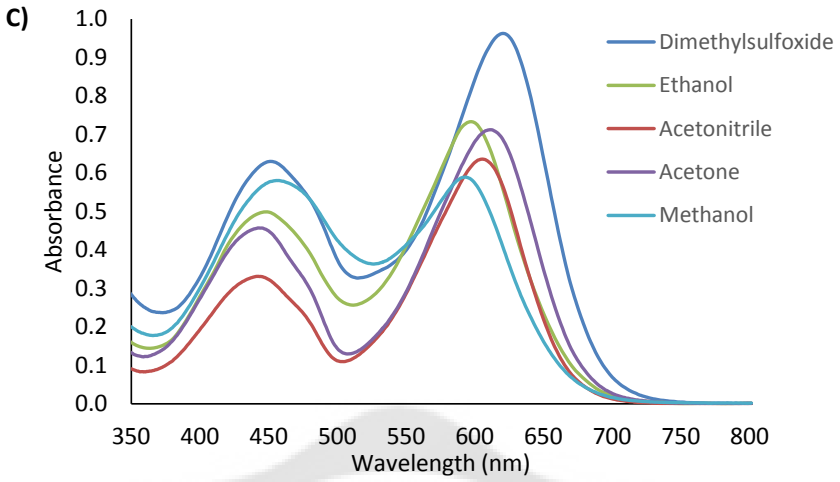

FIGURE 28 Effect of solubility dithizone in different solvents. (Methanol, Ethanol, Chloroform, Acetone, Hexane, Dichloromethane, Acetonitrile and Dimethyl sulfoxide) A) dithizone by dissolving with organic solvents and B) after addition of AgNPs solution (0.2 mg/L). C) The absorbance spectra of dithizone in five organic solvents.

4.2 Characterization of dithizone in three solvents, Ag ion and AgNPs

The absorption spectra of 10 mg/L dithizone in a solution of ethanol showed two absorbance maximum at 450 and 604 nm, respectively. While, the spectral of dithizone in dimethyl sulfoxide showed two maxima at 455 and 620 nm and in acetonitrile reveal the presence of a peak at around 447 nm and 604 nm, respectively. Moreover, the absorbance maximum of 50 mM Ag ion in DI water is located at 301 nm. Whereas, the AgNPs solution in the size of 20 nm presented a bright yellow color and showed an absorption peak at 406 nm with the concentration of 20 mg/L. The absorption maximum at 492.5 nm is shown for the 100 nm AgNPs, the light pink color with the concentration of 20 mg/L as shown in (Figure 29).

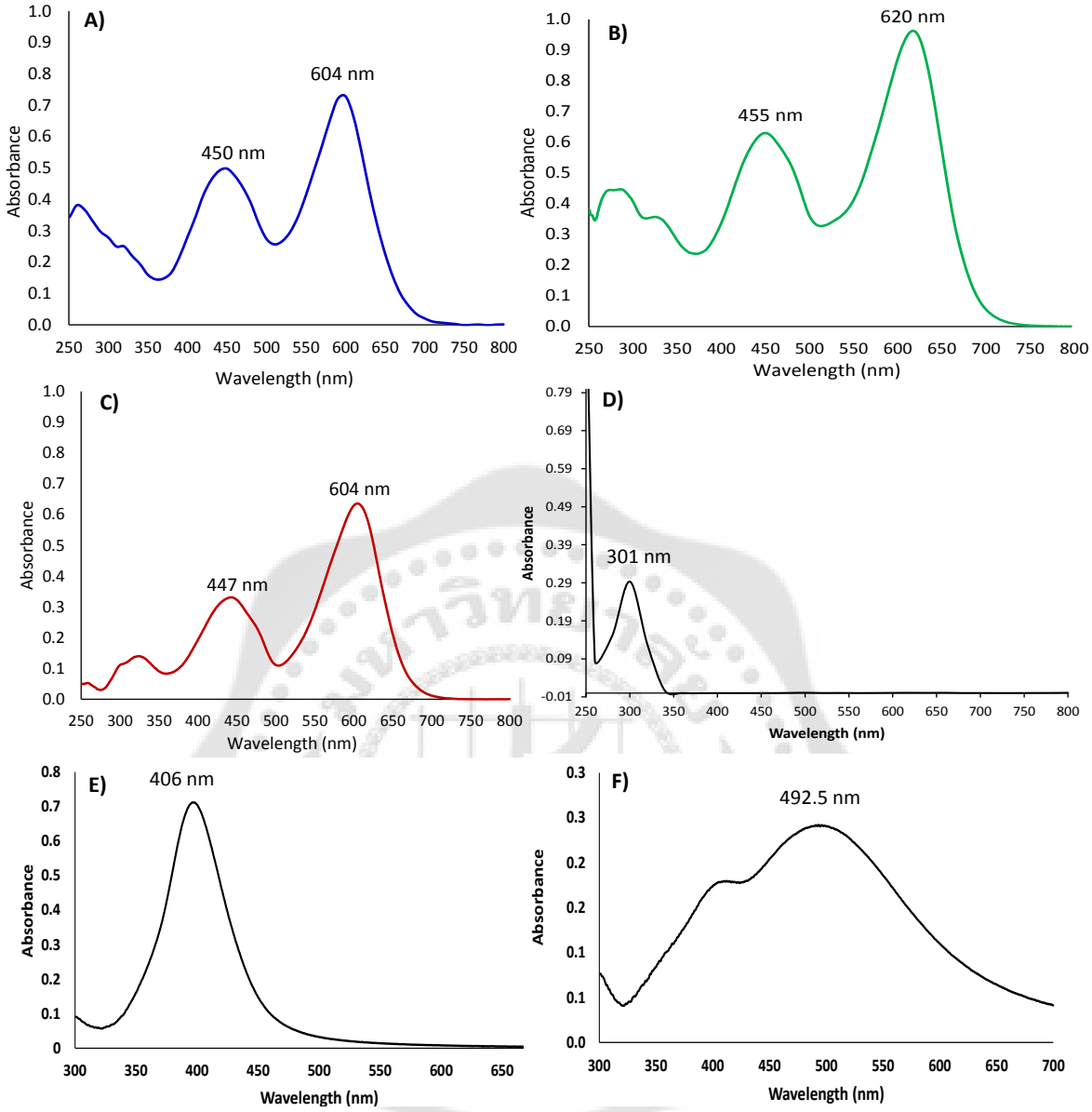

FIGURE 29 The absorbance spectra of A) dithizone (10 mg/L) in an ethanol solvent; B) dithizone (10 mg/L) in a DMSO solvent; C) dithizone (10 mg/L) in a acetonitrile solvent; D) Ag ion solution (50 mM) E) 20 nm AgNPs solution (20 mg/L) and F) 100 nm AgNPs solution (20 mg/L).

4.3 Effect of pH

Initially, the effect of pH on color change between dithizone concentration of 10 mg/L in ethanol solution with 20 or 100 nm AgNPs solution at a pH range from 2-10 were investigated in (Figure 30) and the absorbance spectrum was recorded. The results show that required pH is above pH 6 and the absorbance intensity at 477 nm as show in

(Figure 31), which dramatic increase in the absorbance ratio (A_{477nm}/A_{604nm}) was clearly observed. Therefore, the appeared dithizone results indicated the selectivity for AgNPs and the lowest detection limit at pH 6 that in acidity, medium, AgNPs does not form stable complexes with dithizone and to be formed stable complex with dithizone in alkaline medium with the appropriated pH for the complex. The same results were found by using 100 nm AgNPs of a stable orange colored complex. In addition, the adjusted pH of the $AgNO_3$ solution shows the precipitation of silver hydroxide (AgOH) (data not shown).

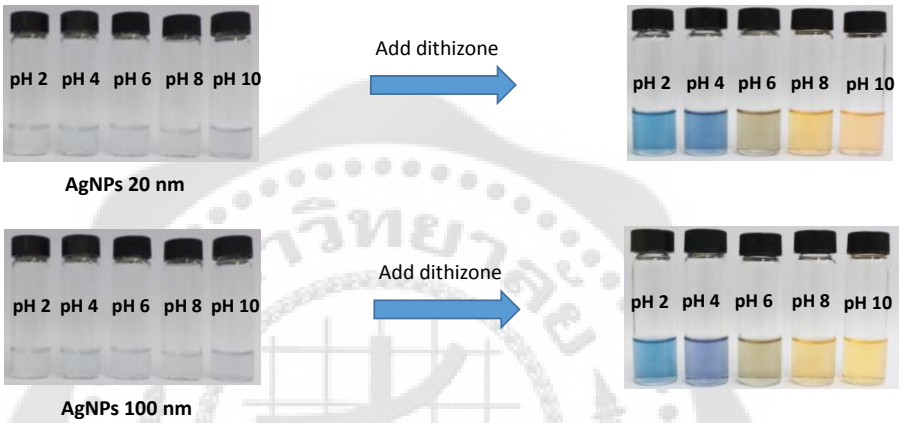

FIGURE 30 Effect of pH on AgNPs-dithizone complex in aqueous system.

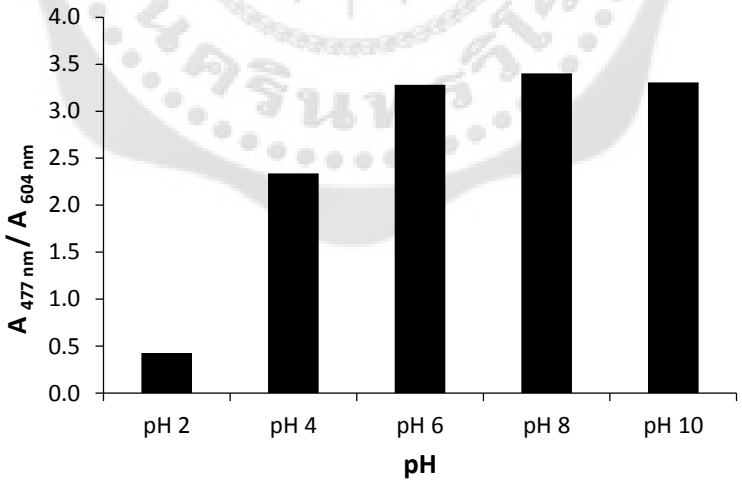

FIGURE 31 The absorbance ratio ($A_{477\ nm}/A_{604\ nm}$) of AgNPs-dithizone complex as function of pH.

4.4 Selectivity of dithizone with other metal ions

4.4.1 Dithizone in ethanol solvent

The colorimetric sensing ability of 10 mg/L dithizone in ethanol solution towards other metal ion solutions (1.951×10^{-5} M) of Na^{+}, K^{+}, Cu^{2+}, Mg^{2+}, Ba^{2+}, Mn^{2+}, Fe^{3+}, Co^{2+}, Ni^{2+}, Cu^{2+}, Ag^{+}, Zn^{2+}, Cd^{2+}, Hg^{2+}, Pb^{2+} and AgNPs of 20 and 100 nm with a concentration of 0.2 mg/L were tested by colorimetric analysis. Initially, the selectivity of the dithizone in the sensing of the metal ions was tested by adding 2 mL of dithizone to a mixture solution containing 2 mL of each metal ion. All of the experiments were prepared at room temperature. Each metal ion appears in naked eyes inspection having the color change of the dithizone after a few seconds of addition 0.2 mg/L of 20 nm AgNPs from green to orange. The same result was found by using AgNPs with the particle size 100 nm as shown in (Figure 32). But the different color appeared for other metal ions. Therefore, there are no significant color changes compared in the presence of other metal ions which is demonstrated in the sensing system being specific to AgNPs that the detection of Ag ion is noticed compared with AgNPs in the different color. Then, we can possibly discriminate between the AgNPs, the Ag ion and other metal ions with the naked eye. Moreover, the absorbance spectra of dithizone solution change after the addition of 1.951×10^{-4} M other metal ions were measured by using UV-Vis spectrophotometry. The result shows that the absorbance spectra of other metal ions with dithizone have no significance. The presence of dithizone resulted in the wavelength of maximum absorbance intensity in both 450 and 604 nm and after addition of 20 and 100 nm AgNPs, a new peak appeared in both at 477 nm and the absorbance band at around 500 nm in the case of Ag ion which caused the color change of the solution from green to pale pink. Therefore, these results indicated that the evaluation approach has a good selectivity and specificity toward AgNPs with the particle size of 20 and 100 nm as shown in (Figure 33).

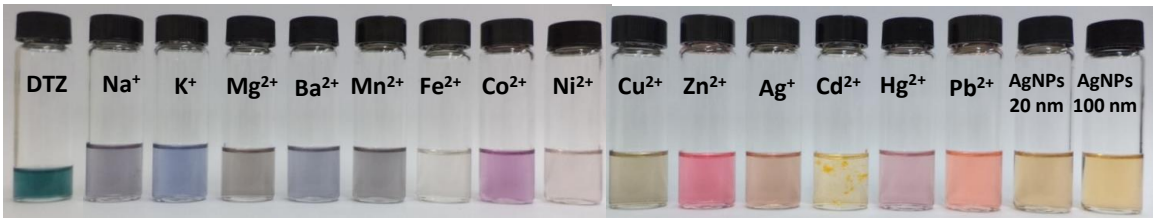

FIGURE 32 Visual color change of the other metal ions (1.951×10^{-4} M) solution after addition of dithizone in ethanol with the concentrations of 10 mg/L.

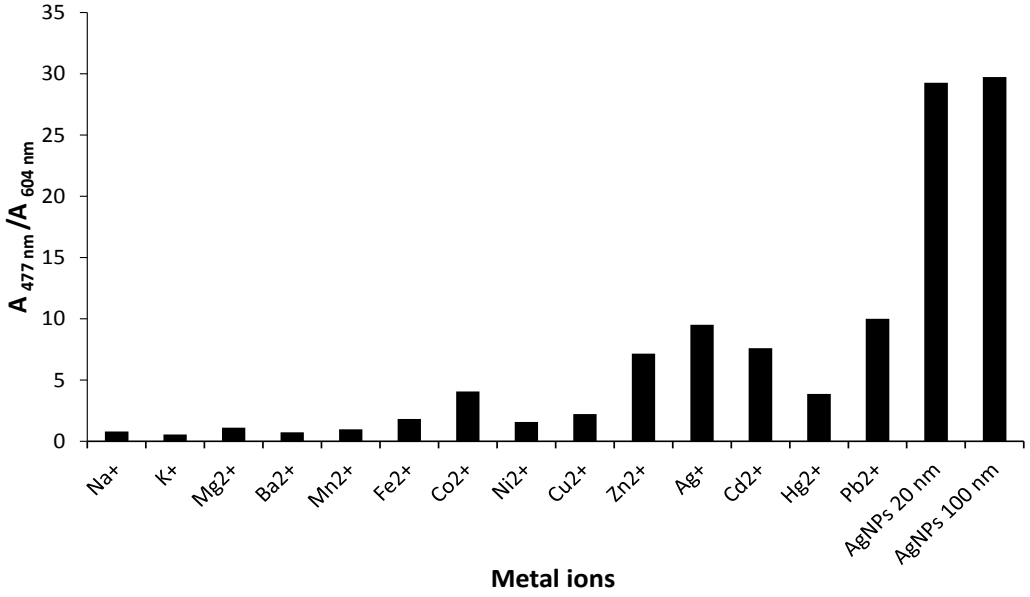

FIGURE 33 Selectivity of the dithizone in ethanol solvent for AgNPs. Concentration of AgNPs was 0.2 mg/L; concentration of each of the other metal ions was 1.951×10^{-4} M.

4.4.2 Dithizone in dimethyl sulfoxide (DMSO) solvent

The absorption spectra of ligand dithizone (20 mg/L) in DMSO solvent was studied upon addition of various metal ions (1×10^{-5} M) such as Na^{+}, K^{+}, Cu^{2+}, Mg^{2+}, Ba^{2+}, Mn^{2+}, Fe^{3+}, Co^{2+}, Ni^{2+}, Cu^{2+}, Ag^{+}, Zn^{2+}, Cd^{2+}, Hg^{2+}, Pb^{2+} , Ca^{2+}, Al^{3+}, Fe^{2+}, Cr^{2+} and AgNPs of 20 and 100 nm with a concentration of 0.2 mg/L. The absorption band at 455 nm and 620 nm after addition of AgNPs solution, the color of the solution changed from green to orange and a new absorption band at 477 nm were found. In the presence of Ag ion, the absorbance band at 500 nm and the color of solution change from green to pale brown were as shown in (Figure 34), In the presence of the selectivity to only AgNPs, a remarkable increase in the absorbance ratio of $A_{477\ nm}/A_{620\ nm}$ were indicated so that it had no significant response to other metal ions as shown in (Figure 35). The same result of color change from green to orange was found by using AgNPs with the particle size 100 nm.

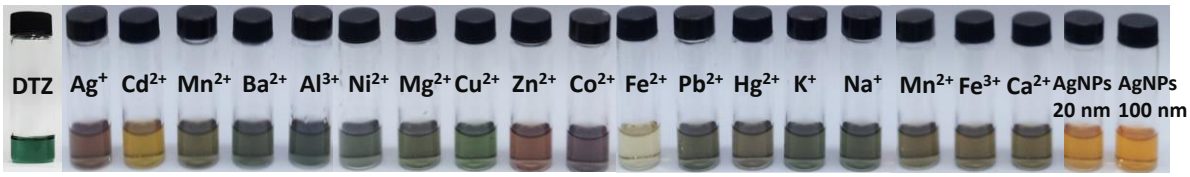

FIGURE 34 Visual color change of the other metal ions (1 x 10^{-5} M) solution after addition of dithizone in DMSO with the concentrations of 20 mg/L.

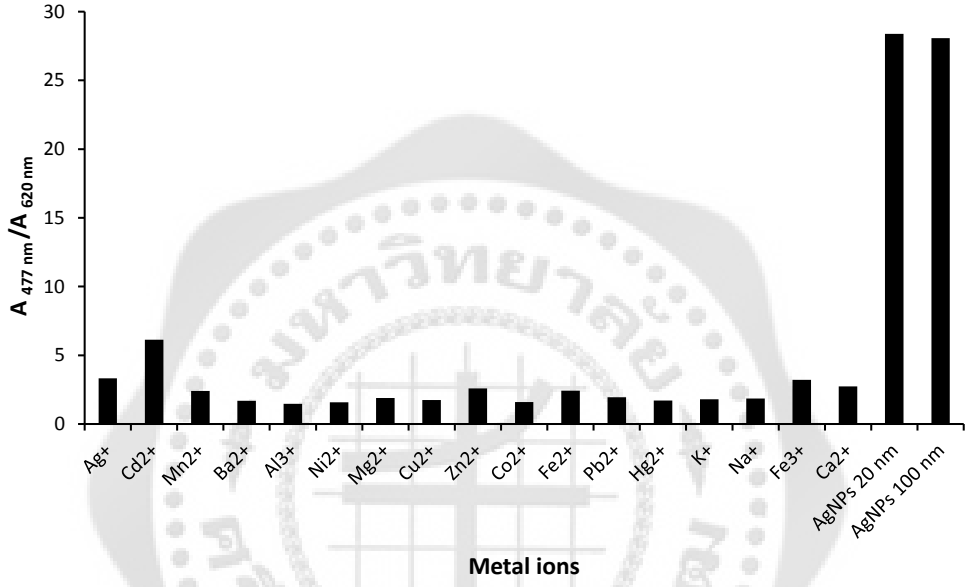

FIGURE 35 Selectivity of the dithizone solution in DMSO for AgNPs. Concentration of AgNPs was 0.2 mg/L; concentration of each of the other metal ions was 1 x 10^{-5} M.

4.4.3 Dithizone in acetonitrile solvent

The studied on the selectivity of dithizone ligand (10 mg/L) in acetonitrile solutions by adding various metal ions (1 x 10^{-4} M) of Na^{+}, Cu^{2+}, Mg^{2+}, Ba^{2+}, Mn^{2+}, Fe^{3+}, Co^{2+}, Ni^{2+}, Cu^{2+}, Ag^{+}, Zn^{2+}, Cd^{2+}, Hg^{2+}, Pb^{2+} , Ca^{2+}, Al^{3+}, Fe^{2+}, Cr^{2+} and AgNPs of 20 and 100 nm with a concentration of 0.6 mg/L. The dithizone ligand revealed an absorbance band at 447 nm and 604 nm. The change in the solution color of dithizone with the addition of these metal ions was studied. In the presence of AgNPs (20 nm and 100 nm), the absorption band at 477 nm and the change in the solution color from green to orange appeared. In the case of Ag ion solution after addition of dithizone, it leads to change in the solution from green to pink as shown in (Figure 36). In order to evaluate the sensitivity of this method and investigate the minimum concentration of AgNPs in aqueous solution by

the color change of the system, The resulting indicated that the dithizone a high selectivity and good selectivity toward AgNPs as shown in (Figure 37).

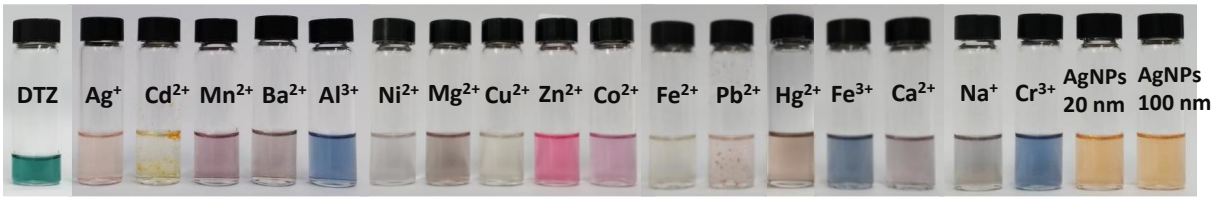

FIGURE 36 Visual color change of the other metal ions (1 x 10^{-4} M) solution after addition of dithizone in acetonitrile with the concentrations of 10 mg/L.

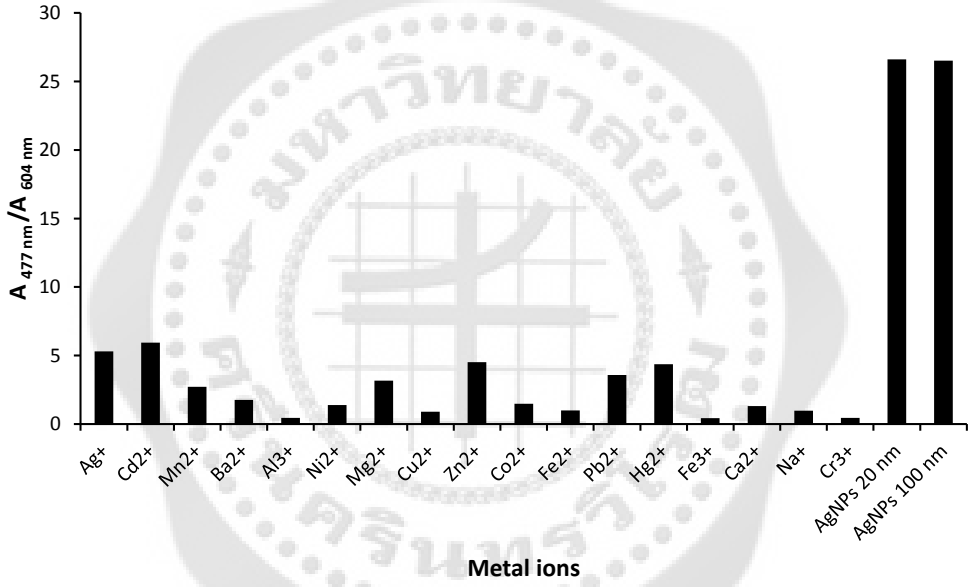

FIGURE 37 Selectivity of the dithizone solution in acetonitrile for AgNPs. Concentration of AgNPs was 0.6 mg/L; concentration of each of the other metal ions was 1 x 10^{-4} M.

All the results show that the dithizone in ethanol, DMSO and acetonitrile solvent after addition AgNPs solution are appeared the color of solution change from green to orange. This indicated that the selectivity of dithizone towards AgNPs. Moreover, the color of the Ag ion solution change from green to pale pink after addition dithizone solution and when adding dithizone solution into AgNPs solution and the Ag ion solution are revealed different color which also exhibited a good selectivity towards AgNPs and Ag ion over other metal ions. In the UV-Vis spectrum, the absorption at 477 nm for AgNPs-

dithizone complex and the absorption peak at about 500 nm are appearing for silver-dithizone complex .The result of dithizone in ethanol and acetonitrile solvent is quite similar.

4.5 Detection limit of dithizone

4.5.1 Dithizone in ethanol solvent

The 5 mg dithizone was dissolved in ethanol solution in the final concentration of 10 mg/L followed by dithizone solution was diluted from stock solution in various concentrations from 5 mg/L to 50 mg/L. After that, the 0.2 mg/L AgNPs (20 nm or 100 nm) were added in difference concentration of dithizone solution showing a color change from green to orange as shown in (Figure 38). In UV-Vis spectrum, the absorption ratios of $A_{477\ nm}/A_{604\ nm}$ show a significant increase after the addition of AgNPs. The results show the high absorption ratio of dithizone concentration at 5 mg/L, 6.67 mg/L and 10 mg/L as shown in (Figure 39), according to the color change of complex. Therefore, the present limit of detection of this dithizone is 5 mg/L which the same results of color change from green to orange and the detection limit of dithizone is 5 mg/L were found by using 100 nm AgNPs.

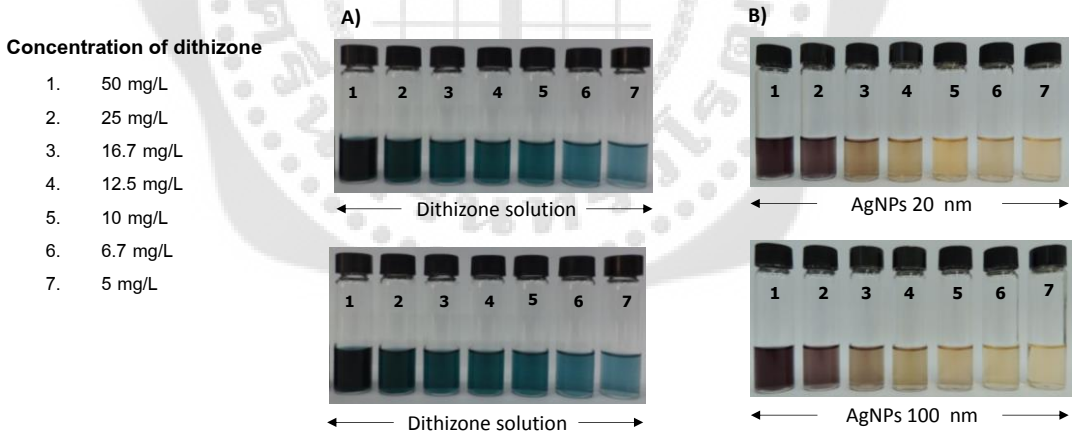

FIGURE 38 Color change of the dithizone solution in various concentrations. A) Dithizone solution concentration of 5 mg/L to 50 mg/L in ethanol. B) After addition of 0.2 mg/L AgNPs in the size of 20 nm and 100 nm, respectively.

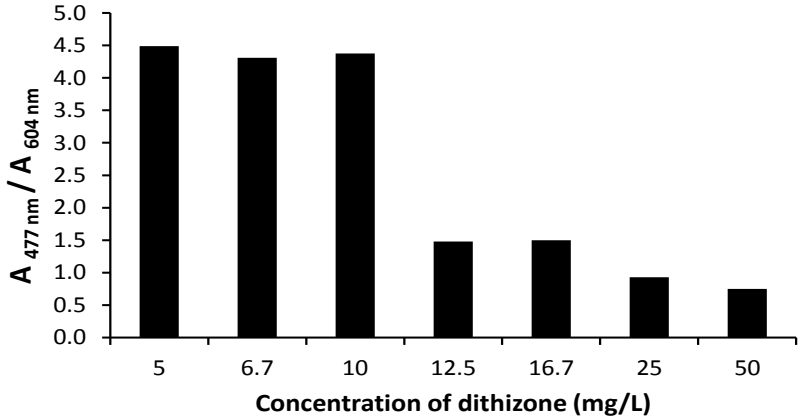

FIGURE 39 The absorption ratio of $A_{477\ nm}/A_{604\ nm}$ of AgNPs-dithizone complex in the presence of 5 mg/L - 50 mg/L dithizone.

4.5.2 Dithizone in dimethyl sulfoxide solvent

In addition, the stock solution of dithizone in dimethyl sulfoxide solvent was diluted in various concentrations from 5 mg/L to 50 mg/L after addition of 0.2 mg/L AgNPs (20 or 100 nm) having the presented color change from green to orange as shown in (Figure 40). The intense color of a complex depends on the concentration of dithizone. However, the absorption ratio ($A_{477\ nm}/A_{620\ nm}$) is increasing with a decrease in the dithizone concentration as shown in (Figure 41). A limit of detection was found to be 5 mg/L according to the intensity color was clear and the same results of color change from green to orange and the detection limit of dithizone is 5 mg/L were found by using 100 nm AgNPs.

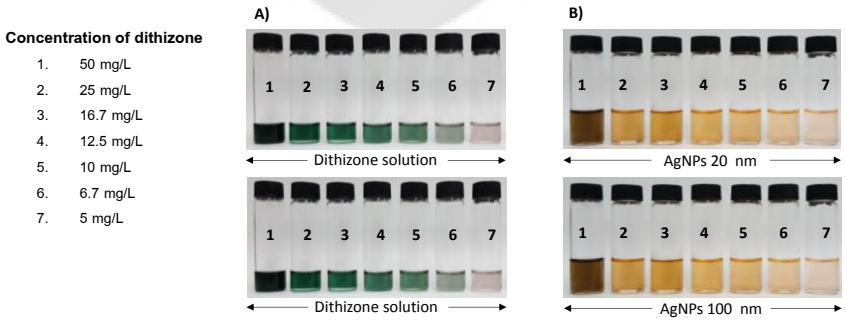

FIGURE 40 Color change of the dithizone solution in various concentrations. A) Dithizone solution concentration of 5 mg/L - 50 mg/L in DMSO. B) After addition of 0.2 mg/L AgNPs in the size of 20 nm and 100 nm, respectively.

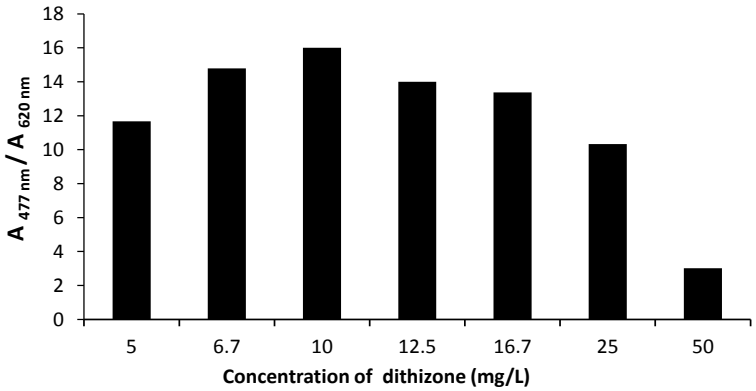

FIGURE 41 The absorption ratio of $A_{477\ nm}/A_{620\ nm}$ of AgNPs-dithizone complex in the presence of 5 mg/L - 50 mg/L dithizone.

4.5.3 Dithizone in acetonitrile solvent

In acetonitrile solution, the stock solution of dithizone was diluted in various concentrations from 5 mg/L to 50 mg/L. AgNPs (20 or 100 nm) was added into dithizone solution. The results show that the color change from green to pale orange as shown in (Figure 42) and the absorbance spectra of complex were recorded. Furthermore, the absorption ratio ($A_{477\ nm}/A_{620\ nm}$) increase as a function of the dithizone concentration in the range of 5 mg/L - 50 mg/L. Then, the color intensity of the complex appeared at 10 mg/L dithizone was clearly related to the absorption ratio as shown in (Figure 43). Therefore, the detection limit of dithizone by the naked eye was found to be 5 mg/L and the same results of color change from green to pale orange and the detection limit of dithizone is 5 mg/L were found by using 100 nm AgNPs.

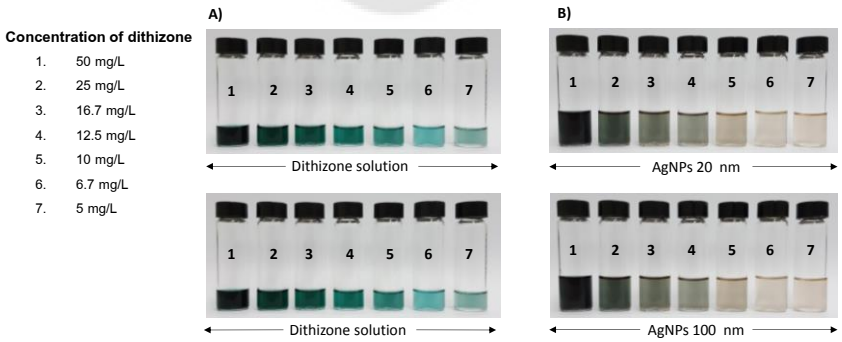

FIGURE 42 Color change of the dithizone solution in various concentrations. A) Dithizone solution concentration of 5 mg/L - 50 mg/L in acetonitrile. B) After addition of 0.2 mg/L AgNPs in the size of 20 nm and 100 nm, respectively.

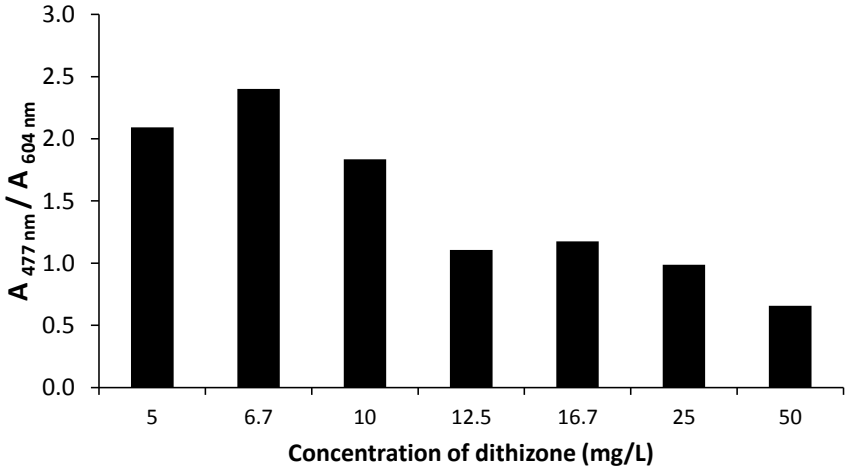

FIGURE 43 The absorption ratio of $A_{477\ nm}/A_{604\ nm}$ of AgNPs-dithizone complex in the presence of 5 mg/L - 50 mg/L dithizone.

4.6 Detection limit of Ag ion

4.6.1 Dithizone in ethanol solvent

To estimate the sensitivity of this method and investigate the minimum amount detectable concentration of Ag ion in aqueous solution, the influence of 10 mg/L dithizone in ethanol concentration on the determination of Ag ion was investigated in the concentration range of 1.95 μM to 97.55 μM Ag ion. The different concentrations of Ag ion aqueous solution was prepared by adding a solution of the dithizone at room temperature. The color change of the solution in the system was monitored as shown in (Figure 44), and related to absorption ratio ($A_{500\ nm}/A_{604\ nm}$) increase as a functions of the Ag ion concentration in the range of 1.95 μM to 97.55 μM as shown in (Figure 45). The results show that the high intensity color of complex was found to be 97.55 μM, the color of the dithizone changes from green to pink for Ag ion. But the lower than concentration of Ag ion about 97.55 μM were clearly no change in color. Therefore, the appeared limit of detection of this Ag ion is 24.39 μM.

Concentration of Ag ion

1. 97.5 μM
2. 48.8 μM
3. 24.4 μM
4. 4.88 μM
5. 3.25 μM
6. 2.44 μM
7. 1.95 μM

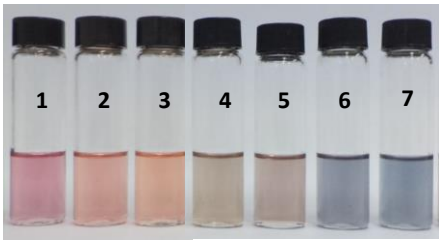

FIGURE 44 Color change of the Ag ion solution in various concentrations after addition of 10 mg/L dithizone in ethanol solvent.

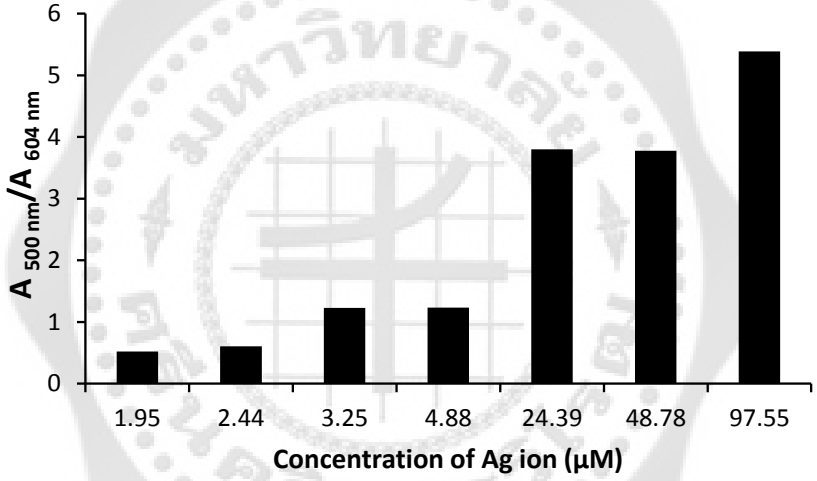

FIGURE 45 The absorption ratio of $A_{500\ nm}/A_{604\ nm}$ of silver-dithizone complex in the presence of 1.95 μM to 97.55 μM Ag ion.

4.6.2 Dithizone in dimethyl sulfoxide solvent

Whereas, the concentration of 8 mg/L dithizone in dimethyl sulfoxide solution to detect different concentration of Ag ions ranging from 1 μM to 6 μM. The color change from green to pink were as shown in (Figure 46) and the absorbance ratio of of $A_{500\ nm}/A_{620\ nm}$ of the mixture solution correlate with the concentration of Ag ions in (Figure 47), the visible color change can be simply remarkable by the naked eyes when the concentration of Ag ion is over 1 μM. Thus, the detection limit of Ag ion was found to be 1 μM.

Concentration of Ag ion

1. 6 μM
2. 4 μM
3. 2 μM
4. 1 μM

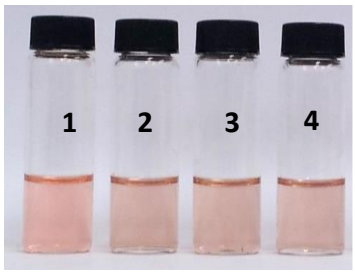

FIGURE 46 Color change of the Ag ion solution in various concentrations after addition of 8 mg/L dithizone in DMSO solvent.

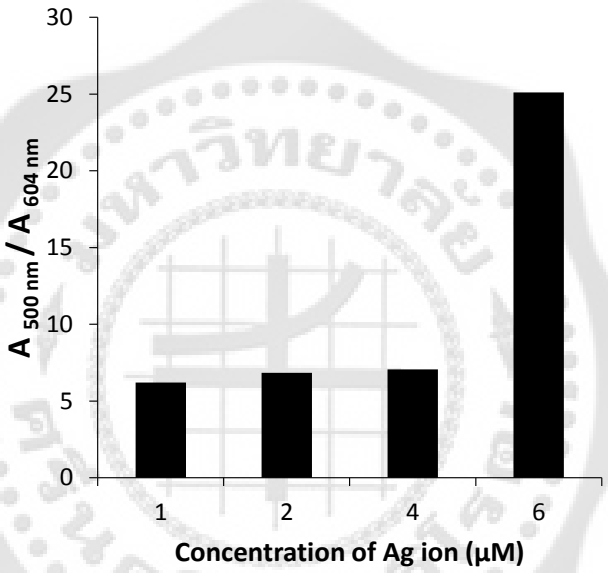

FIGURE 47 The absorption ratio of $A_{500\ nm}/A_{620\ nm}$ of silver-dithizone complex in the presence of 1 μM to 6 μM Ag ion.

4.6.3 Dithizone in acetonitrile solvent

In acetonitrile, the concentration of Ag ion in the ranging from 1 μM to 100 μM was determined using the 10 mg/L dithizone solution. After addition of Ag ion in different concentration, the resulting showed a pink color of solution as shown in (Figure 48), However, the concentration of 1 μM and 10 μM showed no change or slight decrease in the absorption ratio of $A_{500\ nm}/A_{604\ nm}$ according to (Figure 49). Therefore, the detection limit for Ag ion was found to be 100 μM.

Concentration of Ag ion

1. 100 µM
2. 10 µM
3. 1 µM

FIGURE 48 Color change of the Ag ion solution in various concentrations after addition of 10 mg/L dithizone in acetonitrile solvent.

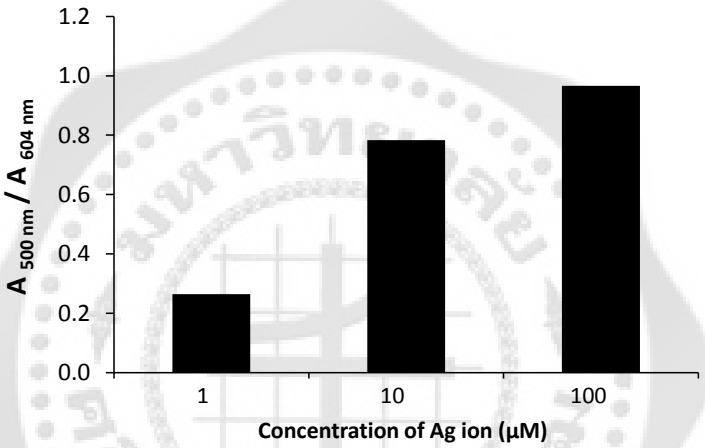

FIGURE 49 The absorption ratio of $A_{500\ nm}/A_{604\ nm}$ of silver-dithizone complex in the presence of 1 µM to 100 µM Ag ion.

From observations, the result of dithizone in dimethyl sulfoxide solvent appeared the lowest limit of detection for Ag ion was found to be 1 µM. Because of the solvent polarity.

4.7 Detection limit of AgNPs for dithizone

4.7.1 Dithizone in ethanol solvent

The preparation of 10 mg/L dithizone in ethanol solution with various concentrations of 20 nm AgNPs ranging from 0.00002 mg/L to 0.2 mg/L were determined. After addition of dithizone solution into the different concentrations of AgNPs, the color of the solution changes from colorless to orange upon concentrations of AgNPs as shown in (Figure 50). As seen from (Figure 51), the absorbance intensity ($A_{477\ nm}/A_{604\ nm}$) was found to decrease with decreasing the concentration of AgNPs in the range of 0.00002 mg/L to

0.2 mg/L. Thus, a concentration of 0.02 mg/L was selected as the detection limit of AgNPs solution which the same results of color change from colorless to orange and the detection limit of AgNPs is 0.02 mg/L were found by using 100 nm AgNPs.

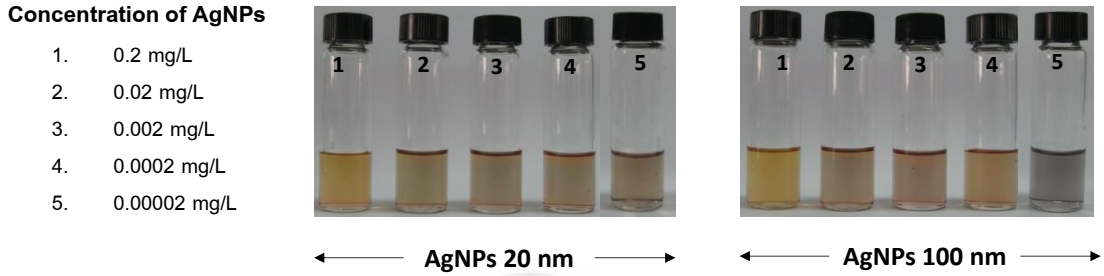

FIGURE 50 Color change of the AgNPs solution in various concentrations after the addition of 10 mg/L dithizone.

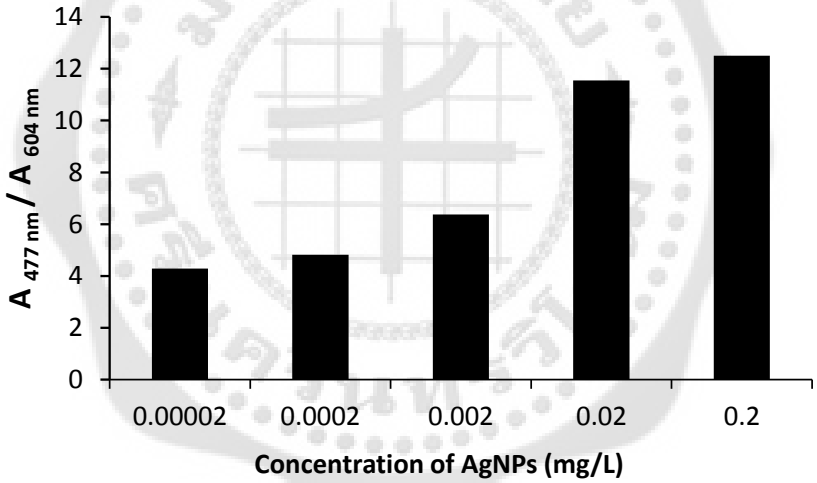

FIGURE 51 The absorption ratio of $A_{477\ nm}/A_{604\ nm}$ of AgNPs - dithizone complex in the presence of 0.00002 mg/L to 0.2 mg/L AgNPs.

4.7.2 Dithizone in dimethyl sulfoxide solvent

Moreover, the 20 nm AgNPs solution was prepared by the difference concentration in the ranging from 0.00002 mg/L to 0.2 mg/L after addition of dithizone in dimethyl sulfoxide solution with the concentration of 10 mg/L. The results show that the color of the AgNPs changes from colorless to orange as shown in (Figure 52). In the UV-Vis spectrum, absorption ratio of $A_{477\ nm}/A_{604\ nm}$ is decreased depending on the concentration of AgNPs according to (Figure 53). Thus, the detection limit for AgNPs is 0.02 mg/L, which

a correlate to higher intensity absorption ratio and the same results of color change from colorless to orange and the detection limit of AgNPs is 0.02 mg/L were found by using 100 nm AgNPs.

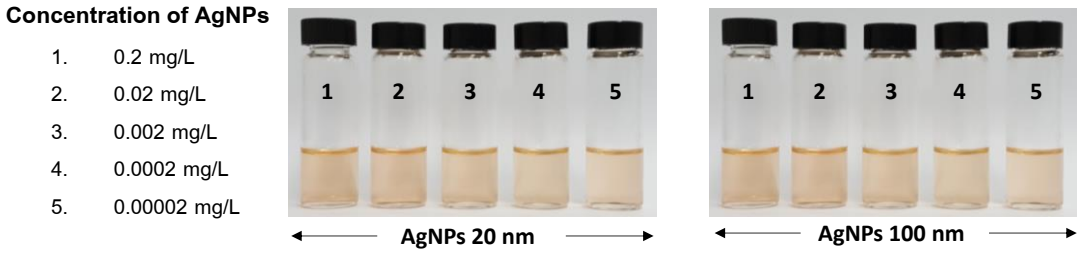

FIGURE 52 Color change of the AgNPs solution in various concentrations after the addition of 10 mg/L dithizone.

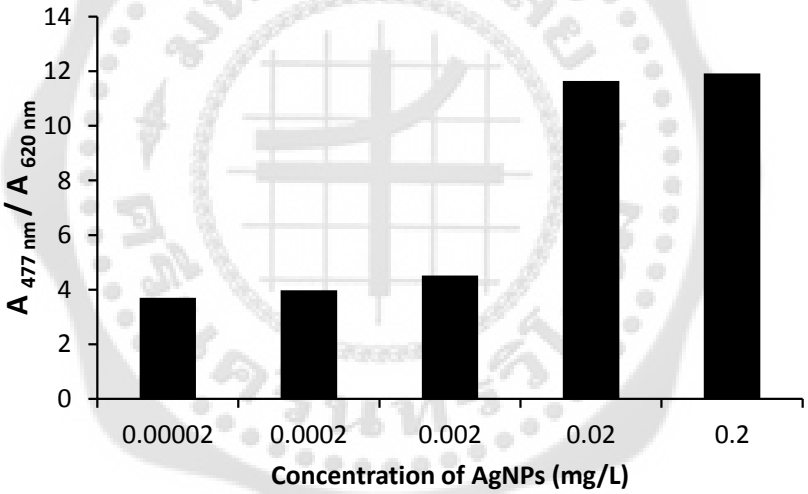

FIGURE 53 The absorption ratio of $A_{477\ nm}/A_{620\ nm}$ of AgNPs - dithizone complex in the presence of 0.00002 mg/L to 0.2 mg/L AgNPs.

4.7.3 Dithizone in acetonitrile solvent

The gradual addition of 10 mg/L dithizone in acetonitrile solution toward the 20 nm AgNPs solution in various concentrations in the ranging from 0.4 mg/L to 0.8 mg/L were studied. The spectral change was a result of the addition of AgNPs concentration having the color change from colorless to orange as shown in (Figure 54). Whereas, the intensity of color was confirmed by the absorption ratio of $A_{477\ nm}/A_{604\ nm}$ of AgNPs - dithizone complex as shown in (Figure 55) and the absorbance maximum spectra

of complex appeared at 477 nm. Therefore, the detection limit for AgNPs was found to be 0.6 mg/L. The same results of color change from colorless to orange and the detection limit of AgNPs is 0.6 mg/L were found by using 100 nm AgNPs.

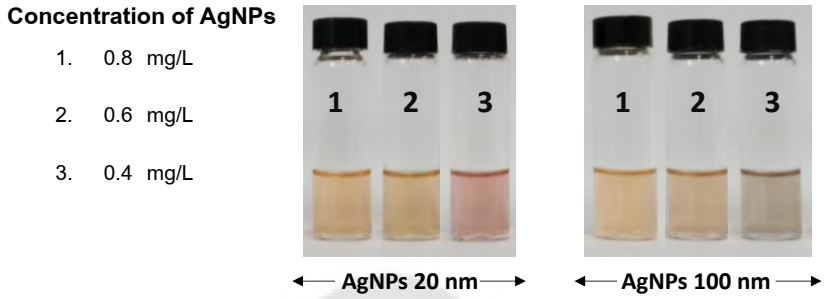

FIGURE 54 Color change of the AgNPs solution in various concentrations after the addition of 10 mg/L dithizone.

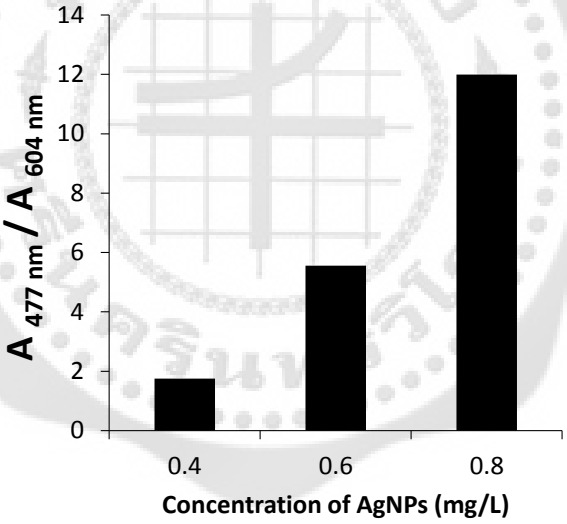

FIGURE 55 The absorption ratio of $A_{477\ nm}/A_{604\ nm}$ of AgNPs - dithizone complex in the presence of 0.4 mg/L to 0.8 mg/L AgNPs.

From all the result, the detection limit for dithizone, Ag ion and AgNPs were optimized. The detection limit of dithizone in different organic solvents of ethanol dimethyl sulfoxide and acetonitrile was determined. The results show the optimum concentration of 10 mg/L dithizone in three solvents. Due to the high intensity of absorption ratio of AgNPs - dithizone complex and the color change of complex could be clearly observed by the naked

eyes. Therefore, the 10 mg/L of dithizone was chosen to prepare for testing in following experiment. And the 10 mg/L of dithizone in different organic solvents were used for determination the detection limit of Ag ion and AgNPs. Comparison of the dithizone dissolving with ethanol, dimethyl sulfoxide and acetonitrile solvents after addition, Ag ion in difference concentration was determined. The results show the detection limit of Ag ion is 1 μM for dithizone (8 mg/L) in DMSO. However, the same concentration of 10 mg/L of dithizone in ethanol and acetonitrile was compared, the resulting show the detection limit for Ag ion was found to be 97.55 μM for dithizone in ethanol and a limit of detection was 100 μM for dithizone in acetonitrile. On the other hand, the detection limits of AgNPs were investigated by adding the same concentration of 10 mg/L dithizone in ethanol, DMSO and acetonitrile solvents. The results show the detection limit of AgNPs was found to be 0.02 mg/L for dithizone in ethanol and DMSO. In acetonitrile solvent, the result shows a limit of detection for AgNPs was 0.6 mg/L. Therefore, the detection limit of silver depends on the concentration and organic solvents including interaction of silver-dithizone complex (Gulam; Takahashi; & Ohga. 2009: 5170-5174; Zaporozhets; Petruniock; & Sukhan. 1999: 865-873).

From all the above results show that the dithizone in acetonitrile solvent was carried out in the next experiments due to the dithizone in acetonitrile solvent are more stable than ethanol and DMSO and can be stored for at room temperature.

5. Applications

In analytical applications, dithizone ligand was prepared by dissolving with acetonitrile solvent.

5.1 Paper based sample

5.1.1 Effect of concentration in paper based

The different solutions with various dithizone concentrations (40 mg/L, 60 mg/L, 80 mg/L and 100 mg/L), were prepared to monitor the colorimetric of the paper based. The dithizone solution was dropped into the loading zone of the paper based in various concentrations. In the experiment, there were prepared deionized water for control testing the paper based. Then, 5 µL of the mentioned dithizone solutions was dropped into the loading zone of paper based on the room temperature. The results show that the color of paper based changes from colorless to green as shown in (Figure 56). Followed by, the 5 µL of deionized water was dropped into a dithizone solution onto the loading zone of this paper based. The result has no significant color change from paper based. Moreover, the paper based was absorbed rapidly with dithizone solution at the room temperature for a few minutes to dry. The intensity of color on paper based depends on the concentrations of dithizone solution.

Concentration of dithizone

1. 100 mg/L
2. 80 mg/L
3. 60 mg/L
4. 40 mg/L

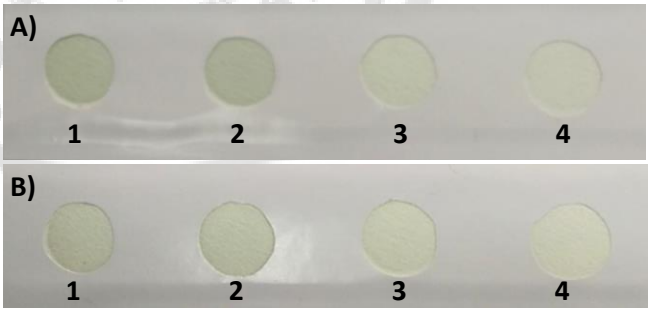

FIGURE 56 Colorimetric responses of paper device A) Modification of the loading of dithizone with in various concentrations (40-100 mg/L). B) After addition of deionized water.

5.1.2 Effect on reaction time in paper based

The effect of time on the colorimetric response of the paper based was investigated that a 80 mg/L dithizone solution was prepared and 5 µL of this solution was dropped into the loading zone of paper based. Then, the paper based is changed of color from colorless to green due to the dithizone solution is green color. Followed by, adding 5 µL of Ag ion solution which the paper based visual color change immediately to pink. After 40 min, the intensity of color on the paper based is gradually decreasing and the change of paper color was not clearly by the naked eyes in (Figure 57), because of degradation and oxidation of metal-dithizone complex (Michalska; & Kowal. 1985: 1119-1125). Therefore, the dithizone on the paper based occur immediately reaction with Ag ion lead to the color change by the naked eyes of these signals.

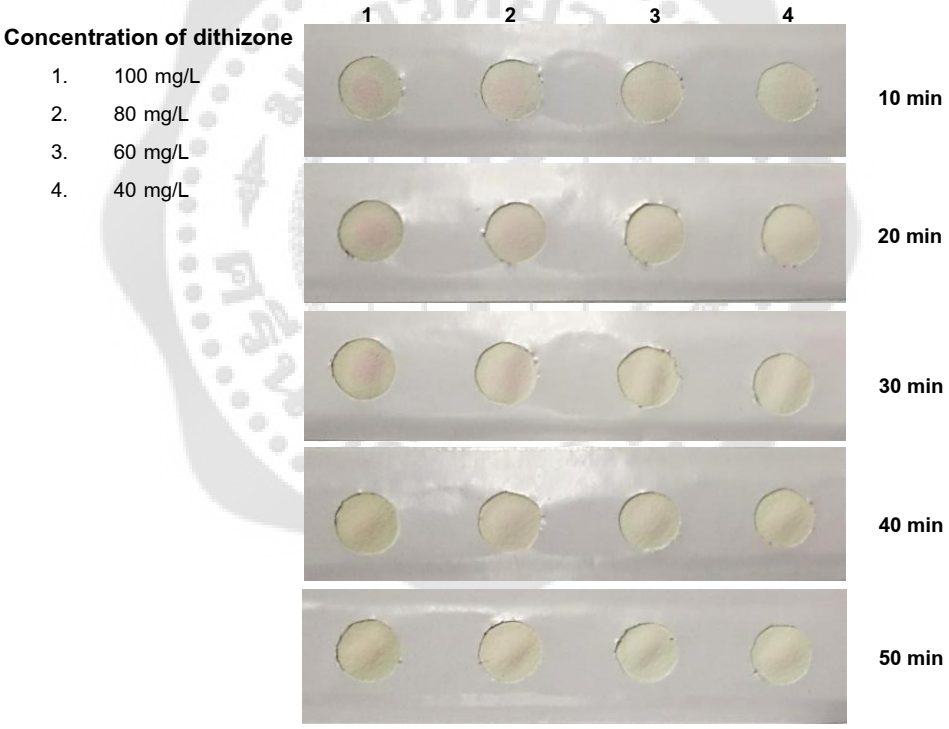

FIGURE 57 Effect of time shows the image of the colorimetric response after adding of Ag ion (100 µM) into paper based with different dithizone concentration of 40 mg/L, 60 mg/L, 80 mg/L and 100 mg/L, respectively.

5.1.3 Detection limit of dithizone, Ag ion and AgNPs in paper based

5.1.3.1 Detection limit of dithizone solution in paper based

To study on the detection limit of the dithizone solution for paper based, after pipetting a 5 µL with various dithizone concentrations of 40 mg/L, 60 mg/L, 80 mg/L and 100 mg/L, respectively, into the test zone of paper based. Followed by, adding 5 µL of Ag ion solution (100 µM) onto the test zone of this paper based. Simultaneously, the results show that the color of paper based changes from green to pink was observed by the naked eyes as shown in (Figure 58). In the case of AgNPs solution 10 mg/L, after addition of the AgNPs solution (5 µL) onto the loading zone leads to change in the paper based from green to yellow which can be remarkable by naked eyes as shown in (Figure 58). The concentrations of dithizone are lower than 80 mg/L show the low intensity of color compared to the other concentrations. Therefore, the limit of detection for dithizone by the naked eye is 80 mg/L. The dithizone solution concentration of 80 mg/L was selected to prepare the testing of paper based on this research.

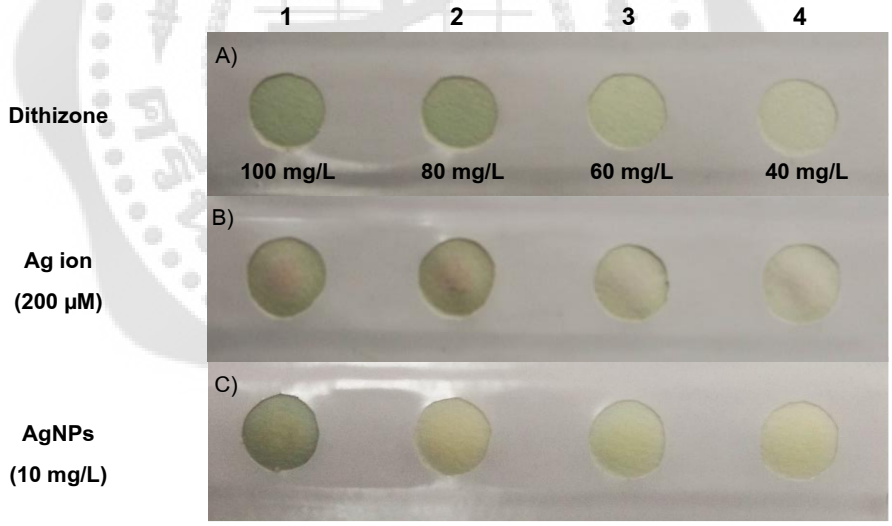

FIGURE 58 Corresponding photographs of the paper based. A) Dithizone solution within various concentrations of 40 - 100 mg/L into the loading zone of paper based. B) After the addition of 200 µM Ag ion. C) After addition of AgNPs (10 mg/L).

5.1.4 Detection limit of Ag ion in paper based

For the detection limit of the Ag ion solution onto the paper based, the Ag ion solution was diluted with DI water to the concentration of 1 μM, 10 μM, 100 μM and 200 μM. The dithizone solution (80 mg/L) was dropped onto the loading zone of paper based. Then, different concentrations of Ag ion solution were dropped to the test zone. A color changes from green to pink were observed as shown in (Figure 59) by the naked eyes upon in various concentrations of Ag ion solution. Therefore, the limit of detection for Ag ion is 100 μM.

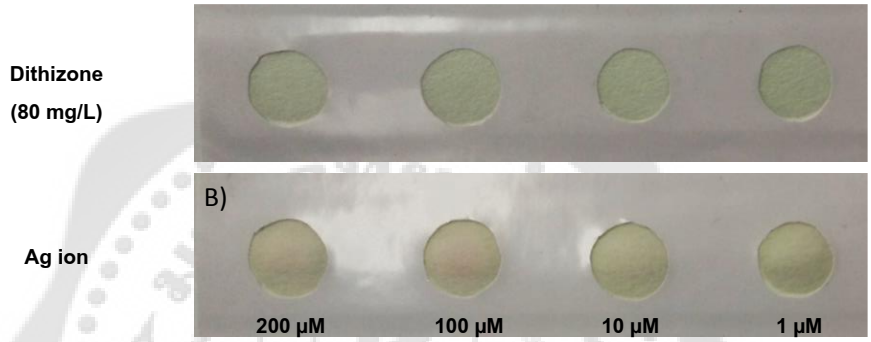

FIGURE 59 Corresponding photographs of the paper based. A) Dithizone solution concentration of 80 mg/L into the loading zone of paper based. B) After addition of Ag ion in different concentration of 1 μM, 10 μM, 100 μM and 200 μM, respectively.

5.1.5 Detection limit of AgNPs in paper based

After addition 5 μL of dithizone solution (80 mg/L) into the loading zone of paper based, followed by, adding 5 μL of AgNPs solutions in various concentrations of 0.4 mg/L, 0.6 mg/L, 0.8 mg/L, 1.25 mg/L, 2.5 mg/L, 5 mg/L, 10 mg/L and 20 mg/L. Therefore, the results of the paper based demonstrate the color change from green to yellow with a detection limit of 10 mg/L for AgNPs as shown in (Figure 60).

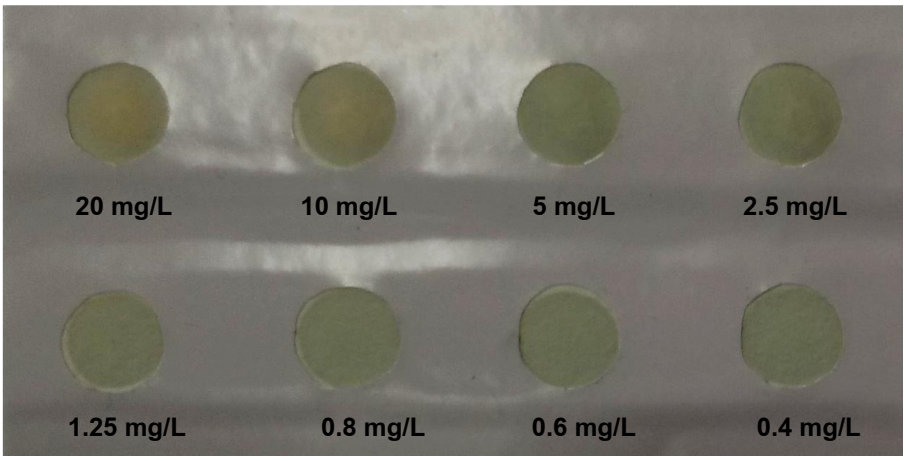

FIGURE 60 Corresponding photographs of the paper based after addition of AgNPs in different concentration of 0.4 mg/L, 0.6 mg/L, 0.8 mg/L, 1.25 mg/L, 2.5 mg/L, 5 mg/L, 10 mg/L and 20 mg/L., respectively.

From all above mentioned result of the detection limit of Ag ion and AgNPs solutions on a paper based, after addition of 5 µL of dithizone solution (80 mg/L) into the loading zone of paper based. The Ag ion and AgNPs solution were added and visual color changes of Ag ion and AgNPs solution from green to pink and green to yellow, respectively with different color of Ag ion and AgNPs solution because of the concentration of silver and size of particles. Moreover, a color change was observed upon the interaction of silver-dithizone through binding of silver to the thiol (-SH) groups on dithizone. The limit of detection for AgNPs is lower than Ag ion.

5.1.6 Analysis of AgNPs in aqueous samples of the paper based

Aqueous samples of commercial, personal care nanoproducts containing silver nano were obtained by purchasing at department stores. The paper based was prepared by loading 5 µL of dithizone solution (80 mg/L). Follow by, adding 5 µL of aqueous sample into the loading zone of paper based. The result shows that the color change from green to orange by naked eyes as shown in (Figure 61).

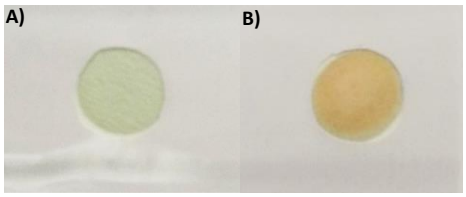

FIGURE 61 Corresponding photographs of the paper based. A) Dithizone solution concentration of 80 mg/L into the loading zone of paper based. B) After addition of aqueous sample.

5.2 Cream based sample

5.2.1 Analysis of spiked AgNPs powder in cream based

About 20 g of the cream base was accurately weighed into a beaker and homogeneously mixed with silver nanoparticles (2 mg) for 20 minutes. The mixture sample was diluted to four concentrations (12.5 mg/L, 25 mg/L, 50 mg/L and 100 mg/L). The 0.4 g of each sample was added with 50 µL of dithizone solution (80 mg/L). After 15 minutes, the color of sample changes from green to orange as shown in (Figure 62).

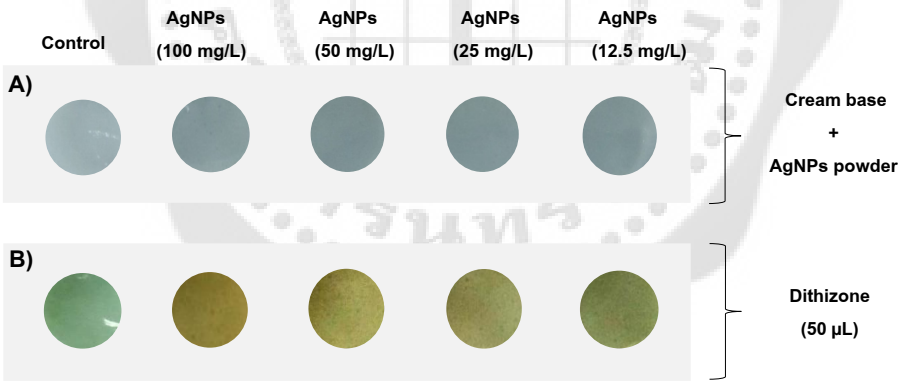

FIGURE 62 Image of the colorimetric response upon reaction with different concentration of AgNPs (12.5 mg/L - 100 mg/L). A) Images of the cream base - AgNPs mixtures before And B) after addition of dithizone solution (80 mg/L).

5.2.2 Analysis of the spiked AgNPs solution in cream based

Cream base 0.4 g was added 50 µL of dithizone solution in a concentration of 80 mg/L, resulting in the color change green color of cream sample by the naked eyes. Then, the addition of DI water into sample have no color change of the sample. While, the AgNPs solutions in various concentrations of 0.4 mg/L, 0.6 mg/L, 0.8 mg/L, 1.25 mg/L, 2.5 mg/L, 5 mg/L and 10 mg/L were prepared. Then, cream sample was added in different concentration of AgNPs solution. After mixtures for 10 min, the color of sample change from green to orange as shown in (Figure 63).

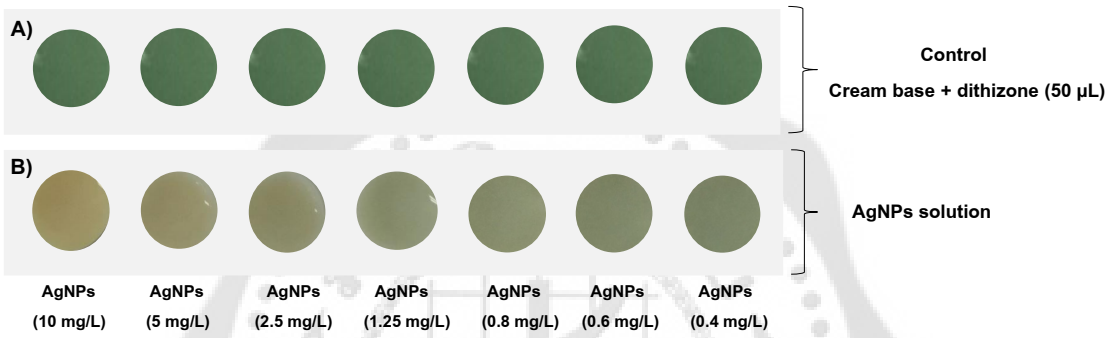

FIGURE 63 The image of visual color change upon addition in various concentrations of AgNPs. A) Images of the cream base - dithizone solution (80 mg/L) mixtures before and B) after addition of AgNPs solution (0.4 mg/L - 10 mg/L).

5.2.3 Analysis of AgNPs in cream sample

Moreover, the samples of commercial, personal care nanoproducts were purchased from department stores. Skin cream nanoproduct was carried out for detection of AgNPs by using dithizone. Then, a 0.4 g of product was added in various volumes of dithizone solution (80 mg/L) after mixtures for 15 min the color of sample change clearly from green to orange as shown in (Figure 64) which its intensity color depends on volume of dithizone solution. However, the trends of color change similar to color of AgNPS solution standard, which color changes to orange.

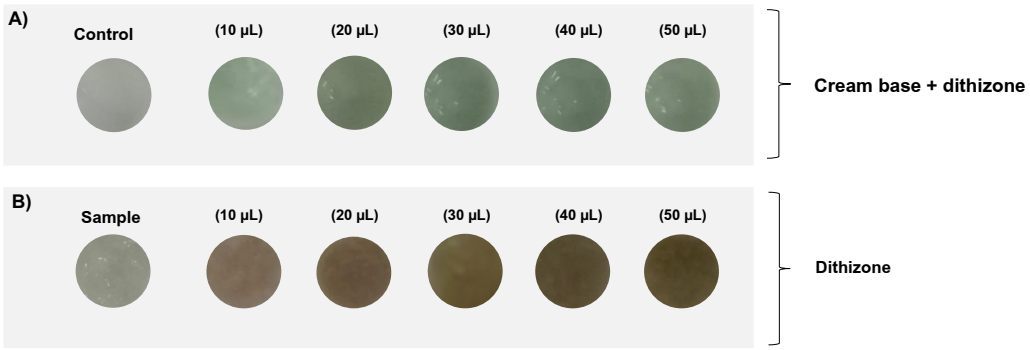

FIGURE 64 The image of visual color change upon addition of dithizone solution into sample (skin cream nanoproduct). A) Cream base with difference volume (10 µL - 50 µL) of dithizone solution (80 mg/L) mixtures. B) The color change of the skin cream sample after the addition of dithizone.

5.3 Aqueous sample

5.3.1 Calibration curve

In this work, dithizone was used for determination the amount of AgNPs in standard AgNPs solution in water. The linearity of the calibration curve confirms the concentration of AgNPs in different solutions. The standard calibration curve of the analysis AgNPs in water, which the calibration curve was plotted between absorbance ratios ($A_{477\ nm}/A_{604\ nm}$) against the AgNPs concentration. A limit of detection of AgNPs was obtained for a signal-to-noise ratio of 3 (3σ) (Shrivastava; & Gupta. 2011:21-25). This method revealed a linear correlation to AgNPs concentration in the range of 0.078 - 0.130 mg/L (the linear equation is y = 81.446x - 3.5553, correlation coefficient R^2 = 0.9957) as shown in (Figure 65). When increasing the concentration of the AgNPs in the solution an increase of the absorption ratio of $A_{477\ nm}/A_{604\ nm}$ was monitored as estimated. The amount of AgNPs was used for this calibration curve.

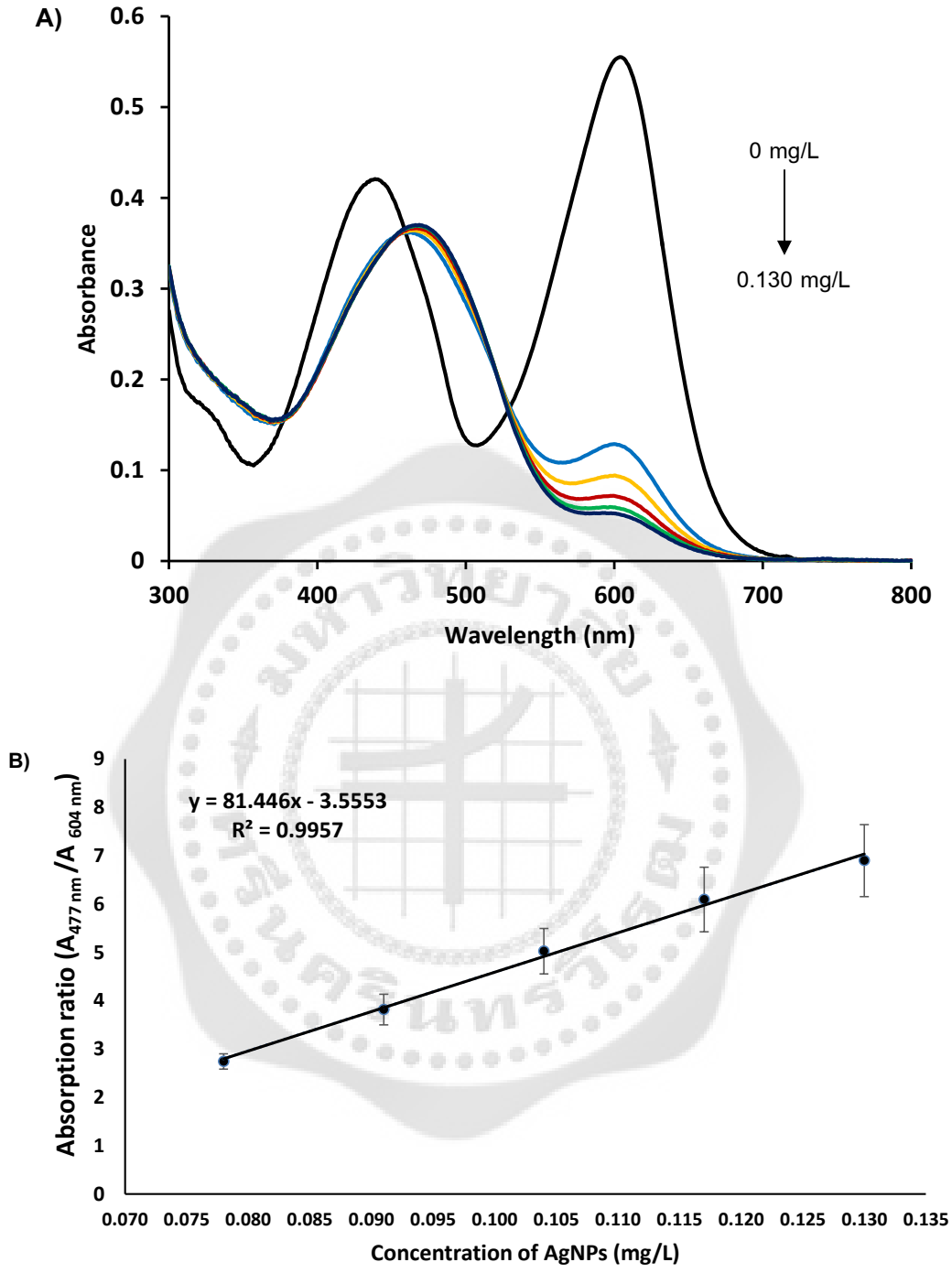

FIGURE 65 A) The UV-Vis spectra of dithizone solutions with various concentrations of AgNPs ranging from 0.078 - 0.130 mg/L (n=3). B) Plot of the absorption ratio of $A_{477\ nm}/A_{604\ nm}$ versus the AgNPs concentration.

5.3.2 Analysis of AgNPs in aqueous sample

Samples of commercial, personal care nanoproducts containing silver nano were obtained by purchasing at department stores. In this work, spray for a shoe was carried out to detect the amount of silver which spray nanoproduct that claimed on their labels to contain ‘‘Nano-silver”. Samples were prepared by filtrating through a whatman filter paper before subjected to further analysis.

Aliquots of the spray product were spiked with standard AgNPs solutions of final concentrations in the range 0.080 - 0.112 mg/L. At different concentrations (0.080, 0.088, 0.096, 0.104, 0.112 mg/L) of AgNPs were added into the prepared spray nanoproduct, and the UV-Vis absorption spectra with added different concentrations of AgNPs were recorded.

To estimate applications for AgNPs analysis in an aqueous media sample, in this research used the dithizone solution sensor to determine the amount of AgNPs in the aqueous media sample. The result show that the linear correlations with regression equation y = 2.7288x + 0.8632 , R^2 = 0.9914) between the absorption value of $A_{477nm}/A_{605\ nm}$ and the concentration of the AgNPs spiked in the sample in the range 0.080 - 0.112 mg/L using the dithizone as shown in (Figure 66). In these resulting, the dithizone obtained recoveries of 98.89%-101.59% of the AgNPs. The relative standard deviations (RSD) of three replicates determination were 1.16% - 3.15% as shown in (Table 13). A limit of detection of 0.071 mg/L was obtained which is lower than the critical standard level of silver allowed in drinking water (WHO. 2008: 434), Therefore, the method has been applied to determine AgNPs spiked in real sample in this study a simple and fast technique to analyze the AgNPs can be found an acceptable detection limit.

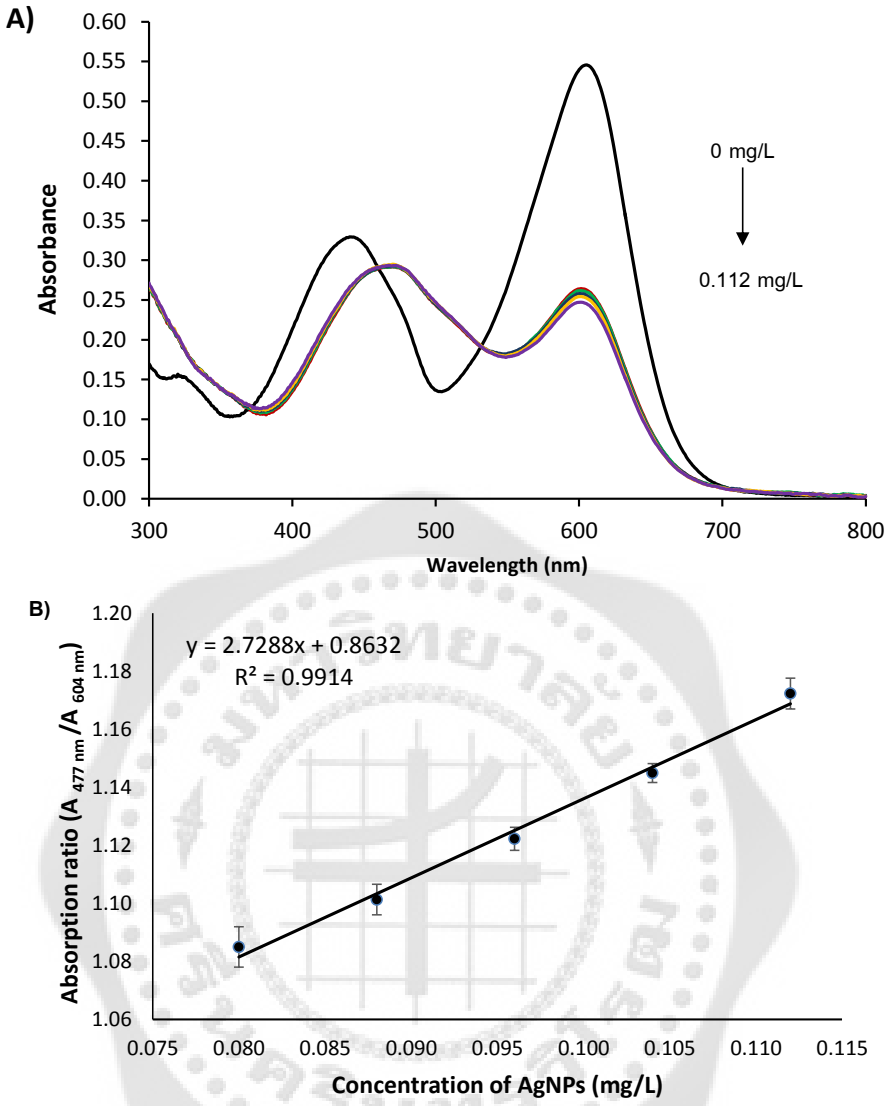

FIGURE 66 A) The UV-Vis spectra of dithizone solutions with various concentrations of AgNPs ranging from 0.080 - 0.112 mg/L (n=3). B) Plot of the absorption ratio of $A_{477\ nm}/A_{604\ nm}$ versus the AgNPs concentration spiked in real sample.

TABLE 13 Quantitative characteristics of the proposed method.

Sample	AgNPs added (mg/L)	Recovered (mg/L)	Recovery (%)	RSD (%)
Aqueous sample (Real sample)	0.080	0.081 ± 0.0026	101.59	3.15
	0.088	0.087 ± 0.0019	99.16	2.22
	0.096	0.095 ± 0.0015	98.89	1.53
	0.104	0.103 ± 0.0012	99.27	1.16
	0.112	0.113 ± 0.0019	101.15	1.71

6. Stability constant (K) and Characterization

6.1 UV-Vis titration of dithizone with Ag ion and AgNPs

6.1.1 UV-Vis titration of silver-dithizone complex

The spectrophotometric titrations between Ag ion at the concentration of 3.32 μM - 33.2 μM with the solution of dithizone in acetonitrile (26.7 μM) were investigated. The absorption spectra changes of dithizone upon addition of solution of Ag ion. The spectral characteristic of dithizone showed two peaks with the maximum absorbance at 447 nm and 604 nm. The spectral change is a result of the addition of Ag ion showing the red shift in wavelength of absorption spectra from 447 to 465 nm and the decreasing of absorbance intensity at 604 nm as shown in (Figure 67). Moreover, UV-Vis titration upon the addition of Ag ion was studied with the measured maximum absorbance at 604 nm corresponding to the formation of a complex between Ag ions and dithizone as shown. The binding of silver-dithizone complex were studied by UV-Vis titration experiments, The spectral data were used to calculate the stability constant between the dithizone and the Ag ion applied by the Benesi–Hildebrand equation 2, (Benesi; & Hildebrand. 1949: 2703-2707; Gaber; et al. 2013: 185-194). Accordinging to (Figure 68), the corresponding stability constant can be determined which is shown in equation 2. Which the stability constant of silver-dithizone complex was K = 4.79 x 10^4 M^{-1}. The corresponding stability constant can be defined by equation 2.;

$$\frac{1}{A - A_0} = \frac{1}{(\varepsilon_{ML} - \varepsilon_L)} + \frac{1}{(\varepsilon_{ML} - \varepsilon_L)\ K[M_0]}$$

Equation 2.

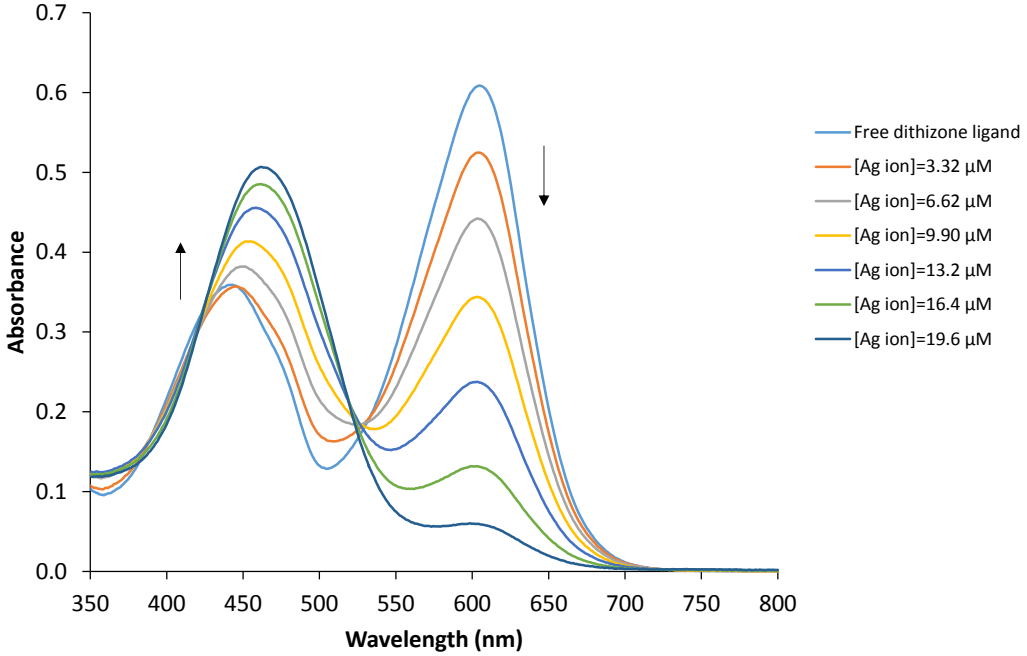

FIGURE 67 UV-Vis spectral titration of dithizone (26.7 µM) in acetonitrile upon addition of (0 - 32 µM) Ag ion.

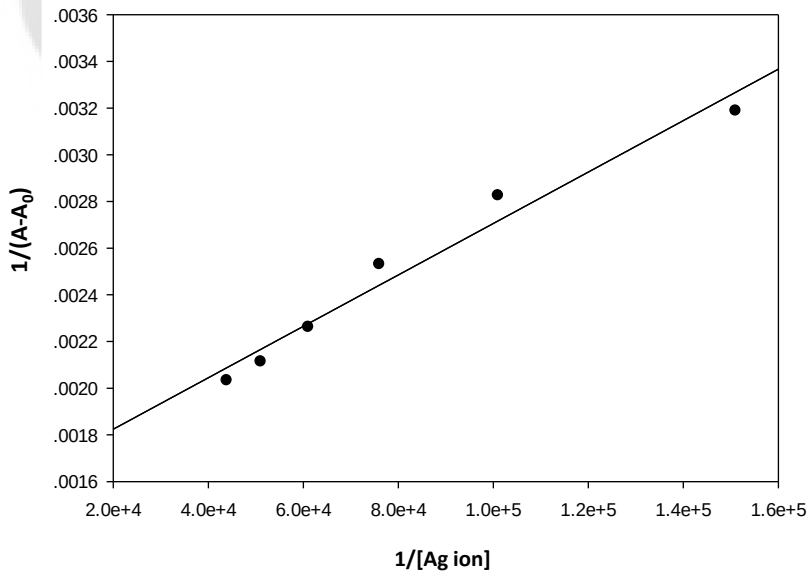

FIGURE 68 Linear dependence of $1/(A - A_0)$ on the reciprocal concentration of Ag ion with dithizone according to Benesi and Hildebrand equation.

6.1.2 UV-Vis titration of AgNPs-dithizone complex

In the subsequent UV-Vis spectrum of dithizone in acetonitrile solvent, it exhibits two absorption bands at 447 and 604 nm. Meanwhile, the gradual addition of 20 nm AgNPs can cause UV-Vis spectrum changes of the absorption band at 447 nm being red shifted to 477 nm and the absorption band showed at 604 nm disappeared as shown in (Figure 69). While is chelating of a complex with the thiol group on dithizone possesses a high affinity to AgNPs showed a critical role in the route of colorimetric recognition which the solution lead to color changes from green to orange. Moreover, the titration of dithizone with increasing amounts of AgNPs has been added constantly until the absorbance intensity being constant. It was observed that the absorbance band at 604 nm of the dithizone gradually decreased and a new absorption band at 477 nm appeared gradually increased with the increasing of AgNPs concentration as shown in (Figure 70) indicating the formation of AgNPs-dithizone complex. Then, stability constants (K) were determined by the UV-Vis spectral changes using Benesi-Hildebrand method (Benesi; & Hildebrand. 1949: 2703-2707; Tayade; et al. 2014:19-26). The corresponding stability constant can be determined using the Benesi-Hildebrand equation as shown in equation 2. Therefore, calculation of the stability constant of UV data was K = 8.223 x 10^5 M^{-1} which a demonstrated plot by adjusted Benesi-Hildebrand plot of $1/(A-A_0)$ verses 1/[AgNPs] as shown in (Figure 71).

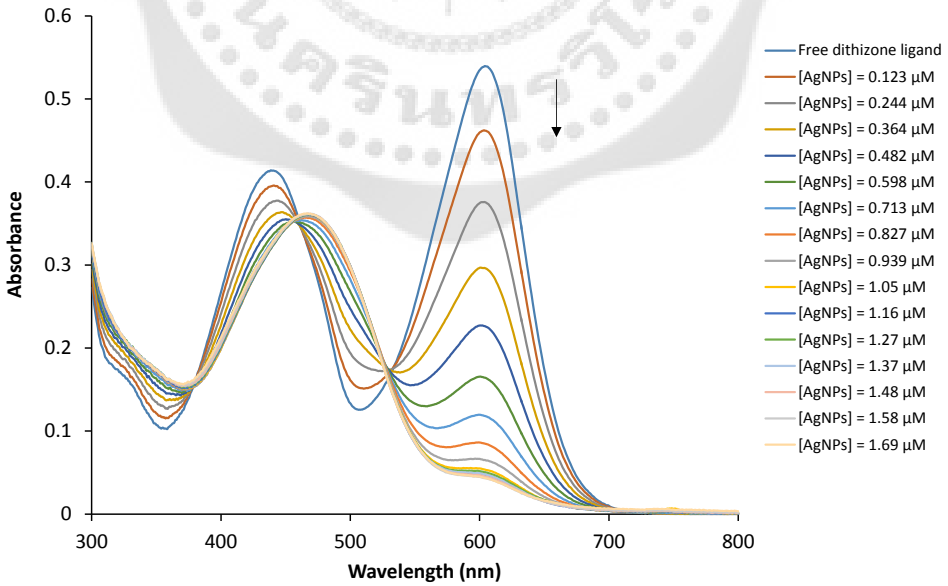

FIGURE 69 Absorption spectra of dithizone ligand on adding different concentrations of AgNPs.

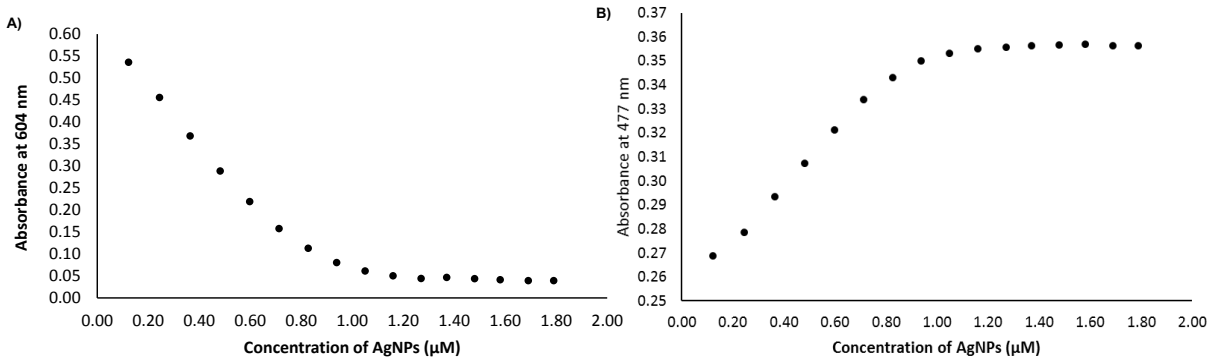

FIGURE 70 Absorbance change of the dithizone by adding different concentrations of AgNPs. A) at 604 nm and B) at 477 nm, respectively.

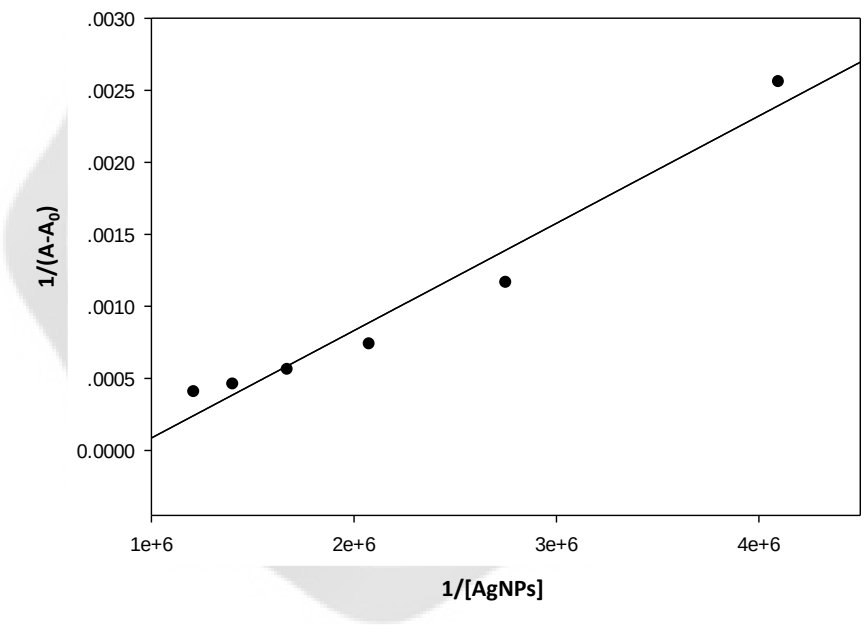

FIGURE 71 Linear dependence of $1/(A - A_0)$ on the reciprocal concentration of AgNPs with dithizone according to Benesi and Hildebrand equation.

Comparison of the interaction between Ag ion and AgNPs with dithizone was considered. The constant of absorbance intensity are indicated the saturation of the complexes, lead to the formation of silver-dithizone complex, according to in the presence of soft metal cations such as Ag ion, prefer “soft” cations due to their stronger interactions with soft sulfur atoms in dithizone (Woznica; et al. 2012: 4437-4442). Therefore, the stability constants (K) values for the complexes of Ag ion and AgNPs with dithizone were calculated

from the plots of $1/(A - A_o)$ versus 1/[Metals], the resulting show the stability constants of silver-dithizone complex was $K = 4.79 \times 10^4\ M^{-1}$ and $K = 8.223 \times 10^5\ M^{-1}$ for stability constants of AgNPs-dithizone complex. The high stability constant of the AgNPs-dithizone complex compared with to the silver-dithizone complex due to the particle size and smaller surface area of AgNPs.

6.2 Characterization of AgNPs-dithizone complex

Moreover, the morphology of AgNPs-dithizone complex were characterized by using transmission electron microscope (TEM). In general, the AgNPs there are spherical in shape and dispersion of particles after binding with ligand occurs by the formation of complexes. The results show that the bigger particles of AgNPs being non-spherical according to (Figure 72), which can cause the adsorption of thiol-ligand on the surface of AgNPs leading to the formation of larger surface complex and may be due to agglomeration (Cure; et al. 2015: 1362-1367).

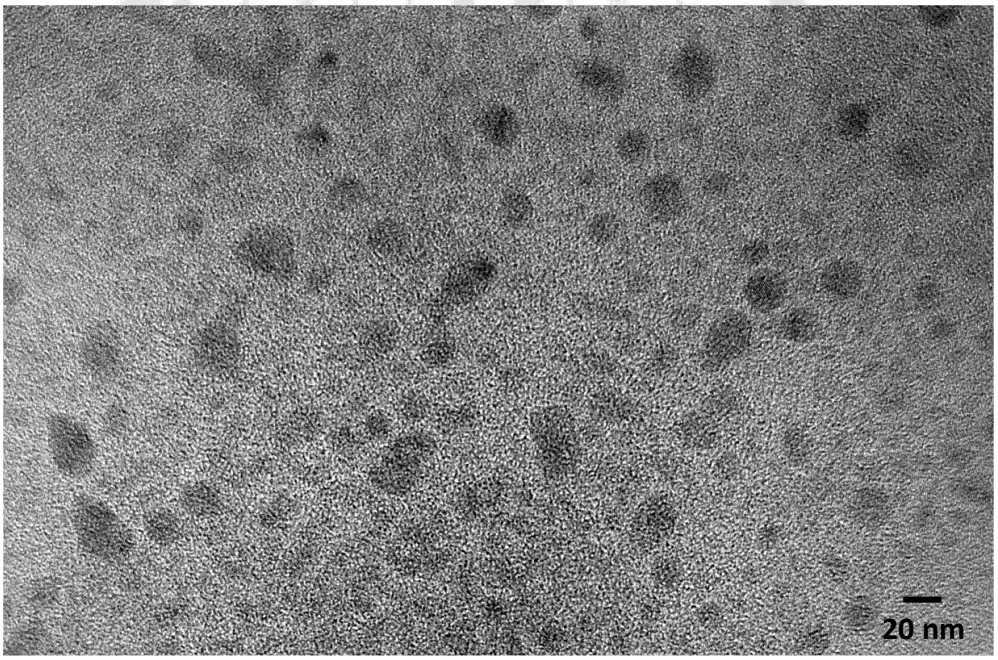

FIGURE 72 TEM image of the complex formation between dithizone and AgNPs.

CHAPTER 5
CONCLUSION

The optimized isomer of dithizone was considered by using the B3LYP/6-31G(d,p) level of calculation. These calculation results indicate that the isomer DIZ-a is classified as the most stable structure of dithizone. The study of interaction between Ag ion and dithizone complex was found that the silver-dithizone complex (2h) was more stable than other complexes with the binding energy of -168.71 kcal mol^{-1}. Moreover, the optimized structure of the dithizone derivative with the nitro group the resulting shows that the structure of the dithizone derivative with the nitro group (DTZ-NO_2-a) is the most stable and similar to dithizone (DTZ-a) due to the symmetrical structure of molecules. While, the interaction between Ag ion and dithizone derivative with the nitro group displayed that the energy of complex (2M) was about -160.86 kcal mol^{-1}. However, the resulting show the binding energy of silver-dithizone complex (2h) is lower than the silver-dithizone derivative with electron-withdrawing group; -SO_3H, -CN, -CF_3, -F, -Cl and -Br complexes. Finally, the structure of complex (2h) is the most stable. After the simulation studies of silver interaction with dithizone and dithizone derivatives were determined and all results were found.

Furthermore, the UV–Vis spectroscopy and FT-IR spectrum were calculated using B3LYP/6-31G (d,p) compared to experimental data which are the result showing the correlation and good agreement. The ^1H NMR of silver-dithizone complex was compared between experimental data and computer simulation system using the B3LYP/6-311+G(2d,p) level of calculation. All results confirmed the possible structure of silver-dithizone complex occurred by an ion exchange process of the interaction between Ag ion and dithizone which the solvent dependence is the main reason for the changes of chemical shifts in the complexes. Meanwhile, the result of interaction between AgNPs and dithizone displayed the AgNP-dithizone complexes (complex (L)) was more stable than other complexes with the lowest binding energy was investigated to be -53.543 kcal mol^{-1}. The behavior of AgNPs clusters adsorbs to the surface of dithizone by occurs via a sulfur atom with a slight gradient. The AgNPs-dithizone complexes were characterized by using transmission electron microscope (TEM) that showed the thiol - ligand absorption on the surface of AgNPs. Furthermore, the absorbance spectral data were used to calculate the stability constant between the Ag ion and AgNPs with dithizone. The result show that the

stability constant was K = 4.79 x 10^4 M^{-1} and K = 8.223 x 10^5 M^{-1}, respectively, which calculated from the plots of $1/(A - A_o)$ versus 1/[Metals]. The results show that the sulfur atoms of dithizone interaction with Ag ion in the ratio of 1:1.

To estimate determined method was applied for the detection of AgNPs in the real sample and the potential application of AgNPs colorimetric sensor in paper based devices. The developed colorimetric sensor has the advantages such as rapidly, simplicity, low cost, saving time and good sensitivity and selectivity for detection AgNPs in the aqueous sample which can be observed by the naked eyes. The selectivity of dithizone in ethanol, DMSO and acetonitrile solvent towards AgNPs, resulting show the color change from green to orange in aqueous media. The results show the detection limit of AgNPs was found to be 0.2 mg/L for dithizone in ethanol and DMSO. In acetonitrile solvent, the result shows a limit of detection for AgNPs was 0.6 mg/L. Therefore, the detection limit of silver depends on the concentration and organic solvents including interaction of silver-dithizone complex.

After that, dithizone in acetonitrile solvent was carried out in the part of an application due to the dithizone in acetonitrile more stable than ethanol and DMSO solvent. On the other hand, paper based sensor were prepared by loading of dithizone solution followed by adding of AgNPs, which observed a color change from green to yellow. The results show that the detection limit was found to be 10 mg/L which the same results were found by using a cream based sensor. Moreover, the dithizone solution was used for detection AgNPs in cream sample. However, the presented method can be applied for the detection of AgNPs in the actual sample. The result show that the linear correlations with regression equation $y = 2.7288x + 0.8632$, $R^2 = 0.9914$) and the detection limit was found to be 0.071 mg/L. Therefore, the sensor can be applied as a convenient and effective method for detection AgNPs in real samples. In the future, the proposed method is useful for screening AgNPs in the actual sample.

BIBLIOGRAPHY

BIBLIOGRAPHY

Abbehausen, Camilla; et al. (2011). Chemical, spectroscopic characterization, DFT studies and initial pharmacological assays of a silver(I) complex with N-acetyl-L-cysteine. *Polyhedron*. 30(4): 579-583.

Adam, Abdel Majid A; et al. (2016). Charge transfer complexation of the anticholinergic drug clidinium bromide and picric acid in different polar solvents: Solvent effect on the spectroscopic and structural morphology properties of the product. *Journal of Molecular Liquids*. 216: 192-208.

Andal V. Kadambi; & Buvaneswari Gopal. (2011). Preparation of Cu_2O nano-colloid and its application as selective colorimetric sensor for Ag^+ ion. *Sensors and Actuators B: Chemical*. 155: 653-658.

Antônio C. Spínola Costa; et al. (2002). Separation and pre-concentration of cadmium, copper, lead, nickel and zinc by solid-liquid extraction of their cocrystallized naphthalene dithizone chelate in saline matrices. *Journal of the Brazilian Chemical Society*. 13: 674-678.

Azizi, Khaled; & Sohrabinia Ali. (2012). A DFT study on the interaction between adsorbed silver on C_{60} and disulfide bond. *Journal of Molecular Graphics and Modelling.* 38: 354-359.

Bae Sung Jin; et al. (2002). Adsorption of 4-Biphenylisocyanide on gold and silver nanoparticle surfaces: Surface-enhanced raman scattering study. *Journal of Physical Chemistry B.* 106: 7076-7080.

Benesi, Alan; & Hildbrand John. (1949). A spectrophotometric investigation of the interaction of iodine with aromatic hydrocarbons. *Journal of the American Oil Chemists Society*. 71: 2703-2707.

Benn Troy M; & Westerhoff Paul. (2008). Nanoparticle silver released into water from commercially available sock fabrics. *Environmental Science & Technology.* 42: 4133-4139.

Bhardwaj Vimal K; et al. (2006). Mesitylene based azo-coupled chromogenic tripodal receptors-a visual detection of Ag(I) in aqueous medium. *Tetrahedron*. 62: 7878-7886.

Blaser Sabine A; et al. (2008). Estimation of cumulative aquatic exposure and risk due to silver: Contribution of nano-functionalized plastics and textiles. *Science of the Total Environment.* 390: 396-409.

Cheng, Guihong; et al. (2012). Dithizone modified magnetic nanoparticles for fast and selective solid phase extraction of trace elements in environmental and biological samples prior to their determination by ICP-OES. *Talanta*. 88: 507-515.

Chiniforoshan, Hossein; et al. (2015). Silver nanoparticles with 4,4-dicyanamidobiphenyl ligand: Synthesis, photoluminescent and electroluminescent properties and DFT calculations. *Journal of Molecular Structure*. 1082: 56-61.

Chwastowska, Joanna; et al. (2004). Determination of platinum and palladium in environmental samples by graphite furnace atomic absorption spectrometry after separation on dithizone sorbent. *Talanta.* 64: 224-229.

Cure, Jeemy; et al. (2015). Monitoring the coordination of amine ligands on silver nanoparticles using NMR and SERS. *Langmuir.* 31: 1362-1367.

Das, Priyadip; et al. (2012). A highly selective and dual responsive test paper sensor of Hg^{2+}/Cr^{3+} for naked eye detection in neutral water. *RSC Advances.* 2: 3714-3721.

Danwittayakul, Supamas; et al. (2008). Simple detection of mercury ion using dithizone nanoloaded membrane. *Journal of the Minerals Metals & Materials Society.*18: 37-40.

Dastjerdi, Roya; & Montazer, Majid. (2010). A review on the application of inorganic nanostructured materials in the modification of textiles: focus on anti-microbial properties. *Colloids and Surfaces B: Biointerfaces.* 79: 5-18.

De Schamphelaere Karel A.C; & Janssen Colin R. (2004). Bioavailability and chronic toxicity of zinc to juvenile rainbow trout *(Oncorhynchus mykiss)*: comparison with other fish species and development of a biotic ligand model. *Environmental Science & Technology.* 38: 6201-6209.

Eschwege Karel G; Conradie, Jeanet; & Kuhn, A. (2011). Dithizone and its oxidation products: A DFT spectroscopic and x-ray structural study. *Journal of Physical Chemistry A.* 115: 14637-14646.

Frisch Michael J; et al. (2003). *Gaussian 03, Revision B.01. Gaussian Inc,* Pittsburgh: Pennsylvania.

Gaber Mohamed; et al. (2013). Cu(II) complexes of monobasic bi- or tridentate (NO, NNO) azo dye ligands: Synthesis, characterization, and interaction with Cu-nanoparticles. *Journal of Molecular Structure.* 1032: 185-194.

Gao, Yuan; & Cranston, Robin. (2008). Recent advances in antimicrobial treatments of textiles. *Textile Research Journal*. 78: 60-72.

Garnuszek, Piotr; et al. (1998). The synthesis, radioiodination and preliminary biological study of the new carboxylic derivatives of dithizone. *Applied Radiation and Isotopes.* 49: 1563-1571.

Ghosh, Soumen; et al. (2015). Amido-Schiff base derivatives as colorimetric fluoride sensor: Effect of nitro substitution on the sensitivity and color change. *Spectrochimica Acta Part A: Molecular and Biomolecular Spectroscopy.* 149: 869-874.

Greene Richard M; & Su, Wen-Pin. (1987). Argyria. *American Family Physician.* 36: 151-154.

Grimme, Stefan; et al. (2010). The mechanism of dihydrogen activation by frustrated Lewis pairs revisited. *Angewandte Chemie International Edition*. 49: 1402-1405.

Gulam Rabani M; Takahashi, Toru; & Ohga, Yasushi. (2009). Dynamic solvent effects on the thermalisomerization of zinc dithizonate. *Physical Chemistry Chemical Physics.* 11: 5170-5174.

International Organization for Standardization. (2008). *Nanotechnologies - Terminology and definitions for nano-objects - Nanoparticle, nanofibre and nanoplate. ISO/TS 27687.* 1st ed. Geneva: Switzerland.

Jiang, Jinqiang; et al. (2012). A novel highly selective colorimetric sensor for Ni(II) ion using coumarin derivatives. *Inorganic Chemistry Communications*. 15: 12-15.

Kaegi, Ralf; et al. (2010). Release of silver nanoparticles from outdoor facades. *Environmental Pollution.* 158: 2900-2905.

Kaur, Navneet; & Kumar, Subodh. (2011). Colorimetric metal ion sensors. *Tetrahedron.* 67: 9233-9264.

Khan, Zaheer; et al. (2011). Effects of solvents on the stability and morphology of CTAB-stabilized silver nanoparticles. *Colloids and Surfaces A: Physicochemical and Engineering Aspects*. 390: 120-125.

Kiwan, Mohamed. (1997). Use of dichloromethane with dithizone as an alternative solvent to carbon tetrachloride restricted by Montreal Protocol. *Talanta.* 44: 947-950.

Lee Kerry J; et al. (2007). *In vivo* imaging of transport and biocompatibility of single silver nanoparticles in early development of zebrafish embryo. *ASC Nano.* 1: 133-143.

Lorenz, Christiane; et al. (2012). Characterization of silver release from commercially available functional (nano) textiles. *Chemosphere*. 89: 817-824.

Lv, Yongjun; et al. (2011). Simple indole-based colorimetric sensors with electron-withdrawing chromophores: Tuning selectivity in anion sensing. *Journal of Fluorine Chemistry.* 132: 973-977.

Mei, Qunbo; et al. (2012). A highly selective and naked-eye sensor for Hg^{2+} based on quinazoline-4(3H)-thion. *Nouveau Journal de Chimie*. 36: 1879-1883.

Michalska, Danuta; & Kowal Andrzei T. (1985). Vibrational spectra of Cu(II), Cu(I), Ni(II), Pd(II), Pt(II) and Hg(II) complexes with dithizone. *Spectrochimica Acta Part A: Molecular and Biomolecular Spectroscopy.* 41: 1119-1125.

Mo, Fanyang; et al. (2013). Recent applications of arene diazonium salts in organic synthesis. *Organic & Biomolecular Chemistry*. 11: 1582-1593.

Morgan Tammie P; & Wood Chris M. (2004). A relationship between gill silver accumulation and acute silver toxicity in the freshwater rainbow trout: Support for the acute silver biotic ligand model. *Environmental Toxicology & Chemistry.* 23: 1261-1267.

Mulfinger, Lorraine; et al. (2007). Synthesis and Study of Silver Nanoparticles. *Journal of Chemical Education*. 84: 322-325.

National Institute for Occupational Safety and Health. (2007). NIOSH Pocket Guide to Chemical Hazards. Washington: D.C.

Pasricha Aneesh; et al. (2012). Comparative study of leaching of silver nanoparticles from fabric and effective effluent treatment. *Journal of Environmental Science.* 24: 852-859.

Pearson Ralph G. (1963). Hard and soft acids and bases. *Journal of the American Chemical Society*. 85: 3533-9.

Safavi, Afsaneh; & Bagheri, Mozhgan. (2005). Design of a copper (II) optode based on immobilization of dithizone on a triacetylcellulose membrane. *Sensors and Actuators B: Chemical*. 107: 53-58.

Salih, Bekir; et al. (1998). Adsorption of heavy metal ions onto dithizone-anchoredpoly (EGDMA-HEMA) microbeads. *Talanta.* 46: 1205-1213.

Shrivastava, Alankar; & Gupta Vipin B. (2011). Methods for the determination of limit of detection and limit of quantitation of the analytical methods. *Chronicles of Young Scientists.* 2: 21-25.

Summers Richard L. (1998). Computer Simulation Studies and the Scientific Method. *Journal of Applied Animal Welfare Science.* 1: 119-131.

Takahashi, Yukiko; Danwittayakul, Supamas; & Suzuki Toshishiqe M. (2009). Dithizone nanofiber-coated membrane for filtration-enrichment and colorimetric detection of trace Hg(II) ion. *Analyst.* 134: 1380-1385.

Tan, Xue-Jie; et al. (2014). Synthesis, characterization and in vitro cytotoxic properties of new silver(I) complexes of two novel Schiff bases derived from thiazole and pyrazine. *Polyhedron*. 71: 119-132.

Tavallali, Hossien; et al. (2013). A novel development of dithizone as a dual-analyte colorimetric chemosensor: Detection and determination of cyanide and cobalt (II) ions in dimethyl sulfoxide/water media with biological applications. *Journal of Photochemistry and Photobiology B: Biology*. 125: 121-130.

----------. (2014). Dithizone as novel and efficient chromogenic probe for cyanide detection in aqueous media through nucleophilic addition into diazenylthione moiety. *Spectrochimica Acta Part A: Molecular and Biomolecular Spectroscopy.* 121: 139-146.

Tayade Kundan C; et al. (2014). Design and synthesis of a pyridine based chemosensor: Highly selective fluorescent probe for Pb^{2+}. *Journal of Fluorescence.* 24: 19-26.

Ullah, Habib; et al. (2014). Density functional theory and phytochemical study of Pistagremic acid. *Spectrochimica Acta Part A: Molecular and Biomolecular Spectroscopy.* 118: 210-214.

Walsh Michael J; & Ahner Beth A. (2013). Determination of stability constants of Cu(I), Cd(II) & Zn(II) complexes with thiols using fluorescent probes. *Journal of Inorganic Biochemistry* 128: 112-123.

Wang, Litao; et al. (2011). Nitro-substituted 3,3-bis(indolyl)methane derivatives as anion receptors: Electron-withdrawing effect and tunability of anion binding properties. *Spectrochimica Acta Part A: Molecular and Biomolecular Spectroscopy.* 78: 726-731.

World Health Organization. (2008). *Guidelines for drinking-water quality.* 3rd ed. Geneva: Switzerland.

Woźnica, Emilia; et al. (2012). Dithizone modified gold nanoparticles films for potentiometric sensing. *Analytical Chemistry.* 84: 4437-4442.

Yang, Xuan; & Wang, Erkang. (2011). A Nanoparticle autocatalytic sensor for Ag^{+} and Cu^{2+} ions in aqueous solution with high sensitivity and selectivity and its application in test paper. *Analytical Chemistry.* 83: 5005-5011.

Yin, Changhai; et al. (2012). Sensitive determination of trace mercury by UV–visible diffuse reflectance spectroscopy after complexation and membrane filtration-enrichment. *Journal of Hazardous Materials.* 233-234: 207-212.

Yu, Hong-Mei; Song, Hua; & Chen, Ming-Li. (2011). Dithizone immobilized silica gel on-line preconcentration of trace copper with detection by flame atomic absorption spectrometry. *Talanta*. 85: 625-630.

Zaporozhets, Olga A; Petruniock, Nicole; & Sukhan, Verma. (1999). Determination of Ag(I), Hg(II) andPb(II) by using silica gel loaded with dithizone and zinc dithizonate. *Talanta.* 50: 865-873.

Zhou, Jing; et al. (2011). Diphenylthiocarbazone (dithizone)-assisted solvothermal synthesis and optical properties of one-dimensional CdS nanostructures. *Journal of Alloys and Compounds.* 509: 6731-6735.

GLOSSARY

LIST OF ABBREVIATIONS AND SYMBOLS

µg/L

Micrograms per liter

µL

Microliter

µM

Micromolar

AAS

Atomic absorption spectroscopy

Ag^+

Silver ion

AgNPs

Silver nanoparticles

$Al(NO_3)_3.9H_2O$

Aluminum nitrate nonahydrate

$BaCl_2.2H_2O$

Barium chloride dihydrate

°C

Degree Celsius

^{13}C NMR

13-Carbon Nuclear Magnetic Resonance Spectroscopy

$CaCl_2$

Cacium chloride

$Cd(CH_3COO)_2.2H_2O$

Cadmium acetate dihydrate

$CoCl_2.6H_2O$

Cobalt chloride hexahydrate

$Cu(NO_3)_2.3H_2O$

Copper nitrate Trihydrate

LIST OF ABBREVIATIONS AND SYMBOLS (continued)

CH_2Cl_2

Dichloromethane

CH_3COOH

Glacial acetic acid

$CH_3COONa.3H_2O$

Sodium acetate trihydrate

CH_3NO_2

Nitro methane

CH_3OH

Methanol

C_2H_5OH

Ethanol

C_3H_6O

Acetone

C_4H_8O

Ethyl acetate

$C_6H_6N_2O_2$

p-nitroaniline

C_6H_{14}

Hexane

cm

Centimeter

CN^-

Cyanide anion

Co^{2+}

Cobalt (II) ion

Cu^{2+}

Copper (II) ion

LIST OF ABBREVIATIONS AND SYMBOLS (continued)

DMSO

Dimethysulfoxide

DMSO-d_6

Dimethysulfoxide-d_6

DTZ

Dithizone

$FeSO_4.7H_2O$

Iron sulfate heptahydrate

FTIR

Fourier transform infrared spectroscopy

G

Gram

h

Hour

HCL

Hydroclhoric acid

HNO_3

Nitric acid

^1H NMR

Proton Nuclear Magnetic Resonance Spectroscopy

H_2SO_4

Sulfuric acid

HASB

Hard soft acids bases

$HgCl_2$

Mercury chloride

ICP-AES

Inductively coupled plasma atomic emission spectrometry

LIST OF ABBREVIATIONS AND SYMBOLS (continued)

ICP-OES

Inductively coupled plasma optical emission spectrometry

ICP-MS

Inductively coupled plasma mass spectroscopy

KBr

Potassium bromide

KCL

Potassium chloride

KHP

Potassium hydrogen phthalate

KI

Potassium iodide

KNO_3

Potassium nitrate

KOH

Potassium hydroxide

M

Molarity

mg

Milligram

mg/L

Milligram per liter

mg/mL

Milligram per milliliter

$MgSO_4.7H_2O$

Magnesium sulfate heptahydrate

mL

Milliliter

LIST OF ABBREVIATIONS AND SYMBOLS (continued)

mg/m^3

Milligram per cubic meter

mM

Millimolar

mm

Millimeter

mmol

Millimole

$MnSO_4.H_2O$

Manganese sulfate monohydrate

N

Nitrogen

NaI

Sodium iodide

$NaNO_2$

Sodium nitrite

NaOH

Sodium hydroxide

$Na_2S.9H_2O$

Sodium sulfide Nonahydrate

NH_3OH

Ammonium hydroxide solution

$NiCl_2.6H_2O$

Nickel chloride hexahydrate

nm

Nanometer

OPDA

o-phenylenediamine

LIST OF ABBREVIATIONS AND SYMBOLS (continued)

$Pb(NO_3)_2$

Lead nitrate

pH

Power of hydrogen

ppb

Parts per billion

S

Sulfur

SPR

Surface plasmon resonance

TLC

Thin-Layer chromatography

TEM

Transmission electron microscopy

UV-Vis

Ultraviolet-visible

v/v

Volume/Volume

w/v

Weight/Volume

XRD

X-ray diffraction

$ZnSO_4.7H_2O$

Zinc sulfate heptahydrate

VITAE

VITAE

Name : Nootcharin Wasukan

Date of Birth : October 1, 1987

Place of Birth : Amnat Charoen

Address : 19/11 Tumbol Mad, Lue Amnat District, Amnat Charoen 37000, Thailand

Educational Background:

June 2008 - March 2011	Bachelor of Science Degree in Chemistry Srinakharinwirot University, Bangkok, Thailand
June 2011 - March 2012	Master of Science Degree in Chemistry Srinakharinwirot University, Bangkok, Thailand
June 2016	Doctor of Philosophy Degree in Applied Chemistry Srinakharinwirot University, Bangkok, Thailand

Scholarships:

June 2011-March 2012	Thailand Graduate Institute of Science and Technology Scholarship (TGIST), National Science and Technology Development Agency (NSTDA) (Grant No. TG-55-17-53-059M)
June 2012 - Present	Thailand Graduate Institute of Science and Technology Scholarship (TGIST), National Science and Technology Development Agency (NSTDA) (Grant No. TG-55-17-55-055D)

Poster presentation:

Wasukan N., Srisung S., Kulthong K., Maniratanachote R. Potential exposure of silver from nanoproducts sold in Thailand. Pure and Applied Chemistry International Conference (PACCON 2012)**,** 11-13 January 2012, The Empress Hotel, Chiang Mai, Thailand.

Wasukan N., Srisung S., Kulthong K., Maniratanachote R. Selective colorimetric detection of silver nanoparticles (AgNPs) in aqueous media using dithizone. ^{6}th International Symposium on Nanotechnology, Occupational and Environmental Health (NanOEH), 28-31 October, 2013 at Nagoya Congress Center, Japan

Wasukan N., Srisung S., Kulthong K., Maniratanachote R. Dithizone-based colorimetric sensors for silver nanoparticles in aqueous media. Pure and Applied Chemistry International Conference (PACCON 2014) **,** 8-10 January 2014 at Centara Hotel & Convention Centre Khon Kaen

Oral presentation:

. **Wasukan N.**, Srisung S., Kuno M., Kulthong K., Maniratanachote R. Evaluation of Dithizone-Based Colorimetric Sensors for Silver Nanoparticles in Aqueous Media. Nanotech France 2016 Conference and Exhibition. Pôle Universitaire Léonard de Vinci**.** 1 - 3 June 2016, Paris, France

International Research:

August 2015 - January 2016	Research project in the research lab of **Professor Wesley R. Harris** at Department of Chemistry and Biochemistry, University of Missouri-St. Louis, Missouri, United states

Proceeding:

May 2012 **Wasukan N.**, Kulthong K., Srisung S., Maniratanachote R. A method to evaluate potential dermal exposure to silver in nanoproducts. Proceedings of NanoThailand 2012, pp.1-4, 2012.

Publications:

April 2015 **Wasukan N.**, Srisung S., Kuno M., Kulthong K., Maniratanachote R. Interaction evaluation of silver and dithizone complexes using DFT calculations and NMR analysis. Spectrochimica Acta Part A: Molecular and Biomolecular Spectroscopy 149 (2015) 830-838.

November 2015 **Wasukan N.**, Srisung S., Kulthong K., Boonrungsiman S., Maniratanachote R. Determination of silver in personal care nanoproducts and effects on dermal exposure. Journal of Nanoparticles Research (2015) 17:425.